Scuola Normale Superiore

Laboratorio di Biologia

PhD in Neuroscience

Multilevel investigation of Tau pathology: from the cytoplasm to the nucleus

Candidate:
Giacomo Siano

Supervisor:
Cristina Di Primio, PhD
Professor Antonino Cattaneo

Abstract

Tau protein has been discovered in 1975 from brain tissues and its main function in neurons is to bind and stabilize microtubules. This observation was followed by the identification of Tau as one of the main actors able to induce neuronal toxicity in a group of neurodegenerative disorders named tauopathies. From these discoveries, the scientific community has invested great efforts to elucidate the mechanisms involving Tau and to find a way to prevent its pathological effects. Tau toxicity is due to its displacement from microtubules, progressive aggregation of the protein and spreading in several brain areas causing neuronal dysfunction and death. These are considered the central events leading to neurodegeneration. However, recently it has been demonstrated that Tau is located not only on microtubules or in the cytoplasmic aggregates but also in other subcellular regions, in particular in dendrites and in the nuclear compartment where it exerts functions related to synaptic transmission and genome protection, respectively.

In order to investigate the dynamics of Tau from physiological conditions to destabilization and aggregation, we developed a FRET-based biosensor, the Conformational Sensitive Tau (CST), able to determine the conformational changes of Tau during the progression of the pathology. We showed that in physiological conditions, in living cells, Tau binds microtubules with a paperclip conformation. After drug treatments or tauopathy-related mutations, the conformation of Tau opens indicating an impairment of Tau binding to tubulin. Finally, by treating cells with different kinds of Alzheimer's aggregates, the CST displaced from microtubules and formed FRET-positive intracellular inclusions demonstrating that it is a powerful tool to study also aggregation. The CST employment allowed the characterization of a particular mutation associated to Pick's disease, Q336H. Remarkably, we found that this mutation induces a closer conformation of Tau and a higher affinity to tubulin, an effect that is opposite to previously discovered mutations.

We applied the CST to develop a cell-based aggregation assay to screen compounds impairing Tau pathology. A first screening identified the ERK kinase inhibitor PD-901 as a compound reducing Tau aggregation. Moreover, to test the

efficacy of therapeutic compounds *in vivo*, a transgenic zebrafish expressing the CST is under development to establish a zebrafish-based aggregation platform.

The signal of the CST is detectable not only in the cytoplasm but also in the nucleus, however, the FRET analysis in this compartment revealed that nuclear Tau conformation is probably more open and relaxed.

We investigated the nuclear function of Tau and we found that the increase in the soluble pool of Tau enhances its translocation into the nucleus and, concomitantly, the nuclear Tau alters the expression of VGluT1, a disease-relevant gene, indicating that Tau has a role in gene expression modulation. We observed that the increase in VGluT1 expression mediated by Tau causes neuronal hyperexcitability in hippocampal primary neurons, an event typical of the first stages of AD. We found that this Tau function is impaired by the P301L mutation and by pathological aggregation.

To identify other possible genes modulated by Tau we performed an RNAseq experiment and we found a global gene expression alteration that strongly resembles the late mild cognitive impairment. The investigation of molecular mechanisms involving nuclear Tau indicates that it competes with HDAC1 for the binding with TRIM28, a nuclear protein involved in heterochromatin formation. This competition causes the delocalization of HDAC1 from the nucleus modifying the chromatin structure and leading to VGluT1 increased levels, suggesting that Tau modulates the gene expression by altering the chromatin condensation.

In conclusion, the CST developed in this study allows to follow in real time the pathological process depicting the early and the late stages of aggregation; thus, it is now at the bases of two screening platforms for the drug discovery and validation in reporter cells and in a transgenic model. In addition, this study demonstrated for the first time that Tau in the nuclear compartment modulates the expression of genes probably by altering the chromatin structure and this role seems to be strongly related to mild cognitive impairment stages when Tau is destabilized and partially aggregated.

Index

Chapter 1

Introduction

1.1 Dementia

Dementia is a general term referring to several different neurodegenerative diseases characterized by mental dysfunctions. The urgency of resolving these pathologies is deeply felt since these diseases have a big impact on our society, with more than 50 million people affected worldwide (Prince et al., 2015). Among the most common dementias, tauopathies represent a conspicuous part. Tauopathies group multifactorial diseases which often differ for development and symptoms, but all of them are characterized by the alteration in structure and function of Tau protein.

1.2 Tau

Tau is a microtubule associated protein (MAP) discovered in 1975, when it was isolated from porcine brain and identified as a factor able to induce tubulin polymerization *in vitro* (Weingarten et al., 1975). Tau is mainly expressed in the central nervous system (CNS) but recently it was found also in other regions of the organism, heart, kidney, lung, testis, pancreas and in fibroblasts (Gu et al., 1996; Ingelson et al., 1996; Sergeant et al., 2005; Vanier et al., 1998). It was also discovered to be expressed in some cancers as breast cancer (Bonneau et al., 2015). Even if Tau can be found in different tissues and conditions, currently it is mainly studied because of its involvement in tauopathies since, in these pathologies, the protein forms toxic aggregates in neurons ultimately leading to dementia.

1.2.1 Gene

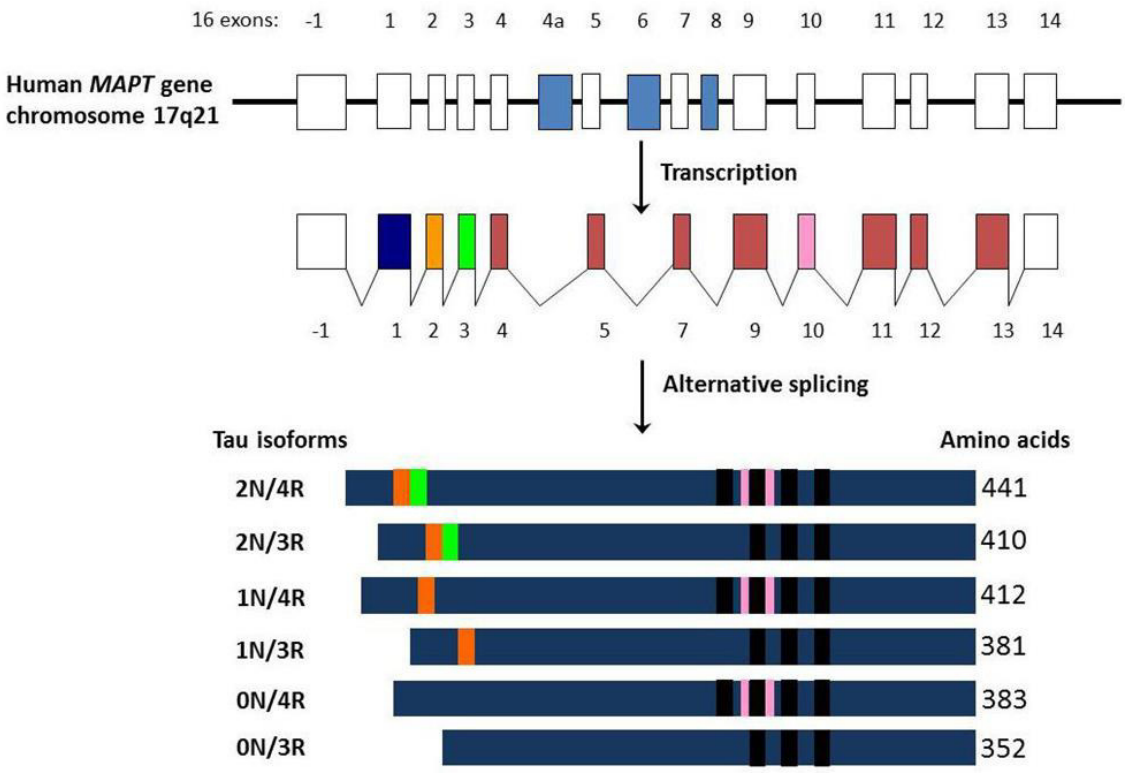

Figure 1.1: MAPT gene and splicing isoforms. Adapted from Luna-Munoz et al., 2013.

Tau protein is encoded by the microtubule associated protein Tau (MAPT) gene located on chromosome 17q21. MAPT contains 16 exons whose alternative splicing yields to six isoforms of the protein. Upstream of exon 1 there are consensus binding sites for transcription factors like AP2 and SP1 (Andreadis et al., 1992; Sadot et al., 1996). The alternative splicing involves exons E2, E3 and E10 leading to isoforms ranging from 352 to 441 aminoacids (Figure 1.1). Splicing of exons E2 or E3 generates isoforms carrying 2, 1 or none particular sequences at the N-terminal end of the protein, while the splicing of E10 determines the presence of a repeated aminoacidic sequence at the C-terminal end (Goedert and Jakes, 1990; Goedert et al., 1989b, 1989a). The expression of different Tau isoforms is specific of brain development. The shortest Tau isoform of 352aa, often referred as foetal Tau 0N3R (splicing of E2, E3 and E10), is characteristic of embryonal brain and is progressively lost during brain development. All the other isoforms are expressed in the adult brain but an additional isoform including E4a was also found to be specific of the peripheral nervous system (PNS) (Goedert et al., 1989a, 1992).

1.2.2 Protein

Tau protein is a hydrophilic polypeptide which appears as a random coiled protein (Cleveland et al., 1977; Hirokawa et al., 1988). It shows very small content in secondary structures (Mukrasch et al., 2009). When bound to microtubules (MTs) Tau shows a preference to assume a loop-like conformation in which the N- and the C-terminal ends are close (Jeganathan et al., 2006; Di Primio et al., 2017). Moreover, in pathological conditions, Tau assumes a β-sheet secondary structure which leads to formation of amyloidogenic aggregates (Daebel et al., 2012).

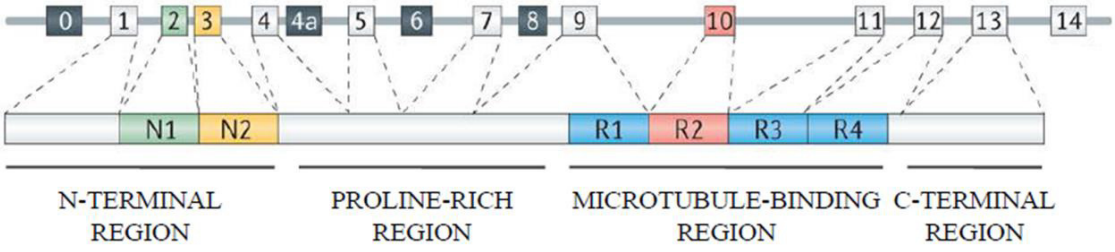

Figure 1.2: Tau protein domains. Adapted from Wang and Mandelkow, 2016.

Tau protein can be divided in two large domains: the projection domain and the microtubule binding domain. The projection domain contains the amino-terminal region (NTD) with high proportion of acidic residues and the proline-rich region (PRD); the microtubule-binding domain is subdivided into a basic true tubulin binding domain with three or four repeats (MTBD) and the acidic carboxy-terminal region (CTD) (Figure 1.2). The six Tau isoforms differ from each other for the presence of three or four microtubule-binding repeats of 31 or 32 residues (isoform 3R or 4R) and for the presence or absence of one or two inserts (29-amino acids) at the N-terminal portion of the protein (Avila et al., 2004; Binder et al., 1985). The projection domain plays several roles such as the determination of space between axonal microtubules, the interaction with other proteins and cation binding (Chen et al., 1992; Hirokawa et al., 1988). Motifs identified in this region include the KKKK sequence involved in heparin binding and the PPXXP/PXXP motifs in the proline-rich region for the binding of Tau with proteins containing SH3 domains such as the tyrosine kinase Fyn (Ittner et al., 2010; Lau et al., 2016; Mondragón-Rodríguez et al., 2012). The repeats of the microtubule-binding domain can be divided in two parts, one composed of 18 residues containing the

minimal region with microtubule binding capacity, while the second region composed of 13/14 residues is known as the inter repeat (Avila et al., 2004). Tau isoforms bind MTs by the MTBD with different affinity depending on the number of repeats: higher for Tau 4R isoforms, lower Tau 3R (Lu and Kosik, 2001).

1.3 Tau function and localization

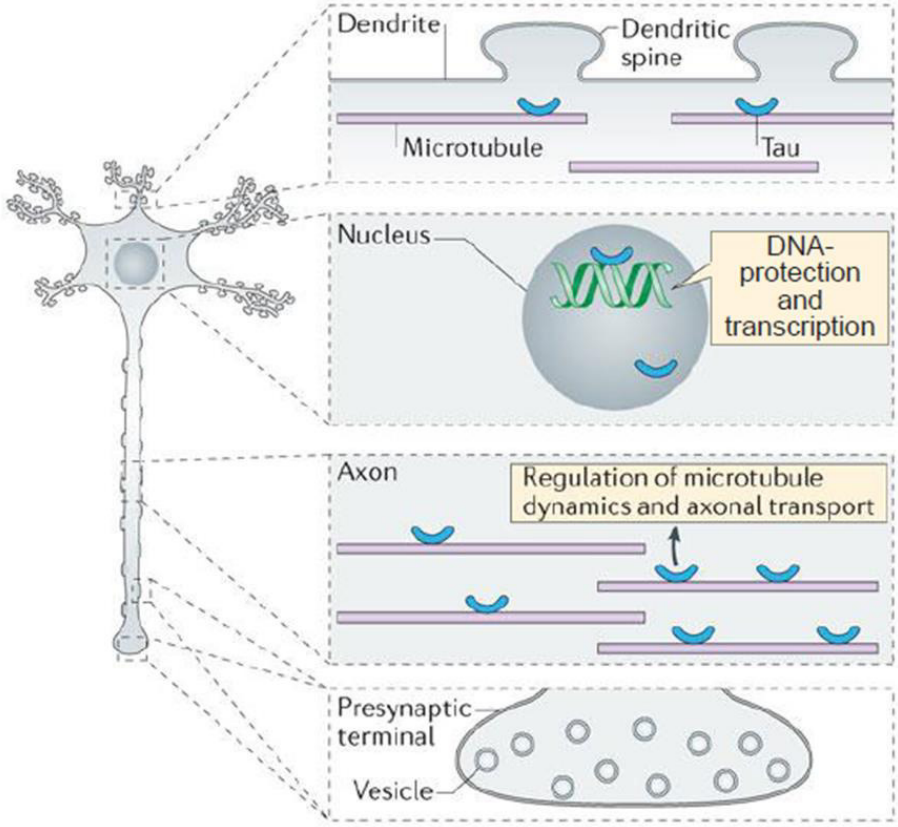

Figure 1.3: Tau subcellular localization and function. Adapted from Wang and Mandelkow, 2016.

Tau was originally found associated to MTs as a protein factor able to induce and stabilize the tubulin polymerization (Weingarten et al., 1975), however, in recent years other functions of Tau have been identified in several subcellular compartments (Figure 1.3). Tau is mostly located in axons, where it interacts with MTs stabilizing them and promoting their assembly (Weingarten et al., 1975). MTBD binds specific pockets in β-tubulin at the inner surface of the MTs while the proline-rich regions, positively charged, are bound to the negatively charged MT-surface; the acidic N-terminal domain branches away from the MT-surface probably because of electrostatic repulsion. Moreover, the β-tubulin pockets of adjacent filaments may be occupied by different repeats of the same MT-binding

domain causing crosslinking of three or four dimers (Amos, 2004; Kar et al., 2003). The projection domain determines spacing between MTs in the axon and may increase the axonal diameter. It interacts with other cytoskeletal components like spectrin and actin filaments allowing Tau-stabilized MTs to interconnect with neurofilaments restricting the flexibility of MTs lattices (Kolarova et al., 2012). Besides regulating MT assembly and stabilization, several evidences associate Tau with the regulation of axonal transport. Tau was seen to detach the cargoes from kinesin without influencing the speed of movement along MTs (Trinczek et al., 1999). *In vitro*, Tau is able to interfere with the dynamics of motor proteins and knock-down of Tau protein is able to increase transport velocity in iPSC-derived dopaminergic neurons (Beevers et al., 2017; Dixit et al., 2008). Moreover, in SHSY5Y cells, Tau is also able to bind p150 subunit of dynactin and to stabilize its binding to MTs, thereby promoting dynein transport (Dixit et al., 2008; Magnani et al., 2007).

Tau protein also localizes in dendrites (Figure 1.3). It has been proposed that it can be found in spines since in brain tissues Tau co-immunoprecipitates with PSD-95 (Ittner et al., 2010). Moreover, upon synaptic activation, Tau moves from the dendritic shaft to spines in cultured neurons and hippocampal slices (Frandemiche et al., 2014). At the synapse, Tau also interacts with Fyn, a tyrosine kinase from the Src-family involved in protein trafficking, by the proline-rich domain which binds SH3 domains of several proteins. Tau is necessary for Fyn localization at the post-synaptic compartment. There, Fyn phosphorylates NMDA subunit NR2B thereby stabilizing its interaction with PSD-95 (Ittner et al., 2010; Lau et al., 2016; Mondragón-Rodríguez et al., 2012). In addition, Tau has a role in signal transmission and synaptic plasticity. Tau reduction results in resistance to pathological network hyperexcitability in a variety of models (DeVos et al., 2013; Holth et al., 2013). It has also been demonstrated that Tau KO shows impaired LTP (Ahmed et al., 2014), but this finding is still debated. Tau is also localized at the axon terminal upon stimulation with NGF (Yu and Rasenick, 2006). Tau is able to potentiate NGF and EGF signalling thus increasing activation of the downstream pathway and influencing neurites extension (Leugers and Lee, 2010). Tau has also been described to have a role in other signalling pathways such as PLC pathway *in vitro* (Hwang et al., 1996). Post-

translational modifications seem to alter Tau distribution, for example phosphorylation in the proline-rich region localizes Tau protein mainly in the somatodendritic compartment, whereas, if the proline-rich region is dephosphorylated or if the phosphorylation occurs in the C-terminal domain, Tau localizes in the distal axonal region (Dotti et al., 1987; Mandell and Banker, 1996).

It has been recently discovered that Tau is involved in miRNA activity. As a matter of fact, Tau interacts with the DEAD box RNA helicase DDX6 involved in translation repression and mRNA decay as well as in the miRNA pathway. Tau/DDX6 interaction increases the silencing activity of the miRNA let-7a, miR-21 and miR-124 affecting the expression of their targets (Chauderlier et al., 2018). Tau has also been localized in many organelles where it can exert non-canonical functions such as ribosomes, mitochondria and endoplasmic reticulum (Tang et al., 2015). Moreover, Tau has been found in the nucleus where it is involved in several functions (Loomis et al., 1990).

1.3.1 Tau nuclear function

In 1990 Tau protein was identified in the nucleus of neuroblastoma cells and in 1995 its nuclear localization was confirmed in human brains. At the beginning, nuclear Tau was detected by immunofluorescence experiments which showed Tau labelling in the nucleus and nucleolus. This evidence was confirmed by subcellular fractionation of chromatin nuclear fraction (Loomis et al., 1990; Rady et al., 1995). The interaction between Tau and chromatin has been further investigated *in vitro* and *in vivo*. *In vitro* experiments demonstrated that the binding of Tau to DNA is mediated by the second half of the proline-rich domain and the R2 of the MTBD (Hua and He, 2003; Qi et al., 2015). Moreover, while hyperphosphorylation of Tau reduces the affinity to DNA, the hypophosphorylated Tau has a higher affinity (Qi et al., 2015).

Other studies clarified that Tau has higher affinity to specific DNA sequences determining also its preferential localization when bound to chromatin. Biophysical studies identified GC-rich sequences as more affine to Tau and demonstrated that the interaction stabilizes the DNA structure when altered by physical agents as high temperature (Vasudevaraju et al., 2012). Fluorescence in

situ hybridization (immune-FISH) in non-neuronal cells revealed that nuclear Tau binds AT-rich α-satellites and colocalizes with nucleolin, supporting the fact that nuclear Tau is localized in the internal periphery of nucleoli (Sjöberg et al., 2006). In addition, by a ChIP-on-chip experiment on primary neurons, it was recently demonstrated that Tau is highly enriched in intergenic chromatin regions even if it is also bound to promoter regions, with a high specificity for the GAGA motifs (Benhelli-Mokrani et al., 2018).

An open question in nuclear Tau field regards possible different functions of Tau isoforms and the effect of post-translational modifications in the nuclear compartment. In adult mice brains 1N Tau isoform is overrepresented in soluble nuclear fraction, while 2N Tau isoform is overrepresented in chromatin-bound fraction (Liu and Götz, 2013). Tau can be found either in a phosphorylated and non-phosphorylated state in the nucleus, probably depending on the sub-nuclear localization. In fact, nucleolar Tau appears to be mainly non-phosphorylated, while in the rest of the nucleoplasm, it can also be phosphorylated (Loomis et al., 1990; Sultan et al., 2011). Moreover, nuclear Tau phosphorylation at specific residues, such as the AT100 epitope, increases with aging, with higher affinity to heterochromatin, suggesting an epigenetic role for Tau (Gil et al., 2017).

One of the first evidence about the function of nuclear Tau was on DNA protection and stability. First *in vitro* experiments showed that Tau is able to increase the dsDNA melting temperature stabilizing its structure and protects DNA from oxidative stress induced by hydroxyl radicals (Hua and He, 2003). This result was further supported by Wei *et al.* demonstrating that Tau binds the minor groove of the double helix preventing damage by peroxidation (Wei et al., 2008). Recently *in vivo* results reported that non-phosphorylated nuclear Tau levels increase in neurons after oxidative stress and hyperthermic conditions which should induce the formation of ROS. By Comet and TUNEL assays and γH2AX immunofluorescence detection in these conditions, it has been observed that Tau protects the genome of cortical and hippocampal neurons from damage. Moreover, it seems that Tau also protects RNA molecules in cytoplasmic and nuclear compartments (Sultan et al., 2011; Violet et al., 2014). Intriguingly expression of mutated Tau in residues related to tauopathies is strongly associated to chromosome aberrant recombination and aneuploidy in mouse and

human samples, supporting the key role of nuclear Tau in genome stability (Rossi et al., 2008, 2013, 2014).

Tau is also involved in chromatin remodelling and gene expression regulation even if the mechanisms are still unclear. A first observation in Tau knock-out mouse models revealed the altered expression of several genes, intriguingly some of them regulates themselves (Gómez de Barreda et al., 2010; Oyama et al., 2004). Increase in nuclear Tau levels is able to induce global chromatin relaxation in Tau overexpressing drosophila and mice, indicating Tau as a factor responsible for the loss of heterochromatin in AD human brains. These alterations result in an increased transcription of genes that are heterochromatically silenced in controls. This observation was shown to be disease relevant since heterochromatin restoration in Drosophila is able to recover the locomotor impairments shown in Tau overexpressing individuals (Frost et al., 2014). More recently, it has been demonstrated that increased Tau levels induce transcription of transposable elements in Drosophila brains and in human AD and PSP brains. Dysregulation of transposable elements is due to both the loss of heterochromatin and the reduction in piwi elements which prevents transposon expression and genomic integration (Guo et al., 2018; Sun et al., 2018). Moreover, it has been demonstrated that Tau not only reduces heterochromatin but it has also a repressive role. As a matter of fact, Tau interacts with TIP5, a transcriptional repressor of rDNA, in the nucleolus and Tau depletion results in an increase of 45S-prerRNA synthesis, suggesting that Tau might be involved in rDNA silencing (Maina et al., 2018). In addition, by ChIP-on-chip experiments, a transcriptional repressive function has been observed towards promoters bound directly by Tau (Benhelli-Mokrani et al., 2018). Other studies support the possible role of Tau in chromatin remodelling. A recent work demonstrated that Tau interacts with the nuclear protein TRIM28 which is able to shuttle it to the nucleus. This was shown tracking the Tau-TRIM28 complex exploiting bimolecular fluorescence complementation and was confirmed observing that TRIM28 overexpression was able to boost Tau shuttling to the nucleus (Rousseaux et al., 2016). Tripartite motif-containing 28 (TRIM28), also known as transcriptional intermediary factor 1b (TIF1b) and KAP1 (KRAB-associated protein-1), is a nuclear protein mainly involved in transcriptional

regulation and chromatin remodelling. TRIM28 acts as a co-repressor of KRAB zinc finger proteins, moreover it interacts with histone deacetylase complexes and methyl transferases (Iyengar and Farnham, 2011). Since Tau is strongly associated to chromatin remodelling and it interacts with TRIM28, it would be interesting to further investigate the nature of this interaction to find out whether TRIM28 or one of its interactors could mediate nuclear Tau functions.

1.4 Tau pathology

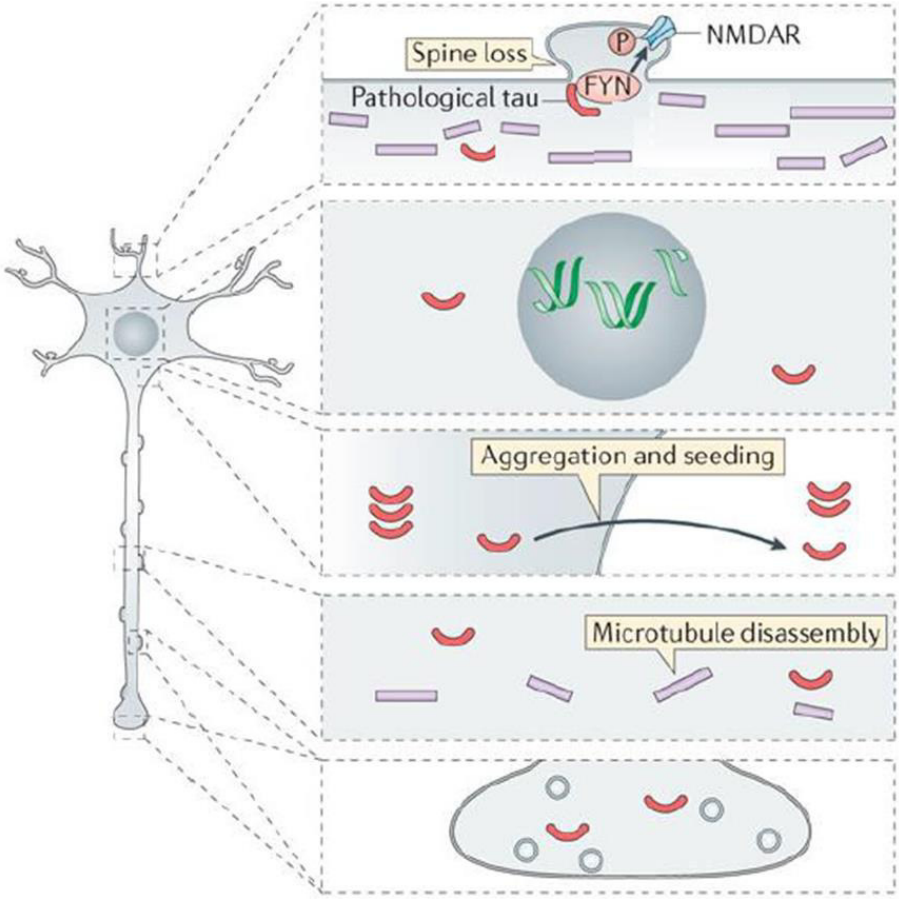

Figure 1.4: Tau pathological changes in subcellular compartments. Adapted from Wang and Mandelkow, 2016.

As stated above, Tau protein is a key player in a group of neurodegenerative diseases named tauopathies and among these Alzheimer's disease is one of the most common and studied. Tauopathies can differ for the progression and symptoms, but all these diseases show a common hallmark that is the pathological destabilization and aggregation of Tau protein. Tauopathies include Alzheimer's disease (AD), Frontotemporal dementia with parkinsonism-17

(FTDP-17), Pick disease (PiD), progressive supranuclear palsy (PSP), corticobasal degeneration (CBD), agyrophilic grain disease (AGD) and Huntington disease (HD), and most of them show both familiar and sporadic forms (Lee et al., 2001). In the first steps of these pathologies, whose mechanisms are still not clear, MTs-bound Tau is post-translationally modified. These modifications lead to Tau displacement from MTs with its increase in the cytoplasmic pool. Post-translational modifications change Tau molecular properties and structure causing the association of Tau monomers into oligomers and then in amyloidogenic aggregates. The molecular mechanisms inducing the toxic effect of Tau aggregation are still debated even if it is strongly supported that the aggregation causes cellular stress and damage to neuronal and non-neuronal cells.

1.4.1 Tau mutations

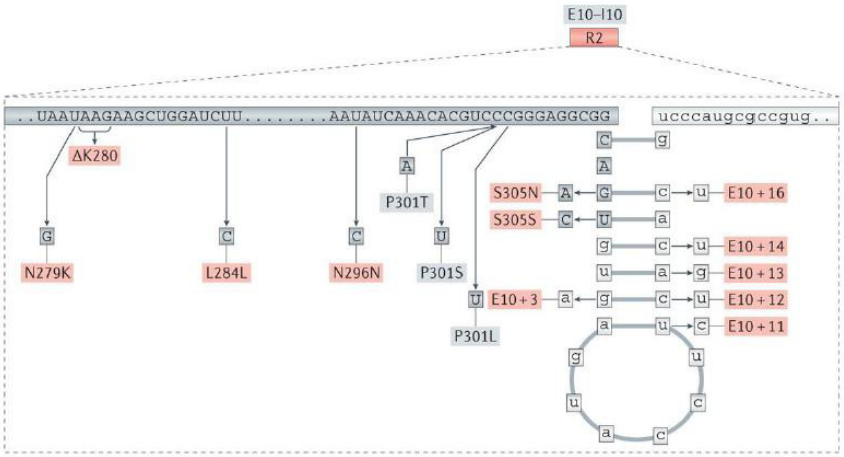

Figure 1.5: Localization of the main MAPT mutations. Adapted from Wang and Mandelkow, 2016

The processes involved in the pathogenesis of tauopathies are still unclear. These diseases can be sporadic or familial and genetic analyses of Tau in patients with familial tauopathies demonstrated that specific mutations are associated to the insurgency of Tau destabilization and Tau failure. Familial tauopathies like FTDP-17 can be caused by several intronic and exonic mutations in MAPT gene such as Δ280K, P301L, P301S and E10+3 (Figure 1.5) (Bugiani et al., 1999; Hutton et al., 1998; Rizzu et al., 1999; Spillantini et al., 1998a). Several studies show that these mutations can induce Tau alterations, making it more prone to destabilization and aggregation. Exonic missense or

deletion mutations destabilize Tau binding to MTs and decrease the ability to induce MT assembly (Goedert et al., 1999). Intronic mutations can affect alternative splicing of E10 thus increasing 4R Tau as observed in patients' brains (Spillantini et al., 1998a). The discovery of mutations altering MAPT splicing suggests that disruption of 3R:4R ratio is sufficient to cause neurodegeneration and dementia, conversely maintaining the physiological 3R:4R ratio appears to be crucial for normal brain functions. The mechanisms around the dementia caused by isoform imbalance is still obscure, but it is hypothesized that it could somehow interfere with Tau binding to MTs thus increasing Tau soluble pool (Liu and Gong, 2008).

An inversion polymorphism arising about 3 million years ago of approximately 900kb on chromosome 17q21 generated two haplotypes, H1 and H2 encompassing MAPT locus (Stefansson et al., 2005). Genome association analyses showed that H1 haplotype is associated with increased risk for PSP and CBD (Baker et al., 1999; Di Maria et al., 2000). In time, variations of each haplotype generated sub-haplotypes which differentially influence the insurgency of tauopathies. For example, the H1c sub-haplotype has been associated with increased risk for PSP and AD (Baker et al., 1999; Myers et al., 2005). In order to explain the pathogenic mechanisms of these haplotypes it has been hypothesized that they can affect Tau expression or Tau splicing. As a matter of fact, reporter genes under H2 promoter show a reduction in transcriptional activity compared to the H1 promoter (Kwok et al., 2004). Moreover, H1/H2 heterozygous neuroblastoma cell line models and human brains indicate that the H1 chromosome induce a significantly higher expression of transcripts including E10 (Caffrey et al., 2006).

Since Tau mutations are strongly associated to Tau pathological behaviour, they are experimentally employed to induce, both in a cellular context and *in vivo*, Tau destabilization and aggregation since wild-type Tau is not able to aggregate spontaneously. In particular, mouse models expressing mutated Tau are largely used to clarify the neurotoxic mechanisms mediated by Tau aggregation and to simulate the progression of tauopathies even if a "perfect" model able to represent all the characteristics of a specific tauopathy is not available yet

(Bondulich et al., 2016; Eckermann et al., 2007; Kremer et al., 2011; Lewis et al., 2000; Schindowski et al., 2006; Yoshiyama et al., 2007).

Intriguingly, mutations in Tau protein seem not only to affect Tau interaction with tubulin leading to aggregation as canonically described (Goedert et al., 1999). Recent studies showed that pathological mutations, along with genomic instability and neuronal damage, cause also an increased probability of tumorigenesis suggesting a role for Tau also in other tissues of the organism (Rossi et al., 2008, 2013, 2014, 2018). Moreover, the P301S mutation associated to FTDP and PiD affects the interaction with DDX6, resulting in an impairment of miRNAs silencing activity (Chauderlier et al., 2018).

1.4.2 Tau post-translational modifications

As described above, Tau protein is exposed to several post-translational modifications that influence both its physiological and pathological behaviour. In particular, it is commonly assumed that Tau modifications, above all hyperphosphorylation and cleavage, are the first events leading to aggregation (Pevalova et al., 2006; Wang and Mandelkow, 2016).

Phosphorylation:

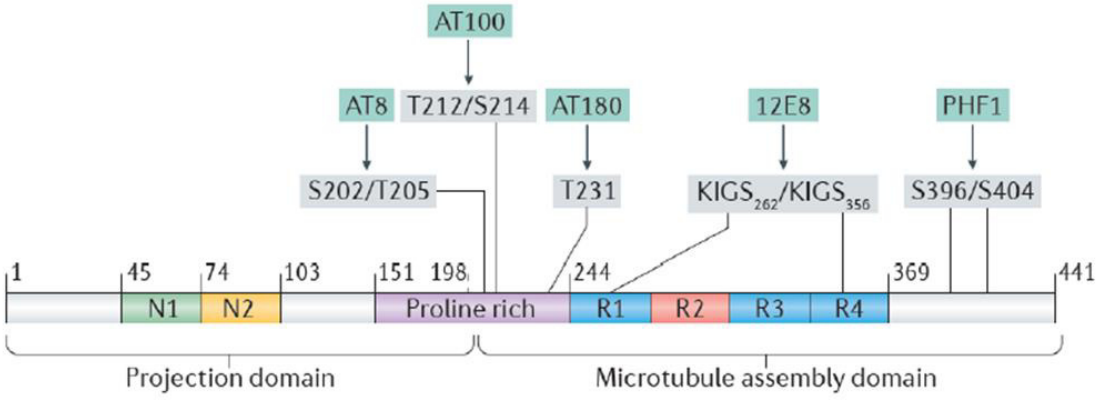

Figure 1.6: Relevant Tau phosphorylation residues. Adapted from Wang and Mandelkow, 2016.

Phosphorylation is the most characterized post-translational modification of Tau. 79 putative serine and threonine phosphorylation sites have been identified. During embryonic development it has been demonstrated that Tau protein is much more phosphorylated than in post-natal period. Tau physiological

phosphorylation seems to control MT dynamics during normal neurite growth and maturation. In tauopathies Tau becomes hyperphosphorylated leading to the formation of amyloidogenic aggregates. Moreover, in recent years, changes in body temperature have been demonstrated to be environmental factors able to alter Tau phosphorylation leading to a predisposition in developing tauopathies (Bretteville et al., 2012; Planel et al., 2004; Tournissac et al., 2019; Vandal et al., 2016; Whittington et al., 2013). By mass spectrometry and antibody detection experiments all six Tau isoforms have been identified in aggregates and have been demonstrated to be phosphorylated at 40 different residues (Avila et al., 2004; Pevalova et al., 2006).

Among critical sites involved in Tau aberrant activity implicated in AD and in other tauopathies, AT8 epitope (Ser199/Ser202/Thr205) has an important role. The phosphorylation of these three residues is sufficient to cause MTs remodelling and instability, diminished mitochondrial transport, cell death and neurodegeneration (Shahpasand et al., 2012). A similar effect is observed by phosphorylation of residues Thr212/Thr231/Ser262 (Alonso et al., 2010). *In vitro* kinetic studies of the binding of unphosphorylated and hyperphosphorylated Tau to tubulin suggest that Ser199/Ser202/Thr205, Thr212, Thr231/Ser235, Ser262/Ser356, and Ser422 are among the critical phosphorylation sites that convert Tau to pathological molecule that sequesters normal microtubule-associated proteins from MTs (Figure 1.6) (Abraha et al., 2000; Alonso et al., 2004; Gong et al., 2005; Haase et al., 2004; Sengupta et al., 1998). The phosphorylation of these residues depends on the activity of both kinases and phosphatases, whose equilibrium plays a key role in Tau pathology.

Kinases:

GSK3β

Glycogen synthase kinase-3 (GSK3β) is expressed ubiquitously but it can be found at high levels in the brain where it localizes predominantly in neurons. It belongs to the PDPK class (proline directed protein kinases), and is a serine/threonine-specific kinase. GSK3β influences Tau behaviour both in physiological and pathological conditions (Pei et al., 1997; Pevalova et al., 2006). Brains of AD patients show a higher immunoreactivity against GSK3β than

control brains, with the kinase predominantly colocalizing with NFTs (Pei et al., 1997). Among the residues phosphorylated by GSK3β, Thr231 has been observed to be strongly related to the beginning of AD. This epitope is an example of primed phosphorylation because it occurs after Ser235 phosphorylation. The modification of Thr231 causes a conformational change in Tau affecting its stability and affinity to MTs (Cho and Johnson, 2003; Daly et al., 2000). Preclinical studies employing GSK3β inhibitors revealed that the block of kinase activity decreases aggregation and protects against axonal degeneration in Tau^{P301L} mice (Noble et al., 2005).

Cdk5

Cyclin-dependent kinase 5 (Cdk5) is a serine/threonine kinase of the PDPK class. It contributes to phosphorylation of human Tau on Ser202, Ser205, Thr212, Thr217, Ser235, Ser396 and Ser404, epitopes phosphorylated in AD brains. Cdk5 interacts with p35 to exacerbate its function. It has been seen that the conversion of p35 in p25 due to pathological conditions causes prolonged activation and mislocalization of Cdk5 and hyperphosphorylation of Tau (Cruz et al., 2003; Lee et al., 2000; Maccioni et al., 2001; Tsai et al., 2004). The knockdown of Cdk5 in AD mouse models strongly decreases the number of neurofibrillary tangles in the hippocampus (Piedrahita et al., 2010).

ERK1/2

Extracellular signal-regulated kinases isoforms 1 and 2 (ERK1/2) belong to the PDPK class of kinases. Analysis on post-mortem AD brains showed that they predominantly colocalize with NFTs (Perry et al., 1999). Consistently, the administration of an ERK2 inhibitor was able to reduce the levels of abnormally phosphorylated Tau and to rescue motor deficits in a mouse model of tauopathy (Le Corre et al., 2006).

JNK

C-Jun amino-terminal kinase (JNK) belongs to the PDPK group of kinases. JNK is able to hyperphosphorylate Tau, moreover immunohistochemical analysis of phopho-JNK showed increased activation of the kinase in the hippocampi of AD patients (Zhu et al., 2001).

Other kinases

Other kinases have an important role in the pathogenesis of tauopathies. PKA is a ubiquitous serine/threonine kinase activated by cAMP. It phosphorylates Tau at Ser214, Ser217, Ser262, Ser396/404 and at Ser416 (Andorfer and Davies, 2000; Carlyle et al., 2014; Zheng-Fischhöfer et al., 1998). CaMKII too seems an important factor inducing Tau aberrant hyperphosphorlation. The function of this kinase is to regulate important neuronal functions including neurotransmitter synthesis and release, modulation of ion channel activity, synaptic plasticity and gene expression. The kinase phosphorylates Tau at Ser262, Ser356, Ser409 and Ser416 that are phosphorylated in brains of AD patients. The phosphorylation of all these residues by PKA and CamKII is strongly associated to Tau pathology since this mechanism influences Tau binding on MTs, cleavage and aggregation (Andorfer and Davies, 2000; Carlyle et al., 2014; Singh et al., 1996; Steiner et al., 1990; Zheng-Fischhöfer et al., 1998).

Phosphatases

Several studies have shown that three major protein phosphatases, PP5, PP2B and PP2A, can dephosphorylate Tau protein. PP2B influences the dynamics of MTs and microfilaments. PP5 is associated with MTs and dephosphorylates Tau in the neuronal cytoplasm. PP2A is localized on MTs and can dephosphorylate Tau by direct interaction or indirectly, regulating the activity of several Tau kinases (Liu et al., 2005; Pevalova et al., 2006). The inhibition or the absence of these phosphatases in cells cause the hyperphosphorylation of Tau suggesting a possible role of these proteins during tauopathy development. Remarkably, in AD brains the impaired activity of PP2A has been observed (Gong et al., 1993).

Other Tau post-translational modifications

Tau undergoes several other post-translational modifications which could influence its functions such as acetylation, glycation, glycosylation and truncation.

As to post-translational modifications, studies on the composition of aggregates revealed that Tau is cleaved at different sites. Tau truncation is characterized by a progressive cleavage of the protein in specific residues which leads to smaller

and smaller fragments prone to aggregation (Gamblin et al., 2003; Guillozet-Bongaarts et al., 2005; Novak et al., 1993; Rissman et al., 2004). Several enzymes have been identified as able to cleave Tau such as caspases but also calpains, thrombin, cathepsins and the aminopeptidase PSA. In particular, in tauopathies, these enzymes are deregulated and target Tau protein inducing and enhancing its destabilization and aggregation (Arai et al., 2006; Cataldo et al., 1997; Nakanishi et al., 1997; Rao et al., 2008; Saito et al., 1993). The study of the progressive Tau cleavage revealed that some residues are cut in early stages of tauopathies and other in late stages. A caspase-cleaved Tau species, cleaved at Asp421, was identified in NFTs (Gamblin et al., 2003). Tau conformational studies suggest that this cleavage is an early event in the pathogenesis of AD (Guillozet-Bongaarts et al., 2005; Rissman et al., 2004). Intriguingly, caspase cleavage at Asp421 can be inhibited by phosphorylation at Ser422 suggesting that some phosphorylations are protective (Guillozet-Bongaarts et al., 2006). Truncated Tau at Glu391 is found in NFTs in tauopathy brains and it is associated to a late stage of the disease. In Tau aggregates a 12KDa fragment from His268 to Glu391containing the MTBD has been identified, and it is referred to as the PHF-core (Novak et al., 1993). Further experiments showed that phosphorylation and truncation work synergically and together they influence Tau aggregation. As a matter of fact, in cells with or without GSK3β, transfected Tau fragment aggregates only in presence of the kinase (Cho and Johnson, 2004).

Another post-translational modification whose importance is becoming relevant is lysine acetylation, which has been revealed to affect Tau properties. This modification neutralizes charges in the MT-binding domain interfering with Tau binding to MTs. Moreover, acetylation of Lys280 increases cytosolic Tau fraction and it's correlated with Tau hyperphosphorylation. It is present mostly in intracellular NFTs rather than in pre-tangles or extracellular aggregates and it precedes Tau truncation (Cohen et al., 2011; Irwin et al., 2012).

Glycosylation is the covalent bonding of sugars to the side chain of a polypeptide which can occur at the amine group of an asparagine (N-glycosylation) or at the hydroxyl radical of serine or threonine (O-glycosylation). These modifications seem to have opposite effect, as O-glycosylation is decreased in AD brain, while N-glycosylation is increased (Wang et al., 1996). Phosphorylation and O-

glycosylation target the same residues, suggesting a mutually exclusive competition. As a matter of fact, in AD patients, a negative correlation has been reported between O-glycosylation level and Tau phosphorylation (Liu et al., 2009). However, it has been reported that the biological effect at each phosphorylation site is different (Gong et al., 2005). Moreover, deglycosylation of PHFs converts them in bundles of straight filaments and successive dephosphorylation results in the release of Tau monomers (Wang et al., 1996).

Oxidation too seems to increase aggregation of monomeric Tau protein because it produces disulphide cross-linking between cysteine residues. Isoforms of Tau containing three repeats (3R) have only one cysteine residue in the MTs binding domain with respect to 4R isoforms which have two cysteines. For this reason, 3R Tau is more prone to aggregate rather than 4R isoform which may form intramolecular disulphide bonds (Barghorn and Mandelkow, 2002).

Other modifications are still under investigation, even if they seem to be related to late stages of Tau pathology. In PHFs and NFTs Tau is also ubiquitinated with the covalent bonding of the 76aa protein ubiquitin. Also glycation, the non-enzymatic linkage between a reducing sugar and the amino side chain of polypeptide, can be identified in PHFs isolated from AD brains while it's not present in normal Tau (Münch et al., 2002; Yan et al., 1995).

1.4.3 Tau aggregation

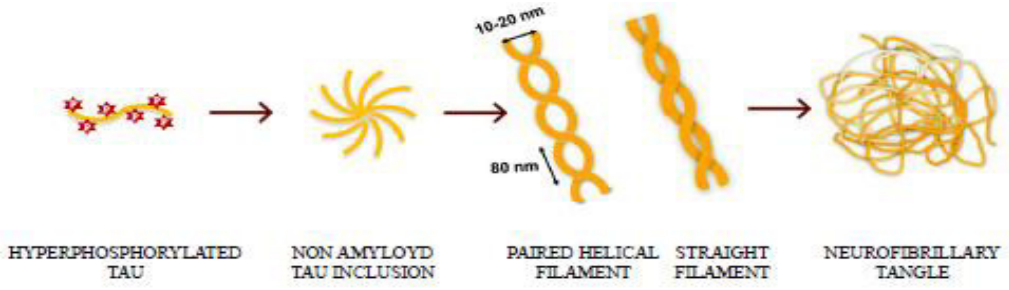

Figure 1.8: Tau aggregation process from monomers to neurofibrillary tangles.

Tau molecule has long stretches of positively and negatively charged regions which don't allow intermolecular hydrophobic association. The β-structure, typical of amyloidogenic proteins, is present in repeated regions, in particular in R2 and R3, which can assemble by their own in filaments (von Bergen et al., 2000). Self-aggregation is inhibited by the presence of intact N- and C-terminal domains but

when Tau undergoes post-translational modifications, the conformational structure changes exposing the sticky repeat regions which lead to formation of aggregates (Alonso et al., 2001). Even if Tau aggregation is a common event of all tauopathies, fibrils isoform composition differs between tauopathies. In AD tangles include both 3R and 4R Tau (Sergeant et al., 1997), in PiD they are mainly made up of 3R (Delacourte et al., 1996) and in PSP, CBD, AGD and FTDP-17 they predominately comprise 4R Tau (Arai et al., 2001; Buée-Scherrer et al., 1996; Togo et al., 2002).

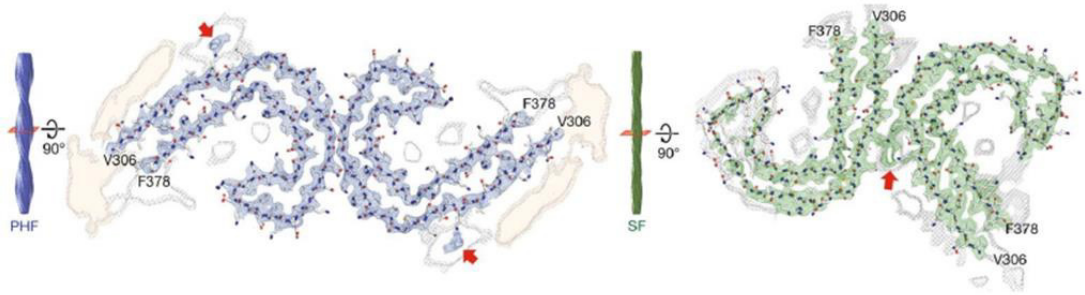

Figure 1.7: PHFs and SFs ultrastructure level. Adapted from Fitzpatrick et al., 2017.

The aggregation process seems to involve several steps. At the beginning, small Tau inclusions with low content in β-sheet structures are formed in a process called nucleation; after that other Tau molecules associate to this core to form paired helical filaments (PHFs) and straight filaments (SFs). Finally, PHFs further self-assemble to form neurofibrillary tangles (NFTs). The formation of Tau fibrils can be experimentally induced by the addition of preformed aggregates which mimic the nucleation step in a process named seeding. It has been demonstrated that the administration of small Tau assemblies in the extracellular medium can induce prion-like homotypic-seeding both *in vivo* and *in vitro* (Clavaguera et al., 2009; Frost et al., 2009). The smallest assembly having these seeding properties is Tau trimer (Mirbaha et al., 2015). Remarkably, in recent papers it has been demonstrated that Tau monomers isolated from tauopathy brains are able to induce Tau aggregation that is specific for the tauopathy the monomer is obtained from. This result opens to new insights suggesting that the monomer possesses peculiar pathological characteristics specific for each tauopathy independently from the oligomerization (Mirbaha et al., 2018; Sharma et al., 2018). It is thought that this occurs because nucleation is the limiting step in Tau

aggregation and if preformed aggregates are administrated, this step can be skipped. Electron-microscopy experiments showed that NFTs consists mainly of 10 – 20 nm PHF (KIDD, 1963) and of 15 – 18 nm straight filaments (SF) (Yagishita et al., 1981). PHFs and SFs also differ at ultrastructure level as both of them consist in two protofilaments with C-shaped subunits but with different symmetry. The N- and C-terminal ends protrude from the core of the aggregate forming the fuzzy coat (Fitzpatrick et al., 2017).

It has been demonstrated that in patients the number of NFTs correlates with the level of cognitive impairment. For this reason, it has been hypothesized that NFTs are toxic for the cell (Arriagada et al., 1992). In tauopathies, Tau is ineffective to keep the cytoskeleton organized in axonal processes because its affinity to tubulin is reduced. This loss of function is due to conformational changes and misfolding which lead to aberrant aggregation in fibrillary toxic structures inside neurons. Tau is redistributed in the somato-dendritic compartment and in isolated processes of affected neurons (Kolarova et al., 2012). The destabilization of MTs affects axonal trafficking in particular the plus-end-directed transport by kinesin (Ebneth et al., 1998). Inhibition of transport slows down exocytosis and the localization of organelles; the absence of these mechanisms causes a decrease in glucose and lipid metabolism, ATP synthesis and a loss of Ca^{2+} homeostasis which lead to a distal degeneration process (Futerman and Banker, 1996; Trojanowski and Lee, 1995). It has been seen that aberrant Tau not only can create aggregates sequestering normal Tau but it can also remove from MTs the two other major neuronal MAPs, MAP1 and 2 (Alonso et al., 1997).

1.4.4 Other mechanisms of cellular toxicity mediated by Tau

Increasing evidences show that NFTs are not the only toxic Tau species in tauopathies, in fact, in AD brains neuronal loss may exceed Tau aggregation (Gómez-Isla et al., 1997). Other pathological mechanisms can be involved in the neurotoxicity mediated by Tau. Dendritic Tau seems to mediate Aβ-induced neurotoxicity in AD since, in absence of Tau protein, Aβ-mediated LTP impairment is prevented (Shipton et al., 2011). Moreover, as already described, dendritic Tau is necessary for Fyn localization and scaffolding at the post-

synaptic compartment. There, Fyn phosphorylates NMDA subunit NR2B thereby stabilizing its interaction with PSD95. Under disease conditions, redistribution of Tau from the axon into the somatodendritic compartment is thought to increase Tau-dependent sorting of Fyn to dendrites, leading to toxic hyperexcitability caused by NMDA receptors. Indeed, the loss of Tau can prevent postsynaptic targeting of Fyn, and as a consequence NMDA-dependent excitotoxicity and memory impairment (Ittner et al., 2010; Lau et al., 2016; Mondragón-Rodríguez et al., 2012). Therefore, Fyn is important to potentiate glutamatergic signalling and it could mediate excitotoxicity in tauopathies. As described above, *in vivo* studies showed that the increase of Tau in the nucleus is associated to global chromatin relaxation resulting in alteration of gene expression. Intriguingly, chromatin relaxation has been shown to be neurotoxic (Frost et al., 2014). Moreover, Tau loss of function induced by mRNA knock down results in an increase of 45S-pre-rRNA synthesis in SHSY5Y (Maina et al., 2018). Other evidences suggested that oligomeric nuclear Tau has a more efficient repressive role than monomeric Tau in mouse models, supporting a global gene expression alteration that can affect neuronal homeostasis (Benhelli-Mokrani et al., 2018). Aberrant Tau influences also miRNA activity, as a matter of fact mutated Tau is less efficient in modulating the activity of miRNA let-7a (Chauderlier et al., 2018). All these evidences strongly support that in tauopathies, Tau is able to induce cellular toxicity since it alters several mechanisms crucial for the correct functioning of the cell.

1.4.5 Tau secretion and spreading

In pathological conditions, Tau aggregation starts in specific areas of the brain and during the pathology progression, Tau inclusions can be found also in other regions indicating a diffusion of amyloidogenic Tau. Its spreading occurs with a standard pattern with close or connected brain areas being affected one after the other (Braak et al., 2006). The mechanisms behind Tau spreading are still under investigation. Tau aggregates were found first intracellularly and the protein detected in the extracellular space was considered as a release from dead cells. On the contrary, further studies reported that Tau is secreted by different neuronal and non-neuronal cell types, associated to exosomes or other membrane vesicles (Kim et al., 2010; Medina and Avila, 2014; Shi et al., 2012). It was also observed that pathological post-translational Tau modifications enhance

its secretion suggesting that the release mechanism is linked to the progression of Tau pathology (Plouffe et al., 2012). Several mechanisms for the uptake have been proposed such as internalization of soluble Tau via receptor-mediated endocytosis, dynamin-driven endocytosis of soluble Tau aggregates or even proteoglycan-mediated macropynocytosis (Medina and Avila, 2014). Spreading could also occur trans-synaptically or via diffusion (Wang and Mandelkow, 2016).

1.5 Molecular tools to investigate Tau by imaging

Due to the key role of Tau in several neurodegenerative diseases, it is crucial to develop molecular tools providing a clear and simple interpretation of the state of Tau protein. These tools can be extremely useful for diagnosis or to screen molecules targeting pathological Tau.

The main approaches to study Tau aggregation rely on biosensors and amyloid binding dyes. Tau biosensors are chimeric proteins containing fluorophores that provide information about the molecular state of Tau. The advantage of fluorophores is that they can be genetically controlled (Kaláb and Soderholm, 2010). An intermolecular sensor that relies on bimolecular fluorescence complementation (BiFC) has been developed. Tau proteins are fused to non-fluorescent N- or C-terminal fragments of V-YFP and when two Tau molecules interact, the fluorophore is reconstituted and the protein fluoresces providing an output for Tau aggregation (Tak et al., 2013). An intermolecular FRET biosensor developed by Kfoury *et al*. is commonly used in laboratories that investigate Tau aggregation. Tau fragments, prone to aggregate, are fused to either YFP or CFP and when two Tau molecules interact, a FRET positive signal is observed. The strong advantage of this biosensor is that it detects Tau aggregation by fluorescence imaging but it is also optimized for FRET cytofluorimetry (Kfoury et al., 2012). Finally, in our laboratory we developed an intramolecular FRET biosensor that will be described later (Di Primio et al., 2017).

Another method to visualize Tau aggregation is the employment of dyes such as Thioflavin T, Thiazin Red and K114. These compounds have high affinity to β-sheet structures typical of amyloidogenic aggregates and can be used in cellular cultures or tissues with the limitation that they need to be fixed by fixation methods. Amyloid binding dyes emits a fluorescence signal when bound to Tau

aggregates which allows to study aggregation dynamics by imaging techniques (Crystal et al., 2003; Luna-Muñoz et al., 2008; Santa-María et al., 2006).

A novel approach is the employment in pre-clinical and clinical studies of molecules for PET imaging. The interest for PET compounds is due to the possibility to accurately and specifically target Tau deposits *in vivo* in patients' brains. The advances of molecular imaging in recent years provided promising Tau-specific tracers such as THK5317, THK5351, AV-1451, and PBB3. The employment of these tracers guarantees the investigation in real-time of Tau deposition patterns *in vivo* for different pathologies, discriminating between neurodegenerative diseases, including different tauopathies, and monitoring disease progression. In AD, the topographical distribution of tracers follows the known distribution of NTFs and is closely associated with neurodegeneration (Okamura et al., 2018; Saint-Aubert et al., 2017).

1.6 Tauopathy animal models

In order to investigate the behaviour of Tau in physiology and, above all, in pathology, several animal models based on the expression of human Tau have been generated. The main model employed for Tau studies is mouse but also *D. rerio* and *Drosophila* are commonly used. The advantage of using animals is obviously that the biological context is complex and closer to human, guaranteeing a higher reliability compared to the *in vitro* conditions. However, the main counterpart is that these models does not develop tauopathies and they need to be genetically modified with Tau molecules prone to pathological aggregation.

Several mouse models have been developed in the last 20 years and most of them are transgenic mice expressing mutated human Tau. The employment of Tau isoforms mutated in specific residues enhances the pathological behaviour of Tau, indeed, in these models Tau is unstable on MTs and forms toxic aggregates spontaneously. Each mouse usually expresses a specific mutation such as Tau^{P301L}, Tau^{P301S} or $Tau^{\Delta K280}$ and all of them lead to aggregation of Tau even if there are differences in the progression and spreading (Allen et al., 2002; Eckermann et al., 2007; Lewis et al., 2000; Terwel et al., 2005; Yoshiyama et al., 2007). Mouse models for Tau pathology can be divided into two groups: the first

resembles pure tauopathies expressing mutated Tau or Tau fragments, the second combines the Tau pathology with the Aβ pathology, a condition resembling Alzheimer's disease. However, tauopathy models share common aspects of pathology development. The expression of mutated Tau causes a progressive neurodegeneration with formation of neurofibrillary tangles around the 6th month (Allen et al., 2002; Lewis et al., 2000; Terwel et al., 2005; Yoshiyama et al., 2007) but there are cases of late aggregation as for Tau$^{\Delta K280}$ model which shows mature tangles only after 24 months (Eckermann et al., 2007). Other models are based on the expression of a Tau fragment which is prone to form intracellular inclusions. In these animals spontaneous aggregation occurs at 9-10 months and progresses with age (Bondulich et al., 2016; Filipcik et al., 2012). All these models show strong neuronal damage worsening with the progression of Tau toxic aggregation. As a matter of fact, common features are the synaptic loss, neuronal death and cognitive deficits which become more severe with aggregation. In some cases also gliosis can be detected suggesting that the neurodegeneration gives rise to an inflammatory process. The main brain areas affected by aggregation and neuronal loss are the spinal cord, cortical areas, amygdala, hippocampus with a spreading which increases with the development of the tauopathy (Allen et al., 2002; Boekhoorn et al., 2006; Bondulich et al., 2016; Filipcik et al., 2012; Van der Jeugd et al., 2011; Kremer et al., 2011; Lewis et al., 2000; Terwel et al., 2005; Yoshiyama et al., 2007). Mutated Tau is also employed for the development of AD mouse models expressing human APP^{SWE} as well. Remarkably, in these animals the presence of both toxic proteins causes a severe Tau and Aβ aggregation suggesting that there is a cooperative effect in the formation of toxic aggregates. Moreover, neuronal and synaptic loss are present and coupled with gliosis. Intriguingly, the brain areas first involved in these processes are slightly different. Indeed, the hippocampus and cortical areas show pathological aggregation followed by spreading in other regions (Lewis et al., 2001; Oddo et al., 2003; Schindowski et al., 2006). Even if a lot of models have been developed and characterized, there is still the lack of a "perfect" model mimicking all the aspects of tauopathies. However, the employment of these animals has been valuable to study pathological mechanisms with cognitive readouts and to test treatments impairing or enhancing Tau toxicity.

Even if the mammalian animal model is the most employed, the long experimental time required to develop the disease, the difficulties in handling and the failure of therapies efficient in human patients induced the scientific community to explore alternative models for specific applications.

During the last decade, Drosophila gained attention as a model system for common human neurodegenerative brain disorders. Most basic molecular and cellular mechanisms are highly conserved between humans and Drosophila and ~70% of all human disease genes have an evolutionary conserved fly homolog, providing a reliable model (Bier, 2005; Bilen and Bonini, 2005). Many Drosophila models have been generated using human Tau. Some are based on wild-type Tau isoforms whereas others express mutated forms such as Tau^{R406W}, Tau^{V337M}, and Tau^{P301L}. To explore specific mechanisms of Tau toxicity or dysfunction, transgenes with targeted mutations and truncations were also generated, with constructs which abolish or mimic Tau phosphorylation or proteolytic cleavage. Together, these models explore the great diversity of tauopathies (Gistelinck et al., 2012). Expression of Tau protein in flies results in neurotoxicity which can be evaluated by morphological readouts of the animal. Roughening of the eye is the most commonly used external phenotype to evaluate toxicity of Tau in Drosophila (Gistelinck et al., 2012). Moreover, Drosophila notum harbours around 200 bristles, which are sensory organs connected at the base with the dendrite of a sensory neuron. Tau toxicity can be quantified by simply counting bristles and overexpression of different variants of Tau leads to bristle loss (Yeh et al., 2010). Other common readouts are the lifespan and pupal lethality, as a matter of fact flies overexpressing Tau show a reduced lifespan and increased death of larvae (Talmat-Amar et al., 2011). All these readouts can be used to easily evaluate the toxic effect of Tau and also to screen genes or drugs altering the toxicity of the protein. Moreover, neuronal cell death can be detected by TUNEL or immunostaining of activated cleaved caspase-3 which indicate increased apoptosis in brains of Tau-expressing flies (Ali et al., 2012; Colodner and Feany, 2010; Talmat-Amar et al., 2011). Neuronal degeneration in Drosophila can also be observed by the presence of vacuoles in brain tissues and can be used as a quantitative readout (Ali et al., 2012; Mershin, 2004; Talmat-Amar et al., 2011). Alterations in axonal transport has also been

observed in flies expressing Tau bearing pathological mutations and PTMs and this causes locomotor defects and altered release of neurotransmitters and neurohormones (Gistelinck et al., 2012). Finally this model can be applied for behavioural tests, in particular olfactory learning and memory in Tau-expressing flies is strongly impaired and almost a complete loss of mushroom bodies is observed suggesting a relevant toxic effect of Tau (Kosmidis et al., 2010; Mershin, 2004). The significant damage caused by Tau in *Drosophila* and the easy readouts led to a relevant use of this model for the identification of Tau mechanisms and interactors related to transport and transmission and for genetic screenings (Gistelinck et al., 2012).

Another animal model which has been considered to study Tau pathological mechanisms is *Danio rerio* (zebrafish). This animal offers several distinct advantages over other vertebrate models: the easy maintenance in laboratory due to its simple habitat conditions, the large clutch size with hundreds of eggs, the transparency of embryos allowing an easy imaging analyses, the feasibility of the genetic manipulation, the vertebrate neural structural organisation and the presence of several orthologue genes similar to humans. Moreover, the small size of larvae allows the high-throughput screenings of neuroactive compounds (Saleem and Kannan, 2018). The zebrafish model has been employed for the study of tauopathies by expressing wild-type or mutated forms of Tau. Interestingly, the pathological features develop much earlier in zebrafish as compared with other available rodent models. Tau expression in zebrafish shows early pathological hallmarks like hyperphosphorylation and conformational changes within the first 2 days of embryonic development. After few days, the larvae develops substantial neurodegeneration displaying pathological features including neurofibrillary tangles by 5 weeks of development (Paquet et al., 2009). Tau aggregation can be observed after Tau overexpression in neurons and these cellular inclusions are positive for pathological phosphorylations in residues related to Tau aggregation and for structural antibodies and dyes (Bai and Burton, 2011; Bai et al., 2007; Paquet et al., 2009, 2010). Moreover, Tau expression in neurons disrupts the cellular cytoskeletal structure (Tomasiewicz et al., 2002). The stereotypic escape response, a behavioural test employed to observe the motility and the response to an external stimuli, has been also

evaluated and at 48 hpf the escape is highly reduced or absent in Tau-expressing larvae (Paquet et al., 2009). Due to the peculiar characteristics of the model and to the effect of Tau overexpression which spontaneously leads to neurodegeneration, zebrafish is considered a promising model to study pathological mechanisms and to develop screenings to impair Tau mediated toxicity.

1.7 Therapeutic approaches against Tau pathologies

Tauopathies are complex multifactorial diseases and the development of therapies has been slow and often inconclusive. Current approaches do not rely on disease modifying drugs, but rather on symptomatic ones and aim to manage behavioural symptoms. Several symptomatic drugs for AD treatment are approved by the Food and Drug Administration and they mainly rely on cholinesterase inhibitors, to prevent the breakdown of acetylcholine described in the brain of AD patients (Birks, 2006) and, at late stages, on NMDA antagonists, to prevent excitotoxicity (Wang and Reddy, 2017). However, these treatments can be unsatisfactory as they cannot halt the progress of the pathology. For these reasons, many efforts have been spent to study the two main lesions in AD, i.e. amyloid plaques (APs) and NFTs in order to come up with a disease modifying treatment. However, all the attempts targeting APs failed in blocking or curing the disease (Makin, 2018; Wischik et al., 2014). Consequently, an increasing interest toward the role of Tau in the etiology of tauopathies has arisen. Recently active or passive immunization showed great potentialities in preventing Tau aggregation, leading to promising clinical trials that are still in progress. As to the passive immunization, the injection of selected antibodies against pathological Tau has been considered and several approaches have been exploited leading to clinical trials (Novak et al., 2018a; West et al., 2017). Recent evidences showed that the reduction of total Tau in adult brains doesn't affect physiological functions and prevents toxicity caused by Tau aggregation. This study opened to a new approach employing ASOs molecules to target Tau expression and reduce the aggregation in patient's brains (Devos et al., 2017; DeVos et al., 2018). Actually the most promising therapeutic intervention is the active immunization by the AAD1vac, a vaccine against pathological Tau. Preclinical studies on mice models revealed that this vaccine specifically reduces

Tau pathological aggregates in the brain and currently it is employed in a clinical trial for AD. The phase II for the evaluation of side effects in patients has recently concluded and further investigations are in progress to determine the therapeutic effect (Kontsekova et al., 2014; Novak et al., 2018c, 2018b, 2018a).

Another possibility to treat Tau pathology is to target hyperphosphorylation since Tau phosphorylation is a key event in the pathology. Many kinase inhibitors have been approved for the treatment of cancer and other diseases, opening to the possibility of a therapeutic application of existing drugs also for neurodegenerative diseases. Among these molecules, PD-901 is a potent inhibitor of ERK pathway whose effect on Tau pathology was previously described. It is currently in clinical trial for the treatment of lung cancer and sold tumors (ClinicalTrials.gov Identifier: NCT02022982; NCT02039336; NCT03905148). Another interesting kinase inhibitor is D-JNKI-1, a cell-penetrating peptide that inhibits JNK pathway which is currently in clinical trial for the treatment of acute hearing loss (ClinicalTrials.gov Identifier: NCT02809118; NCT02561091).

1.8 Förster Resonance Energy Transfer

Förster or fluorescence resonance energy transfer (FRET), is a mechanism of energy transfer between two light-sensitive molecules described in 1948 by Theodor Förster (Förster, 1948). Generally, an excited fluorophore can lose its exceeding energy by emitting a photon or by non-radiative dissipation. In the FRET mechanism, if two fluorophores are sufficiently close each other, one can transmit its energy to the other. The excited fluorophore, the donor, can return to its ground state by non-radiative transfer of energy from its excited dipole to the dipole of the acceptor one. The acceptor fluorophore in turn can return to its ground state by different mechanisms including photon emission, non-radiative dissipation or again energy transfer to another acceptor molecule. No light photons are transferred to the acceptor and no acceptor fluorescence is required for resonance energy transfer to occur. In order for FRET to happen some conditions must be considered. The donor emission spectrum must overlap the acceptor excitation spectrum. Moreover, FRET efficiency is influenced by the distance (R) of the molecules involved. The efficiency decreases at the 6^{th} power

of R and increases with R_0, the distance at which the probability of the energy transfer between the donor and the acceptor is 50% (Förster distance): E = $R_0^6 / R_0^6 + R^6$. The orientation of the dipoles also influences FRET efficiency infact no FRET occurs when the dipoles are perpendicular while it's maximal for parallel dipoles (Kaláb and Soderholm, 2010; Shrestha et al., 2015). However, it has been demonstrated that in a biological context, the impact of dipoles orientation is less significant than the parameters described above since both donor and acceptor fluorophores can acquire all possible random orientations during the donor's lifetime (Shrestha et al., 2015). The choice of the fluorophores is fundamental for an analysis based on FRET technique. The most commonly used donor-acceptor pairs in biology are synthetic organic dyes and fluorophores. However, also other molecules have been introduced such as synthetic nanoparticles, non-natural autofluorescent aminoacids, genetically encoded protein tags targeted by synthetic dyes and bioluminescent donors. Synthetic organic dyes are small molecules with favourable photochemical and spectral properties respect fluorophores. The advantage of fluorophores is that they can be genetically controlled outweighing the fact that are large molecules (Kaláb and Soderholm, 2010). FRET is a useful technique to study protein interactions and conformational changes in the same molecule and it has also been applied in several Alzheimer's disease studies. Takahashi et al exploited FRET strategy to construct a sensor detecting Aβ oligomers using CFP and YFP respectively as donor and acceptor fluorophores (Takahashi and Mihara, 2012). Kinoshita et al used FRET to visualize the interaction between APP and β-secretase from the surface of cells to the endosomal compartment (Kinoshita et al., 2003). In another study the method has been employed for the detection of Tau aggregation by the expression of Tau repeat domains fused to CFP and YFP (Holmes et al., 2014). Other studies employs FRET to study localization of Tau protein on MTs (Nouar et al., 2013). These examples are indicative of the different applications in which FRET can be used in a biological context, to study the interaction between proteins or to detect conformational changes inside the protein.

1.9 Aim of the thesis

This work is focused on the study of molecular mechanisms involved in Tau pathology. First, a Tau intramolecular biosensor named Conformational Sensitive

Tau (CST) has been developed and characterized to study Tau conformational changes. CST revealed the 3D conformations of Tau in physiological and pathological conditions. In particular, we demonstrated that Tau assumes a loop-like conformation when bound to MTs while soluble cytoplasmic Tau shows a more relaxed conformation. Moreover, destabilizing conditions related to tauopathies, such as Tau mutations, induce a conformational change towards a more open structure and a higher solubility of Tau protein. Finally, CST is also sensitive to Tau aggregation, with the formation of FRET positive aggregates. The CST allowed to characterize a peculiar Tau mutation associated to Pick's disease, Tau^{G336H}, which shows a higher stability and a closer loop-conformation on MTs, determining an opposite effect with respect to previous characterized mutations.

The CST has been applied for the development of *in vitro* and *in vivo* aggregation screening platforms. As to the *in vitro* platform, CST reporter cells displaying aggregates were treated with several kinase inhibitors in order to screen potential therapeutic molecules. Among these molecules, we identified a ERK pathway inhibitor actually used in oncological clinical trials, PD-901, as a drug able to reduce Tau pathological aggregation. An *in vivo* screening platform with CST expressed in a zebrafish model has been developed with the aim to obtain a more complex but easy-to-use model for high-throughput screenings of potential therapeutic compounds.

The CST analysed in the nuclear compartment revealed that 3D conformation of nuclear Tau is different from Tau bound to tubulin. The role of nuclear Tau has been investigated in non-neuronal and in neuronal cell lines. We demonstrated that Tau is able to induce a significant increase of mRNA and protein levels of the Vesicular Glutamate Transporter 1 (VGluT1), a disease-relevant gene, in all the considered cell lines. The modulation of VGluT1 is due to the increase in the nuclear amount of Tau protein. Intriguingly, pathological mutation P301L or Tau aggregation lead to a loss of nuclear Tau function, preventing VGluT1 expression. To determine the global effect on gene expression mediated by Tau, a transcriptome experiments on differentiated SHSY5Y showed an alteration of all the glutamate release pathway. A comparison with microarray data on hippocampi of patients affected with AD at different stages revealed that cellular

system overexpressing Tau mimics the first steps of AD. Finally, experiments to clarify the nuclear mechanisms mediated by Tau suggested that Tau in involved in epigenetic mechanisms. In particular, it interacts with the nuclear protein TRIM28 thus competing with HDAC1 which is delocalized from the nucleus to the cytoplasm. This mechanism seems to modulate VGluT1 expression revealing that Tau nuclear function is closely related to chromatin remodelling.

Chapter 2

Materials and methods

2.1 Chimeric constructs cloning

The Conformational Sensitive Tau (CST) has been generated by cloning the cDNA encoding the Tau isoform D (383aa) into the BspEI site of the plasmid pECFP-EYFP already available in the lab (EYFP cloned in frame with ECFP into pECFP-C1 from Clontech at the BspeI site). Both the forward and reverse cloning primers contain the RSIVT linker sequence between the BspEI site and the Tau sequence (forward primer: 5'- GTC GTT TCC GGA AGA TCT ATT GTC ACT ATG GCT GAG -3'; reverse primer: 5'- AAC GAC TCC GGA AGT GAC AAT AGA TCT CAA ACC CTG -3'). The monolabeled constructs pECFP-Tau and pTau-EYFP have been generated by subcloning the Tau cDNA into the BspEI site of plasmid pECFP-C1 and pEYFP-N1 (Clontech Laboratories, Inc., Saint-Germain-en-Laye, France)(FWD-BspEI-TAU: 5'- AAT TAT TCC GGA ATG GCT GAG CCC CGC CAG-3' ; REV-BspEI-TAU: 5'- ACT TGA TCC GGA CAA ACC CTG CTT GGC CAG -3'; FWD-BspEI-RSIVT-TAU: 5'- AAT TAT TCC GGA AGA TCT ATT GTC ACT ATG GCT GAG CCC CGC CAG-3'; REV-BspEI-RSIVT-TAU: 5'- ACT TGA TCC GGA AGT GAC AAT AGA TCT CAA ACC CTG CTT GGC CAG -3'). The cDNA encoding human Tau isoform htau23 (352aa) was derived from pET28-his-3C_Tau352 (Addgene). To obtain a mammalian expression vector, htau23 was digested at XbaI/XhoI site and cloned in pEGFP-C1 by substituting GFP sequence in NheI/XhoI cloning site. Tau-NLS has been generated by digestion and cloning of the 3xNLS (pDonor-tBFP-NLS-Neo was a gift from Kazuhisa Nakayama Addgene plasmid # 80766; RRID: Addgene_80766) in the XhoI/BamHI site. Tau-NES has been obtained by PCR amplification of NES (pmTurquoise2-NES was a gift from Dorus Gadella; Addgene plasmid # 36206; RRID: Addgene_36206) and cloning in EcoRI/BamHI site. Mutagenesis experiments were performed on CST and Tau sequences by employing Site-Directed Mutagenesis Kit Q5 (New England BioLabs). The primers for Tau mutagenesis are: S199A/S202A/T205A (AT8mut) Fwd 5'-CCC AGG CGC ACC CGG CAG CCG CTC CCG C -3'; Rev 5'- GCG CCG GGG GCG CTG TAG CCG

CTG CGA TCC CC -3'; P301L Fwd 5'-AAACACGTCCTGGGAGGCGGC-3'; Rev 5'-GATATTATCCTTTGAGCCACACTTGGACTG-3'; ΔK280 Fwd 5'-AAGCTGGATCTTAGCAAC-3'; Rev 5'-ATTAATTATCTGCACCTTCC-3'; P301S 5'-AAACACGTCTCGGGAGGCGGC-3'; Rev 5'-GATATTATCCTTTGAGCCACACTTGGACTG-3'; Q336H Fwd 5'- AGG AGG TGG CCA CGT GGA AGT -3'; Rev 5'-GGT TTA TGA TGG ATG TTG CC -3'. For bacterial expression of Tau^{P301S}, mutated Tau was digested at NdeI/BamHI sites and cloned in pET11a plasmid already available in the lab. The plasmid pEZX-VG::Gfp was generated by GeneCopoeia. The pTagRFP-tubulin plasmid was purchased from Evrogen (FP145).

2.2 Cell Culture, transfections and treatments

HeLa cells and immortalized hippocampal neurons HT22 were maintained in Dulbecco's modified Eagle's medium (DMEM) (GIBCO) supplemented with 10% FBS. SH-SY5Y (ATCC® CRL-2266TM) cells were maintained in DMEM/F12 (GIBCO) supplemented with 10% FBS. SH-SY5Y were differentiated with 10 μM retinoic acid (Sigma-Aldrich) for 5 days followed by 50ng/ml BDNF (Alomone) in DMEM/F-12 medium not supplemented with FCS for three days. The day before the experiment cells were seeded at 10^5 cells in six-well plates or in Willco dishes (Willcowells). Lipofection was carried out with Effectene (QIAGEN) or Lipofectamine2000 (Thermo-Fisher) according to manufacturer's instructions. Primary hippocampal neurons were obtained from postnatal day (P)0 B6/129 mice. Hippocampi were dissected and triturated in cold calcium-free Hank's balanced salt solution with 100 U/ml penicillin, 0.1 mg/ml streptomycin, and digested in 0.1% trypsin, followed by inactivation in 10% FBS DMEM (GIBCO) with 100 U/ml DNase. Neurons were seeded on poly-D-lysine-coated glass coverslips. For initial plating, neurons were maintained in Neurobasal-A medium (Invitrogen) supplemented with 4.5 g/l D-glucose, 10% FBS, 2% B27 (Invitrogen), 1% Glutamax (Invitrogen), 1 mM pyruvate, 4 μM reduced glutathione, and 12.5 μM glutamate. From the following day on, neurons were grown in Neurobasal-A medium (Invitrogen) supplemented with 2% B27 (Invitrogen), 1% Glutamax (Invitrogen), and 1 μg/ml gentamicin. For IF experiments, neurons at day in vitro (DIV) 18 have been used. Cells were treated with: PTX (Sigma) 1μM for 10 min; Noc (Sigma) 1μM for 30 min; Colchicine (Sigma) 1μM for 24 hours;

Staurosporin (Sigma) 10μM for 45min/4h; Epothilone D (Santa Cruz Biotechnology) 1μM for 30 min; TSA (Sigma) 800 nM for 16 h. For cellular aggregation induction, cells were plated in glass bottom dishes and 1.2 μg of Tau fibrils were delivered to cells with μl of Lipofectamine 2000 transfection reagent diluted in 300 ml of Opti-MEM Reduced Serum Medium (Gibco). Cells were treated for 2h, then DMEM/F-12 was added back to cells. The day after Tau seeding, cells have been treated with 1 μM PD-901 or 6 μM D-JNKI-1 for 48h in the presence of fibrils, while 10 μM Staurosporine (STS) or 200 nM okadaic acid (OA) were administered 72h after Tau seeding for 45 min. AD brain lysates have been provided by Abcam (ab29969, ab29971) and cells have been treated with 10μg for 48h. AβOs have been collected from 7PA2 cells conditioned medium as described by 46, and 500μl of AβOs have been added to 1 ml of complete medium for 96h. Microtubules labeling in live cells has been obtained by SiR-tubulin Kit (excitation wavelength l = 633 nm) (SPIROCHROME) in FRET experiments to avoid interference in FRET signal.

2.3 Transgenic zebrafish

Danio rerio was raised and bred at a temperature of 28 °C with a photoperiod of 14h light/10h dark. Animal care was performed in strict accordance with protocols approved by the Italian Ministry of Public Health and the University of Pisa Ethical Committee, in compliance with EU legislation (Directive 2010/63/EU). Zebrafish embryos were obtained by natural spawning, staged according to the hours post fertilization and raised at 28 °C in 1× E3 medium (NaCl 5.0 mM, KCl 0.17 mM, $CaCl_2$ 0.33 mM, $MgSO_4$ 0.33mM, 0.1% methylene blue) in Petri dishes. For the generation of the CST transgenesis vector, CST sequence has been cloned under the HuC promoter in the Tol2-elavl3-GCaMP6s plasmid (Tol2-elavl3-GCaMP6s was a gift from Misha Ahrens Addgene plasmid # 59531; RRID: Addgene_59531) at AgeI site which removes the GCaMP6 sequence. Eggs were harvested and injected at zygote stage. For microinjection borosilicate microcapillaries were used. Capillaries were pulled with a micropipette puller (P97, Sutter Instrument). For transient CST mRNA injection, capped CST mRNA was prepared by employing the mMESSAGE mMACHINE SP6 transcription kit (Invitrogen). The needles were filled with 2 μl of water solution containing 100ng/μl of CST mRNA, 0.4 M KCl and 1% phenol red. For the generation of

transgenic zebrafishes, the needles were filled with 2 µl of water solution containing 20–30 ng/µl of plasmid DNA, 20–30 ng/µl of Tol2 transposase mRNA, 0.4 M KCl, and 1% phenol red as visual control of successful injections. Embryos were injected with approximately 2 nl of mix solution and the drop volume was estimated under a microscope using a calibrated slide. Injections were performed under the Nikon C-PS stereoscope. F_0 fishes were screened under fluorescence microscope at 24 hpf for zebrafish larvae. Six different founders were selected for line establishment.

2.4 Silencing mediated by lentiviral shRNAs

MISSION® TRC shRNA bacterial glycerol stocks containing Tau shRNAs (MAPT MISSION shRNA SHCLNG-NM_010838) were purchased from SIGMA. A lentiviral vector containing scramble shRNA was used as control. For the generation of viral vector stocks, HEK 293T cells were transfected with 10µg of the packaging plasmid pCMVΔR8.91, 5µg of VSV-G and 20µg of the gene transfer plasmid. The cell culture supernatant was collected twice, at 48h and 72h after transfection and filtered through a 0.45µM pore size filter. Viral vectors were titered by quantification of p24 antigen in cell culture supernatants with an enzyme-linked immunoabsorbent assay (Innogenetics, Gent, Belgium). Differentiated SHSY5Y cells were transduced with lentiviral particles supplemented by 10µg/ml polybrene (Millipore) for six hours. Cells were collected and analysed 72 hours after transduction.

2.5 Tau Purification and Aggregation

BL21 bacterial cells were transformed with pET11a-P301S-hTau plasmid. Cells were lysed according to direct boiling method described in (KrishnaKumar and Gupta, 2017) in 50mM MES pH 6.25 buffer. The lysate was purified using a cation-exchange chromatography. Column was equilibrated with MEF buffer supplemented with 0.5mM DTT. Tau was eluted with MES buffer with 1M NaCl. Heparin-assembled P301S Tau fibrils were prepared as described in (McEwan et al., 2017) 20mM sodium phosphate buffer pH 7.4 supplemented with 0.5mM DTT.

2.6 Cell Survival

For cells survival analysis, SHSY5Y cells were plated on in 24-well plates. Cells were treated with 0.5, 1 and 2 mM PD-901 or 3, 6 and 12mM D-JNKI-1 for 48 h, while 5, 10 and 20mM Staurosporine (STS) or 100, 200 and 400nM okadaic acid (OA) were administered 45 min. Then cells were harvested using trypsin and alive cells count was performed using the Scepter Cell Counter (Millipore).

2.7 Coimmunoprecipitation

Total cell extracts were prepared in ice-cold RIPA buffer (150 mM NaCl RIPA) supplemented with protease and phosphatase inhibitors (Roche). The lysate was quantified using Bradford assay (Thermo Fisher Scientific) and 2mg of protein were incubated with 2µg of primary antibody overnight at 4°C. 20µl of agarose resin conjugated protein G (Santa Cruz) or magnetic beads conjugated protein G (BioRad) were incubated for 2h at 4°C. Samples were washed in ice-cold RIPA. Finally, samples were analysed by Western blot.

2.8 Western Blot

Total protein extracts were prepared in lysis buffer supplemented with protease and phosphatase inhibitors. To guarantee the maximum reproducibility and the minimal contamination in the fractionation experiments, the Subcellular Protein Fractionation Kit for Cultured Cells (Thermo-Fisher) was used according to manufacturer's instructions. Briefly, the protocol enables segregation and enrichment of proteins from five different cellular compartments. The first kit reagent, when added to the cell pellet, causes selective membrane permeabilization, releasing the soluble cytoplasmic contents named Cytoplasmic Fraction (CF). The second reagent dissolves plasma, mitochondria and ER-Golgi membranes. After recovering intact nuclei by centrifugation, a third reagent yields the soluble nuclear extract named SNF. An additional nuclear extraction with micrococcal nuclease is performed to release chromatin-bound nuclear fraction named CBF. The last reagent extracts the cytoskeletal proteins. For preparation of Triton-X insoluble fraction, cells were lysed in Triton-X lysis buffer (1% Triton-X 100 in PBS with protease and phosphatase inhibitors) and the extract was centrifuged at 16000g for 15min. The supernatant was designated as Triton X-100 soluble fraction. The pellet was dissolved in Triton-X lysis buffer

supplemented with 1% SDS, sonicated and boiled. This fraction was designated to be Triton X-100 insoluble fraction. Proteins were quantified by BCA (Thermo-Fisher). For each sample 10-20-30µg were loaded. Proteins were separated by SDS-PAGE and electro-blotted onto Hybond-C-Extra (Amersham Biosciences) nitrocellulose membranes. Membranes were blocked with 5% skimmed milk powder in TBS, 0.1% Tween 20. Primary antibodies for WB: mouse anti-Tau (Tau5) 1:1000 ab80579 (AbCam); rabbit anti-actin 1:10000 (A300-485A BETHYL LABORATORIES); goat anti-Hsp70 1:1000 (sc-1060 Santa Cruz); rabbit anti-histone H2b 1:2000 (Santa Cruz); mouse anti Tau-C3 1:500 (Abcam), mouse anti Tau13 1:1000 (Santa Cruz), rabbit anti GFP 1:1000 (Abcam); mouse anti-GAPDH 1:15000 (Fitzgerald); rabbit anti-VGluT1 ab77822 1:500 (AbCam); rabbit anti-HDAC1 1:500 (Santa Cruz); rabbit anti-TRIM28 1:1000 (Abcam); rabbit anti-pTau (Ser202, Thr205) 1:500 (Thermo Fisher Scientific); rabbit anti-pTau (Ser356) 1:500 (Thermo Fisher Scientific); anti anti-pTau (Thr231) 1:500 (Thermo Fisher Scientific). Secondary antibodies for Western blot analysis were HRP-conjugated anti-mouse, anti-rabbit, or anti-goat purchased from Santa Cruz Biotechnology, Inc., Santa Cruz, CA, USA. Western blot quantification has been performed using ImageJ software.

2.9 Immunofluorescence and immunohistochemistry

Cells were seeded on chamber slides (LabTek) and after transfection and/or drug treatment were fixed with cold methanol for 4 min. Soon after fixation cells were permeabilized with 0.1% Triton X-100 and blocked for 30 min with the blocking solution (PBS+Tween 0,1% + BSA 1% fresh). Primary antibody incubation has been done in blocking solution for 1h or O/N. Zebrafish embryos were manually dechorionated, fixed in 4% paraformaldehyde at the desired developmental stages and stored in methanol at −20°C. Permeabilization has been performed in ice cold acetone / PBS and then in PBS+ triton 1%. Embryos were blocked for 1h in blocking solution (PBS 1% Triton + 10% FCS) at room temperature followed by incubation with peroxidase blocking solution (0.1% H_2O_2 diluted in blocking buffer) O/N at 4°C. Primary antibody incubation has been done in blocking solution O/N. After secondary antibody incubation, DAB substrate was added 3h at room temperature followed by DAB+H_2O_2. Primary antibody used are: mouse anti α-tubulin 1:1000 (Sigma-Aldrich); mouse anti-tau (Tau-13) 1:500 (Santa

Cruz); rabbit anti-VGluT1 ab77822 1:250 (AbCam); DAPI 1:15000 (Sigma); rabbit anti-pAT8 1:100 (Abcam); rabbit anti-VGluT1 ab77822 1:250 (AbCam); rabbit anti-HDAC1 1:200 (Santa Cruz); rabbit anti-TRIM28 1:200 (Abcam); rabbit anti-pTau (Ser202, Thr205) 1:50 (Thermo Fisher Scientific); anti anti-pTau (Thr231) 1:50 (Thermo Fisher Scientific). Excess antibody was eliminated by several washes with PBS 1X and secondary antibody incubation was performed in blocking solution for 1h. Secondary antibodies for IF: Alexa Fluor 633; Alexa Fluor 488 (Life Technologies). Chamber slides were mounted by using Vectashield mounting media (Vector Laboratories). For Tau aggregates staining, samples were incubated with 1 mM K114 (Sigma-Aldrich) for 10 min.

2.10 Real-time PCR

Total RNA was extracted by Nucleospin (Macherey-Nagel) and retro-transcribed by Reverse Transcriptase Core kit (Eurogentec) according to manufacturer's instructions. Real-time PCR was performed using the iTaqTM Universal SYBR® Green Supermix (BioRad), and performed for 40 cycles of amplification with denaturation at 95°C for 15s, annealing at 60°C for 25s, extension at 72°C for 20s. The primers employed were: Actin: fwd 5'-TCCATCCTGGCCTCACTGTCCAC-3', rev 5'-GAGGGGCCGGACTCATCGTACT-3'; Tau: fwd 5'-GTGACCTCCAAGTGTGGCTCATT-3', rev 5'-CTTCGACTGGACTCTGTCCTTG-3'; VGluT1: fwd 5'-GAGGAGTGGCAGTACGTGTTCC-3', rev 5'-TCTCCAGAAGCAAAGACCCC-3'.

2.11 RNA sequencing

Sequencing procedure was performed in Ctrl and Tau-overexpressing differentiated SHSY5Y cells using Illumina methodology (Bentley et al., 2008). Around 2.5 µg of total RNA was used for library preparation (Illumina, TruSeq™ RNA Sample Prep Kit v2) using the manufacturer's description. Libraries were sequenced using a HiSeq2000 (Illumina) running in 50bp single-read mode using sequencing chemistry v2. This resulted in around 29-54 million reads per sample with 50bp length. Reads were extracted in FASTQ format using CASAVA v.1.8 (Illumina). FASTQ formatted reads were used for following analysis. Read mapping was performed using Bowtie (Langmead et al., 2009). On average, 50%

of all reads could be mapped uniquely and were used for counting afterwards. All transcripts were used for further analysis. The read counts were normalized with respect to the size of the individual transcript contigs and to the total amount of mappable reads obtained for the particular sample, resulting in reads per kilobase and million mapped reads (RPKM) values (Mortazavi et al., 2008) for each transcript contig.

2.12 Transcriptome analysis

Differentially expressed genes (DEGs) were identified by applying the statistical tests of the edgeR, DESeq and baySeq packages (Anders and Huber, 2010; Hardcastle and Kelly, 2010; Robinson et al., 2010), while DEGs were selected according a FDR < 0.05 by all three tests. The RPKM counts were clustered in order to identify common expression profiles. DEGs were used for Gene Ontology analysis with ClueGO plug-in (Bindea et al., 2009). The attribute used to import the network in the tool was “name” and the comparison was made with Homo sapiens identifiers. As statistical test “Enrichment (Right-sided hypergeometric test)” was used, with correction for multiple testing and a p-value threshold of 0.05. Moreover, the options “Use GO Term Fusion” and “Use GO Term Grouping” were selected. DEGs clustering was performed by considering three different databases: KEGG, GO and Interactome. In order to characterize the cellular system, a transcriptome meta-analysis was performed employing a public transcriptomics dataset sourced from the Gene Expression Omnibus (GEO) platform hosted on NCBI (https://www.ncbi.nlm.nih.gov/geo/). The gene dataset considered is GSE84422 which includes 1053 post-mortem brain samples across 19 brain regions from a total of 125 patients dying at different AD stages, with 50-60 subjects per brain region. Patients are clustered by AD severity into 4 groups according to clinical dementia rating (CDR), Braak NFT score, sum of NFT density across different brain regions, average neuritic plaque density and average CERAD. Gene expression profiling has been done on the Affymetrix Human Genome U133A Array (GPL96), Affymetrix Human Genome U133B Array (GPL97), Affymetrix Human Genome U133 Plus2.0 Array (GPL570) (Wang et al., 2016). In order to import datasets and create subsets by diagnosis and brain region R packages “GEOquery”, “Rcpp” and “tidyselect” were used. To compare different platforms, platform-specific IDs were converted into Entrex

Gene IDs using the corresponding R annotation databases from Bioconductor, available via bioMart (version 3.8). Multiple platform IDs matching the same gene were summarized in a single entry with gene expression as the mean of probe expression. Probes mapping on the same gene with discordant logarithmic fold change (logFC) were excluded from the analysis. The patients included in the GSE84422 dataset were classified by Alzheimer disease stage into early mild cognitive impairment (E-MCI), late MCI (L-MCI) and Alzheimer's disease (AD) and each subset was compared to our SHSY5Y data. For an overview of the global transcriptome profile, we considered all the genes with at least a small mean fold change (log2 fold change > 0.1) and p-value < 0.05 in our dataset. We compared the differentially expressed genes in our dataset (FDR < 0.1) to all the genes in the hippocampal dataset. Finally, we assessed the correlation of the most significant genes in both datasets. In-built R "plot" function was used to draw scatterplots comparing gene expression in the different conditions. Enrichment of GO terms in SHSY5Y transcriptome compared to hippocampal L-MCI dataset was assessed by overrepresentation analysis (ORA) as described above. The direction and magnitude of the fold change of genes in the most differentially represented pathways was compared to that of patients with L-MCI in dataset GSE84422.

2.13 Image Acquisition and Analysis

For FRET experiments images were acquired with the TCS SP2 laser-scanning confocal microscope (Leica Microsystems, Milan, Italy) equipped with galvanometric stage using a 63/1.4 NA HCX PL APO oil immersion objective. A heated and humidified chamber mounted on the stage of the microscope was used for live imaging experiments in order to maintain a controlled temperature (37°C) and CO_2 (5%) during image acquisition. An Argon laser was used for ECFP (l = 458 nm) and EYFP (l = 514 nm), a Gre-Ne laser for RFP (l = 543 nm) and a He-Ne laser for l = 633 nm. For the quantification of morphological parameters such as the total filament length and the number of crossover points the filament tracer option of the IMARIS Bitplane software has been exploited. In detail, these two parameters are deduced by a software plugin that, based on connectivity and fluorescence intensity, automatically detects and segments filamentous structures revealing information about the topology of filaments as

the sum of the lengths of all lines and the number of crossover points within the filament. For IF experiments a Leica TCS SP8 confocal laser-scanning microscope (Leica Microsystems, Mannheim, Germany) equipped with Leica Application Suite (LAS) X software was used. All frames were captured by means of HC PL APO CS2 40X/1.30 (*) oil objective, a format size of 2048 x 2048 pixel and a sequential scan procedure. All confocal frames were taken by a suitable scanning power and speed along with gain level to achieve the greater signal definition and avoid any background noise. (*) N.A.=1.30. For colocalization experiments, K114 was excited at 380 nm and its fluorescence emission was collected between 530 and 600 nm. ECFP was excited at 458 nm and its fluorescence emission was collected between 470 nm and 500 nm. The two channels were excited sequentially in order to minimize the bleed-through. Images underwent background subtraction and were analysed using Costes approximation method (Costes et al., 2004) in the ImageJ plugin “Coloc2”. Threshold regression was set to Costes and Costes’ significance test was performed. Point spread function was set to 2.0. Costes randomisations were set to 100.

2.14 FRET and FRAP Experiments

For sensitized emission FRET experiments, each image was recorded in a spectral mode, by selecting specific regions of the emission spectrum. The donor ECFP was excited at 458 nm and its fluorescence emission was collected between 470 nm and 500 nm (donor channel) and between 530 nm and 600 nm (FRET channel). The acceptor EYFP was excited at 514 nm and its fluorescence emission was collected between 530 nm and 600 nm (acceptor channel). The donor and acceptor fluorophores were excited sequentially. The ImageJ software was used for images analysis and FRET quantification. Briefly, FRET images were corrected from cross-talk between donor and acceptor channel using Youvan’s method: $F_{index} = I_{FRET} – A \times I_D – B \times I_A$, where I_{FRET}, I_D and I_A are the images of the sample in the FRET, donor and acceptor channel, respectively, after background subtraction and A and B are the fraction of the donor and acceptor leak-through into the FRET channel, respectively. I determined the A parameter in cells expressing only the donor (pECFP plasmid) by acquiring images in donor and FRET channels. A plot of the intensity of each pixel of the

FRET channel image as a function of the intensity of the same pixel in the donor channel image (regression graph) was automatically generated by the ImageJ plugin (FRET and colocalization Analyzer) and then fitted with a linear equation from which A parameter was derived. Images displaying saturated pixel has been discarded. For the evaluation of the B parameter cells transiently expressing only the acceptor (pEYFP plasmid) have been acquired in FRET and acceptor channel and then subjected to same process of A in the ImageJ plugin. Typical values in our experimental conditions are A = 0.1 and B = 0.25, respectively. Normalized FRET (NFRET) was performed with the ImageJ software plugin ‘‘pixFRET’’ (Feige et al., 2005) by using: NFRET = $F_{index}/\sqrt{(I_D \times I_A)}$ (Xia and Liu, 2001). Mathematically, NFRET values should range between 0–1; the plugin automatically multiplies these values 100; NFRET intensities images were represented in false-colour obtained by using the ‘‘fire’’ lookup table option in ImageJ software. Due to the mathematical subtractions in F_{index} calculation, NFRET negative values in some pixels are considered as zero. In FRET experiments investigating intramolecular and intermolecular FRET, to obtain a comparable amount of Tau I transfected cells with 300 ng of CST or 150 ng ECFP-Tau + 150 ng EYFP-Tau (ML/2); to obtain a comparable amount of fluorophores I transfected cells with 300 ng ECFP-Tau+ 300 ng EYFP-Tau (ML). Since in a transient transfection the expression of the transgene varies from cell to cell, to perform a reliable NFRET quantification in ML samples I selected cells that express comparable amount of fluorescence intensity in the donor and acceptor channel with respect of CST; to perform the NFRET quantification in ML/2 samples I selected cells that express about half the amount of fluorescence intensity in the donor and acceptor channel with respect of CST. I measured the level of expression by fluorescence intensity in individual cells, under the microscope. FRAP experiments were performed by using the FRAP module coupled to the confocal microscope and consists of three different phases: (1) a pre-bleach phase, in which 10 frames of 512x512 pixel images at 1000 Hz have been recorded in order to define the initial level of fluorescence intensity; (2) a photobleaching phase, in which a selected circular ROI with a radius of 2 mm in the cytoplasm of the cell was excited at higher laser power (50% for EYFP) for five frames at 1000 Hz; (3) a post-bleaching phase, in which 120 images have been recorded in order to follow the recovery of the fluorescence intensity in the

selected ROI. Fluorescence recovery was extracted from images of the bleached ROI and subjected to the following manipulation steps: (1) background subtraction; (2) first normalization to the initial pre-bleach value of fluorescence intensity; (3) correction for the fluorescence loss: in particular, I evaluated the fluorescence of the whole cell for each time point, before and after the photobleaching phase; then I multiplied every element of the data of the bleached ROI by ($F_{pre\text{-}wholecell}/F_{post\text{-}wholecell}$), where $F_{pre\text{-}wholecell}$ means prebleach intensity within the whole cell, $F_{post\text{-}wholecell}$ stands for postbleach intensity at any given time point. In any case, I set up the experimental parameters of acquisition in order to avoid strong photobleaching (5%–10%); (4) additional normalization to set the first post-bleach point to zero. At least 30 separate FRAP experiments for each sample has been performed. FRAP recovery curves have been fitted by a two phase exponential association function.

2.15 Patch-clamp recordings and electrophysiological data analysis

Recordings were performed on primary neuronal cultures, by adapting the procedure described in Piacentini et al. (Piacentini et al., 2017). Cells were continuously bathed using Tyrode's solution containing: NaCl 150 mM, KCl 4 mM, $MgCl_2$ 1 mM, $CaCl_2$ 4 mM, Glucose 10 mM, HEPES 10 mM, pH 7.4 with NaOH. Borosilicate glass pipettes were pulled with a P-97 puller (Sutter, CA) to a resistance of 5-6 MΩ when filled with an internal solution containing: K-Gluconate 145 mM, $MgCl_2$ 2 mM, HEPES 10 mM, EGTA 0.1 mM, Mg-ATP 2.5 mM, Na-GTP 0.25 mM, phosphocreatine 5 mM, pH 7.35 with KOH. Miniature Excitatory Postsynaptic Currents (mEPSCs) were recorded while holding the neuron at a command potential of -70 mV. Data were acquired using a MultiClamp 700A amplifier, connected to a Digidata 1322A digitizer (Molecular Devices, CA). Data were analyzed using Clampfit 10.7 (Molecular Devices) as described in Mainardi et al. (Mainardi et al., 2017). An event template was constructed and used to detect mEPSCs; stringency of detection was ensured by setting the "template match threshold" to 4. After event detection, the cumulative distributions for mEPSC amplitude and frequency (the latter as interevent interval) were calculated.

2.16 Statistical analysis

For Western Blot and quantitative real-time PCR, statistical significance was assessed by non-parametric Kruskal-Wallis test followed by pairwise Mann-Whitney test. For imaging experiments statistical significance was assessed by Student's t-test or one-way ANOVA followed by Tukey multiple comparisons test. For qPCR, gene expression was calculated with Pfaffl method (Pfaffl, 2001). Each sample was run in triplicate and at least three biological replicates were performed for each experiment. All results are shown as mean ± SEM from at least three independent experiments. Significance is indicated as * for $p<0.05$, ** for $p<0.01$, *** for $p<0.001$ and **** for $p<0.0001$. For patch-clamp recordings, statistical significance was assessed using the Kolmogorov-Smirnov test.

Chapter 3

Results

3.1 Tau conformations in live cells by the CST biosensor

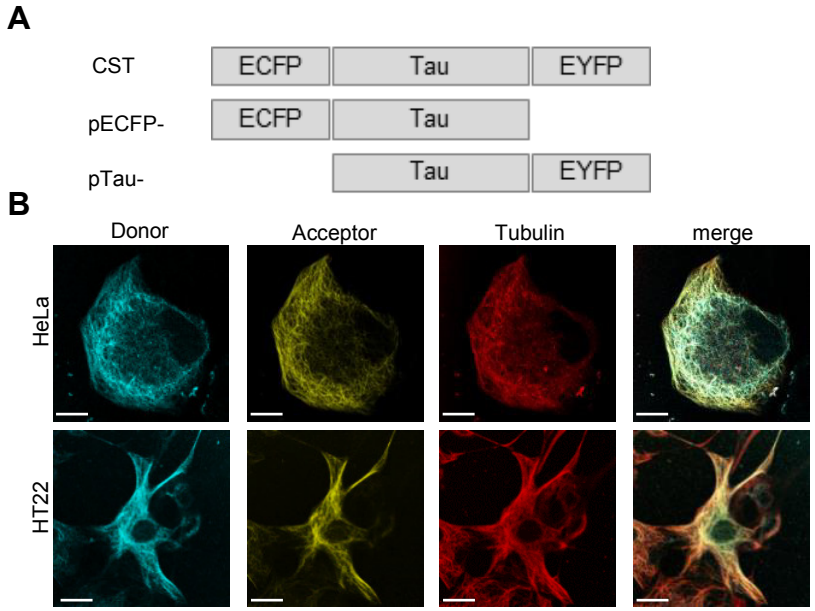

Figure 3.1. Conformational Sensitive Tau sensor (CST) construct colocalizes with tubulin in cells. A. Schematic representation of chimeric constructs. B. Imaging of HeLa and HT22 cells co-transfected with CST and Tubulin-RFP plasmids; donor channel (blue), acceptor channel (yellow), Tubulin (red). White scale bar = 10 μm.

As described above, Tau is an intrinsically disordered protein whose structure in normal conditions is still unclear since it is not possible to analyse it by current molecular approaches. If Tau structure is difficult to elucidate, the conformation of the protein is a simpler target of investigation. *In vitro* studies suggested that Tau assumes a conformation in which its ends are close to each other (Jeganathan et al., 2006; Sabbagh and Dickey, 2016). However, these experiments have been performed in conditions which does not take into account the complexity of a cellular system. In order to investigate the conformation that Tau assumes in physiological and pathological conditions, we generated a conformational biosensor called Conformational Sensitive Tau (CST). The CST is a chimeric protein made of a Tau-D isoform (0N4R) fused at the N-terminal end with a ECFP and at the C-term with a EYFP (Figure 3.1A). The presence of these fluorophores allows to study in real time and in a cellular context the conformation that Tau

assumes in different conditions. Due to the peculiar architecture of the chimeric protein, it is expected that, depending on the conformation of Tau, a FRET signal could be generated by the decreased distance between the N- and C-termini of Tau molecules, thus realizing a context-dependent Conformational-Sensitive Tau sensor. First, we demonstrated that the CST expressed in HeLa cells, that do not express endogenous Tau, and in immortalized hippocampal HT22 cells colocalizes with tubulin-RFP, indicating that the CST maintains Tau physiological function of binding MTs (Figure 3.1B).

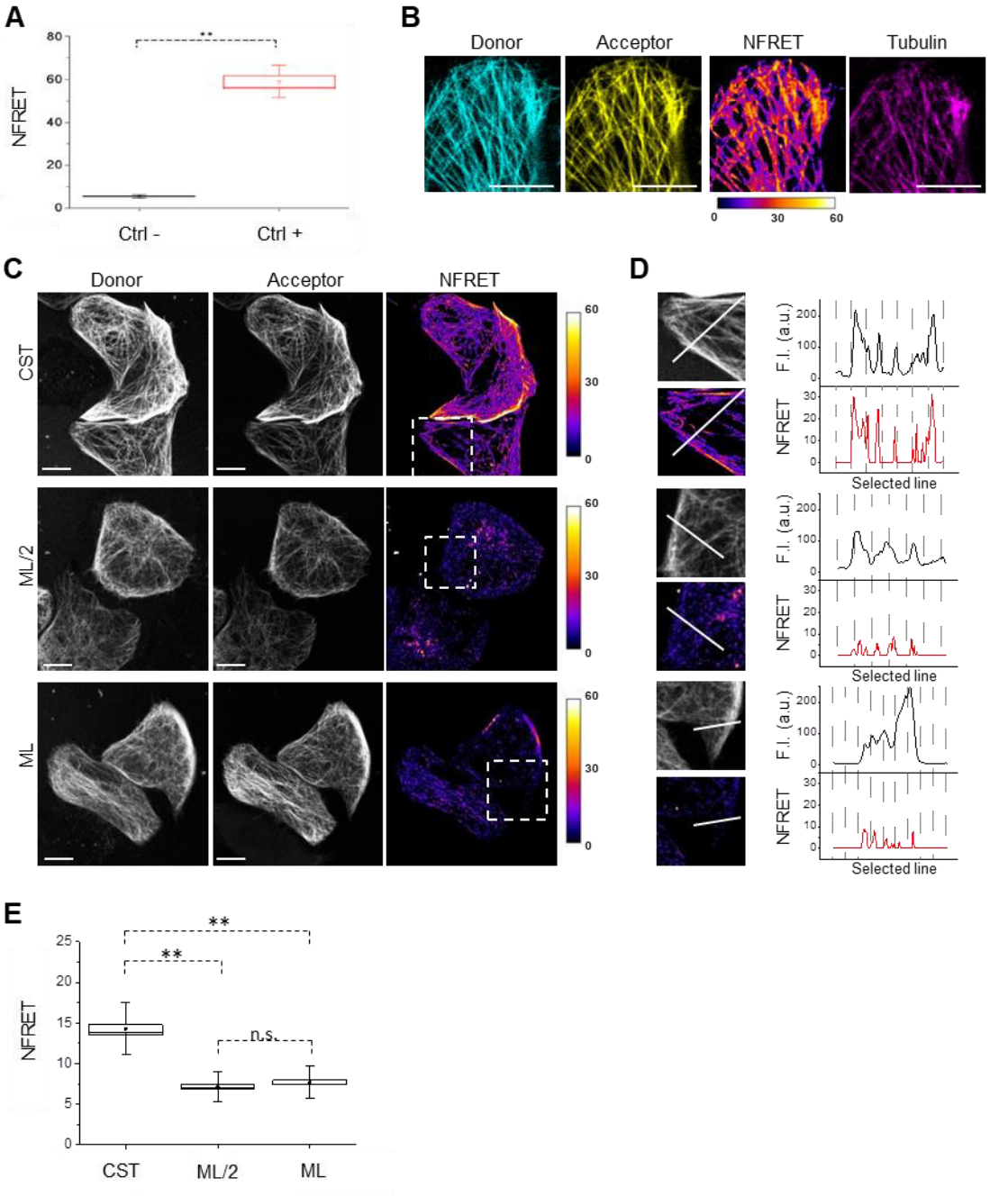

Figure 3.2. The CST displays a positive intramolecular FRET signal on MTs. A. NFRET analysis of positive and negative controls in HeLa cells. B. NFRET signal localization along MTs. Donor (blue), acceptor (yellow), NFRET (false color) and tubulin labeled with Sir-tubulin (magenta). C. FRET measurements in Hela cells expressing CST, ECFP-Tau and Tau-EYFP at comparable Tau levels to CST (ML/2) or ECFP-Tau and Tau-EYFP at comparable fluorophore levels to CST (ML). Donor (grey), acceptor (grey) and Normalized FRET (NFRET) images (false color). White scale bar = 10 mm. D. Magnification of the outlined box in C and Fluorescence intensity profile (F.I.) along the white line (black graph) and NFRET intensity profile along the white line (red graph). E. Box plot of NFRET values calculated on MTs network in CST (40 cells), ML/2 (50 cells) and ML (60 cells). Box spans the standard error of the mean (black square) while whiskers indicates the standard deviation (**$p < 0.01$ ANOVA one-way test).

To exploit the CST as a conformational probe, the quantitative sensitized emission FRET microscopy for the detection of protein conformational changes has been used. FRET parameters have been optimized in cells expressing the donor and the acceptor fused into a chimeric construct (ECFP-EYFP) (See **Materials and Methods**), as a FRET positive control, and in cells expressing both the donor and the acceptor from separate plasmids (pECFP and pEYFP), as a FRET negative control (Figure 3.2A). Imaging analysis in HeLa expressing the CST showed a positive FRET signal which colocalized with tubulin, suggesting that N- and C-terminal ends of Tau protein are close each other on MTs (Figure 3.2B). In order to determine if this FRET signal is due to an intermolecular or intramolecular interaction between Tau terminal ends, cells co-expressing monolabeled Tau constructs (ECFP-Tau and Tau-EYFP) have been compared with cells expressing the CST. Since each CST molecule contains two fluorophores, we considered either cells expressing the same levels of monolabeled Tau, with respect to CST cells (half amounts of fluorophores, ML/2) or cells expressing double levels of monolabeled Tau, with respect to CST cells (hence same amount of fluorophores, ML) (Figure 3.2C). Along selected lines at the intersection with MTs, the CST displayed NFRET values in the range of 15–30 (Figure 3.2D). In cells expressing monolabelled Tau, in both conditions the NFRET signal was significant lower than cells expressing the CST (Figure 3.2E). This result demonstrated that the FRET signal was mainly due to an intramolecular interaction between the N- and C-termini in the same protein, suggesting for the first time that Tau bound to MTs assumes a loop-like conformation.

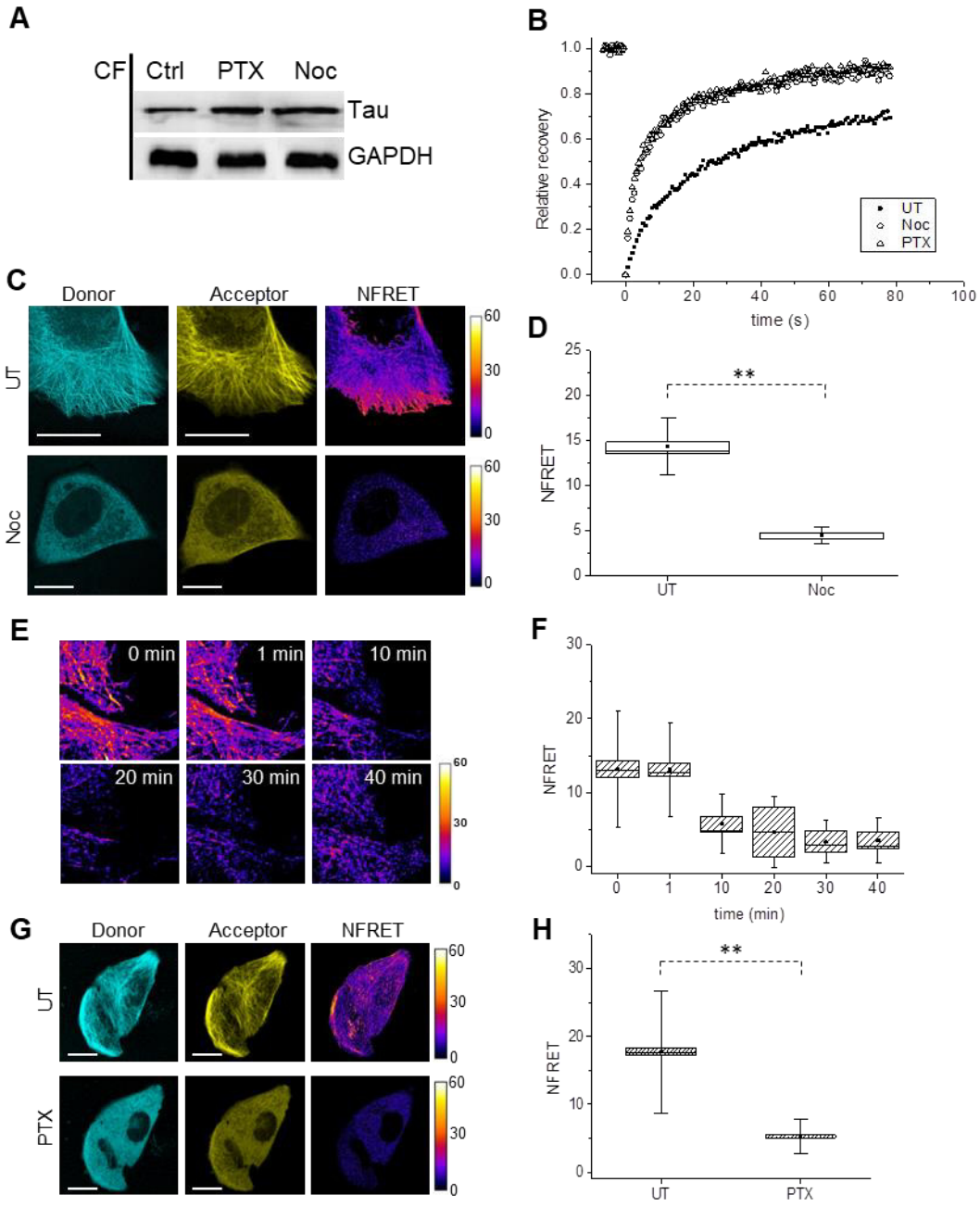

Figure 3.3. Loss of NFRET signal in cells treated with MT interfering drugs. A. Western blot of the cytoplasmic fraction in reporter cells untreated (UT) or treated with Nocodazole (Noc) or Paclitaxel (PTX). B. FRAP relative recovery curves of CST in untreated cells (black square), treated with Nocodazole (empty circle) or Paclitaxel (empty triangle). C. Donor (blue), acceptor (yellow) and NFRET images (false color) in CST reporter cells untreated (UT, upper panels) or treated with Nocodazole (Noc, lower panels). White scale bar = 10 μm. D. Box plot of NFRET values in untreated cells (40 cells) along MTs and in Nocodazole treated cells (20 cells) in random points in the cytoplasm. Box spans the standard error of the mean (black square) while whiskers indicates the standard deviation (**p < 0.01 ANOVA one-way test). E. Real-time FRET analysis of Nocodazole treated reporting cells. NFRET is displayed in false color. F. NFRET quantification of E at different time points. G. Donor (blue), acceptor (yellow) and NFRET images (false color) in CST reporter cells untreated (UT, upper panels) or treated with Paclitaxel (PTX, lower panels). White scale bar = 10 μm. H. NFRET quantification of G along MTs in untreated cells or in random

points in PTX treated cells. Box spans the standard error of the mean (black square) while whiskers indicates the standard deviation (**p < 0.01 ANOVA one-way test).

To analyse the conformation of Tau monomers soluble in the cytoplasm and not bound to MTs, CST reporter cells were treated with Nocodazole (Noc), a MTs disrupting drug. Treated cells were first analysed by subcellular fractionation, to isolate the cytoplasmic fraction (CF) of CST reporter cells. The CF contains the pool of proteins soluble in the cytosol and it allows to quantify the unbound Tau fraction in response to treatments. As shown in figure 3.3A, the treatment with Noc induced an increase in the soluble pool of the CST after MTs destabilization, in fact the signal of Tau in the CF was higher than untreated cells. This evidence has been confirmed by FRAP experiments. FRAP technique distinguishes the freely diffusing pool of proteins, compared to the pool bound to other structures (Azoury et al., 2008; Himmel et al., 2009). The rate of fluorescence recovery indicates how fast fluorescent molecules fill the bleached area and the protein mobility is determined by both diffusion and binding interactions (Breuzard et al., 2013). The recovery curve showed a significant increase of the CST mobile fraction in nocodazole-treated cells (CST: 76±3%; Noc: 91±4%), indicating a higher amount of unbound CST in the cytosol (Figure 3.3B). In these treated cells the NFRET signal was strongly reduced (CST: 14.43±0.73SE; Noc: 4.87±0.64SE), supporting the fact that soluble Tau assumes a different conformation with respect to molecules bound to MTs (Figure 3.3C-D). In particular, the low NFRET indicates a relaxed conformation in which the terminal ends are distant. A time course analysis of the FRET signal in cells treated with nocodazole showed that the loss of NFRET parallels the MTs disruption, and just 10 min after addition of nocodazole the NFRET drops by almost 50% (Figure 3.3E-F). This result demonstrated that CST can be used to monitor the state of association of Tau to cellular MTs.

To determine whether the loss of FRET signal is a consequence of MTs disruption or only of the detachment of Tau from MTs into a soluble pool, CST reporter cells were treated with the MTs stabilizing drug Paclitaxel (PTX), which induces the stabilization of MTs and competes with Tau for its binding to MTs (Hernández et al., 2013; Kar et al., 2003; Makrides et al., 2004). As shown by Western blot and FRAP experiments, PTX treatment induced an increased signal

in the CF compared to untreated cells and a shift of the recovery curve (CST:76±3%; PTX: 93±3%), meaning that the competitive effect of PTX with Tau caused the CST delocalization from the MTs to the cytosol (Figure 3.3A-B). FRET analysis showed a loss of NFRET signal in soluble Tau similar to the one observed with nocodazole treatment (PTX: 5.14±0.61SE), supporting the fact that Tau assumes a relaxed conformation in the cytoplasm in a way independent from the integrity of the MT network. In conclusion, these results demonstrated that, in the cell, Tau molecule bound to MTs assumes a structured hairpin folding conformation, while it remains as an unstructured protein when it is not bound to MTs.

3.2 Pathological point mutations alter Tau mobility and conformation

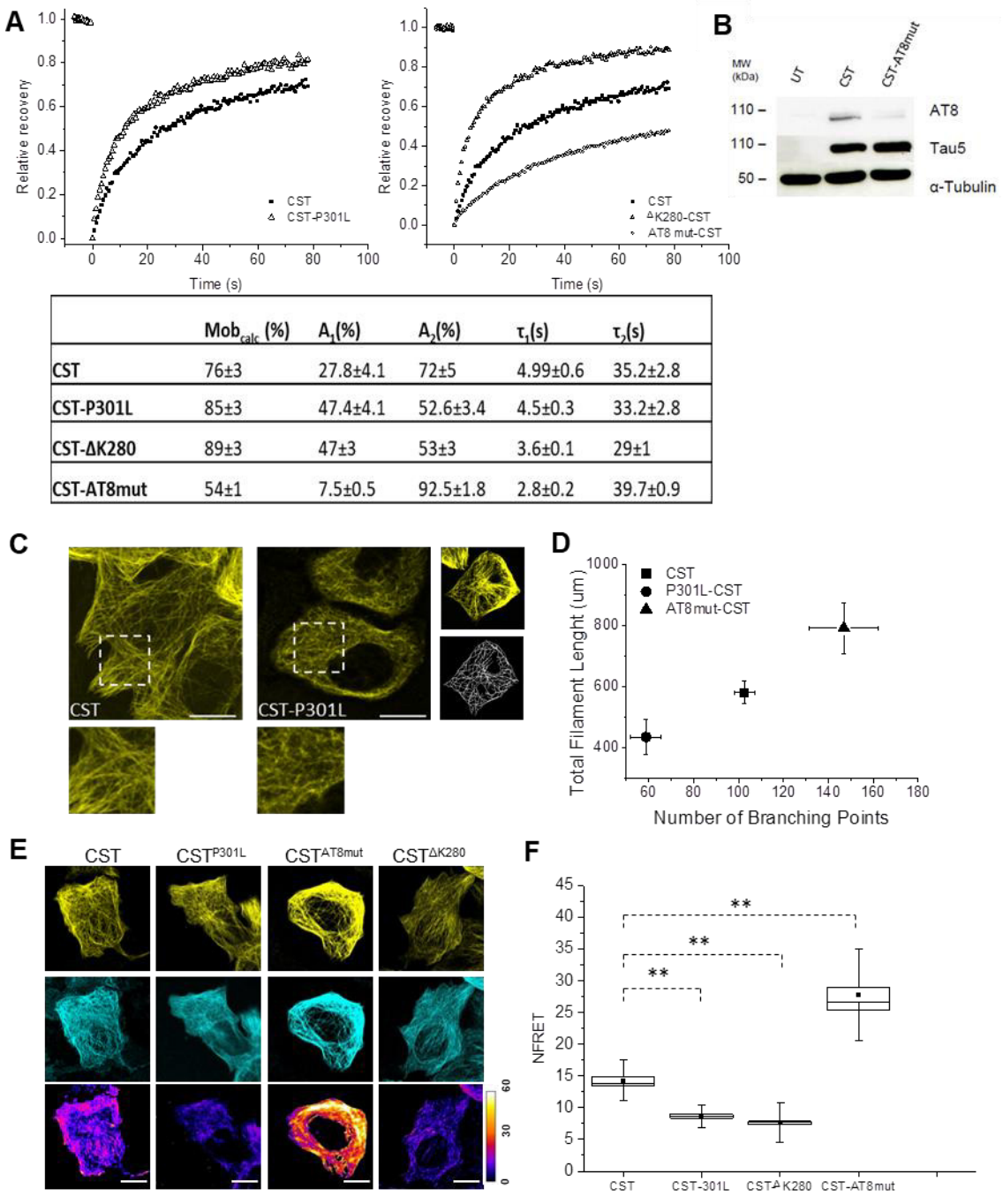

	Mob_{calc} (%)	A_1(%)	A_2(%)	τ_1(s)	τ_2(s)
CST	76±3	27.8±4.1	72±5	4.99±0.6	35.2±2.8
CST-P301L	85±3	47.4±4.1	52.6±3.4	4.5±0.3	33.2±2.8
CST-ΔK280	89±3	47±3	53±3	3.6±0.1	29±1
CST-AT8mut	54±1	7.5±0.5	92.5±1.8	2.8±0.2	39.7±0.9

Figure 3.4. Point mutations alter Tau conformation and mobility. A. FRAP relative recovery curves of CST, CST^{P301L}, $CST^{\Delta K280}$ and CST^{AT8mut} and related mobility analysis. B. Phospho-AT8 epitope detection by western blot of cells expressing CST or CST^{AT8mut}. C. Example of network analysis by confocal imaging of reporter cells (Acceptor channel, yellow) expressing CST and CST-P301L. White boxes are image magnifications. D. Morphological analysis of fluorescent network density in reporter cells expressing CST (n = 10), CST^{P301L} (n = 10) and CST^{AT8mut} (N=10). Data shown are mean and SEM. E. NFRET images (false colour), donor (Blue), acceptor (yellow) of reporter cells. White scale bar = 10 µm. F. NFRET quantification along MTs of cells

expressing CST (n = 40), CST^{P301L} (n = 35), CST^{DK280} (n = 20) and CST^{AT8mut} (n = 20). Box spans the standard error of the mean (black square) while whiskers indicates the standard deviation (**p < 0.01 ANOVA one-way test).

In order to characterize the effect of mutations related to tauopathies on Tau conformation, we mutated the CST with the destabilizing P301L or ΔK280 point mutations (Dayanandan et al., 1999; Hasegawa et al., 1998a; Hutton, 2006; Momeni et al., 2009; Spillantini et al., 1998b). Moreover, we investigated the effect of the mutation at the AT8 epitope (AT8mut) by substituting the unphosphorylatable aminoacid Ala to Ser199, Ser202 and Thr205 commonly phosphorylated in pathological conditions (Bertrand et al., 2010; Bibow et al., 2011; Braak et al., 1994). Reporter cells expressing the different Tau mutants were analysed by FRAP experiments, to analyse the effect on Tau motility. Recovery curves revealed that CST^{P301L} and $CST^{\Delta K280}$ displayed an overall higher mobile fraction with respect to CST^{WT} indicating that the destabilizing mutations increase Tau mobility. Remarkably, the rapid diffusion phase doubled, highlighting that these mutations have an impact on the balance between diffusive and binding phases. The time constants of both diffusing and bound phases were not altered, indicating that the CST integrity was maintained (Figure 3.4A). As seen by Western blot experiments, the CST was partially phosphorylated at the AT8 epitope (Figure 3.4B). Phospho-AT8 is associated to a reduced affinity of Tau with tubulin, MTs destabilization and Tau aggregation (Bertrand et al., 2010; Bibow et al., 2011; Braak et al., 1994). In order to impede the destabilization induced by this modification, we mutated the AT8 epitope with alanine to prevent the phosphorylation and then we analysed the effect on the CST (Figure 3.4B). FRAP measurements on this mutant revealed that the CST^{AT8mut} FRAP recovery curve was slower than that of CST^{WT} (CST^{WT}: 76±3; CST^{AT8mut}: 54±1), thus indicating a lower mobile fraction (Figure 3.4A). This result suggested that the prevention of AT8 phosphorylation increases the stability of Tau on MTs. Furthermore, to investigate the impact of different mutations on MTs organization, a network analysis was performed by exploiting the IMARIS software. The total filament length and the number of branching points of the MT network were considered. Reporter cells expressing the destabilizing mutation CST^{P301L} showed a significant reduction of both parameters compared to CST^{WT}, resulting in a reduced MT network complexity. On the contrary, CST^{AT8mut}, which

increases the stability of Tau on MTs, resulted in a network with a higher complexity then cells expressing CST^{WT}, as indicated by the significant increase in filament length and branching points (Figure 3.4C-D). These results confirmed that Tau mutations can alter the affinity of Tau to MTs thus influencing the MT network complexity. In order to investigate whether the different affinities for MTs could correspond to different Tau conformations we performed a FRET analysis. We observed a significant reduction of NFRET signal on MTs for CST^{P301L} and $CST^{\Delta K280}$ compared to CST^{WT} (CST^{P301L}: 8.21±0.41SE; $CST^{\Delta K280}$: 7.44±0.29SE) indicating that the destabilizing mutations P301L and ΔK280 not only affect Tau binding with tubulin but also alter Tau conformation on MTs (Figure 3.4E-F). This result indicates that Tau pathological mutants, even when associated to MTs, have a conformation that disadvantages FRET events. On the contrary, the stabilizing mutation AT8mut led to a significant increase of the NFRET signal (CST^{AT8mut}: 28.84±1.54SE) indicating that the terminal ends of CST^{AT8mut} bound to MTs are closer than CST^{WT} (Figure 3.4E-F). Overall these results demonstrate that the pathological mutations P301L and ΔK280 consistently alter both the protein conformation and the interaction of Tau with MTs, conferring it an increased mobility. On the other hand, the mutant CST^{AT8mut} assumes a conformation where N- and C-termini interaction is favoured and which is also associated to a slower mobility and a higher stability of Tau on MTs.

3.3 The pathological mutation Q336H increases the stability of Tau on MTs

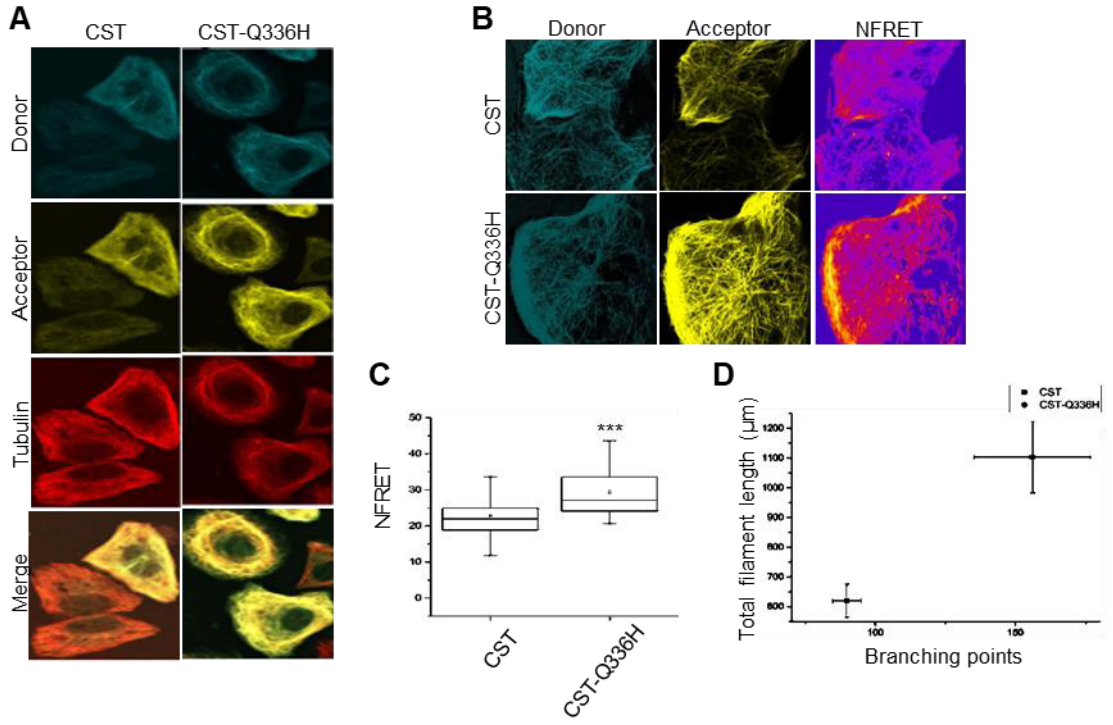

Figure 3.5. The pathological mutation Q336H promotes a closer loop conformation of Tau and a more complex network. A. Imaging of HeLa cells expressing CST or CST^{Q336H} and signal localization along MTs. Donor (blue), acceptor (yellow), tubulin (red). B. NFRET images (false color), donor (Blue), acceptor (yellow) of reporter cells. C. NFRET quantification of cells expressing CST (n = 20) and CST^{Q336H} (n = 20). Box spans the standard error of the mean (black square) while whiskers indicates the standard deviation (***p < 0.001 t-student test). D. Morphological analysis of fluorescent network density in reporter cells expressing CST (n = 10) and CST^{Q336H} (N=10). Data shown are mean and SEM.

The CST demonstrated to be a very sensitive and reliable tool in detecting the stability and conformation of Tau, thus it is possible to exploit it to clarify the effect of pathological mutations still not properly characterized. With this purpose, we selected a Tau mutation, discovered in a patient affected with Pick's disease, whose effect on Tau behaviour has not been investigated, the missense Q336H mutation. *In vitro* experiments revealed that Tau^{Q336H} promotes tubulin polymerization more than Tau^{WT}, an uncommon behaviour for Tau pathological mutations previously described (Tacik et al., 2015). Colocalization experiments on HeLa cells expressing CST^{Q336H} showed that the mutated protein is localized on MTs (Figure 3.5A). FRET analysis indicated that the CST^{Q336H} displayed a significant higher NFRET compared to cells expressing CST^{WT} suggesting that this mutation induced a folding with a reduced distance between the terminal

ends of Tau (Figure 3.5B-C). To further evaluate the impact of this mutation on MT network, we performed a network analysis on total filament length and on the number of branching points, in cells expressing CST^{WT} or CST^{Q336H}. Remarkably, CST^{Q336H}-cells showed a significant increase in both filament length and branching points, indicating that this mutation is clearly associated to a higher complexity of the MT network (Figure 3.5D), an opposite result compared to the effect of the P301L or DK280 mutations previously described. In conclusion, the exploitation of CST for the characterization of the Q336H mutation revealed that this mutation related to Pick's disease, leads to a closer conformation of Tau molecule and to a higher MT complexity suggesting a stabilizing effect that is quite uncommon for Tau pathological mutations.

3.4 CST is sensitive to Tau aggregation

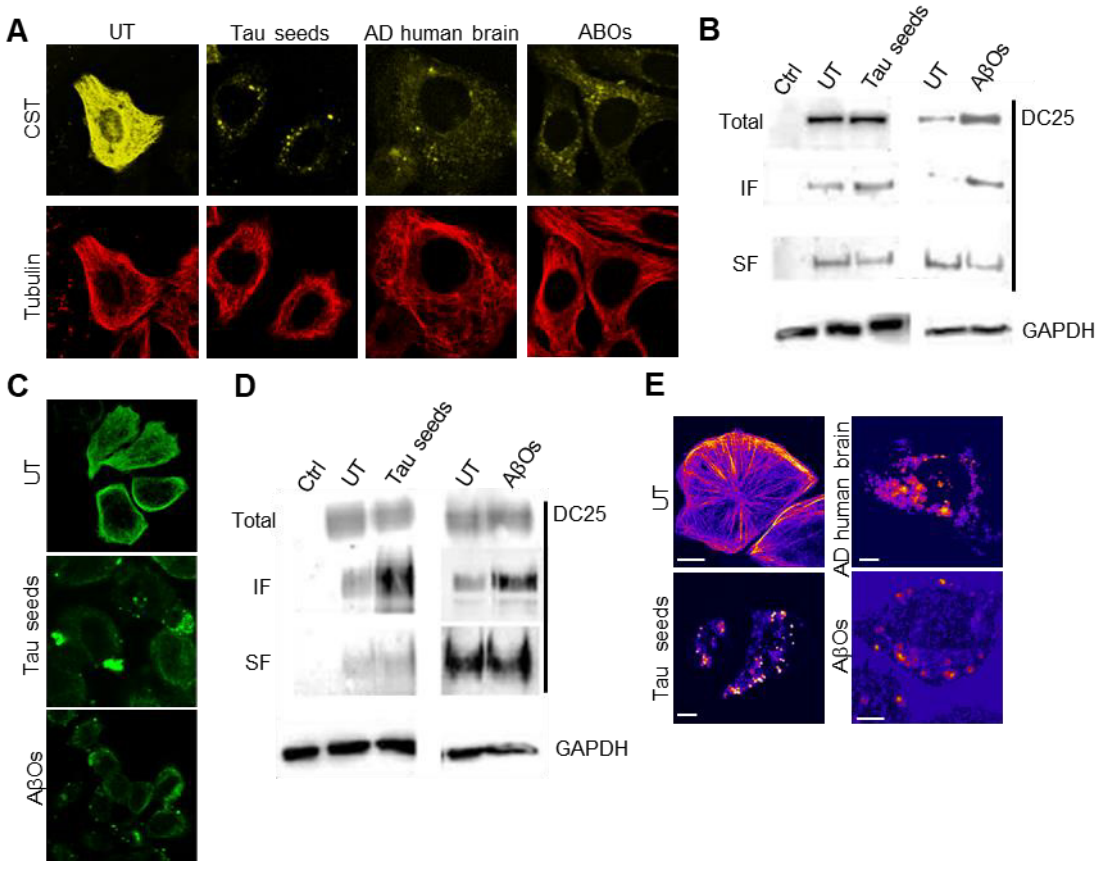

Figure 3.6. CST is sensitive to pathological aggregation in cells treated with homotypic or heterotypic seeds. A. Imaging of CST expressing cells untreated (UT) or treated with AD human brains, Tau seeds or AβOs. CST reporter cells have been treated for 48h with Tau seeds 200nM, for 96h with 10µg of AD human brain lysate or with AβOs. Tubulin is represented in red B. Western blot of Sarkosyl soluble (SF) and insoluble fractions (IF) of reporter cells treated with Tau seeds or AβOs. C. Immunofluorescence of Tau expressing cells treated with Tau seeds (middle

panel) and AβOs (lower panel). Cells expressing unlabeled Tau are stained with anti Tau13 antibody (green). D. Western blot of Sarkosyl soluble (SF) and insoluble fractions (IF) of cells expressing unlabeled Tau and treated with Tau seeds or AβOs. E. FRET images of untreated and treated reporter cells.

Several studies demonstrated that misfolded Tau drives its aggregation and spreading in tauopathy disease progression. We exploited the CST sensor to detect seeding induced by agents potentially involved in Tau self-aggregation. To this aim, CST reporter cells were first exposed to synthetic Tau seeds added in culture medium. Synthetic seeds have been prepared from 4R recombinant Tau fragment (297-391) (Kontsekova et al., 2014). As expected, after 48h treatment, CST was completely displaced from MTs and cytoplasmic inclusions appeared (Figure 3.6A). CST reporter cells were then exposed to protein extracts from AD human brains. Lysates from AD brain induced a significant relocalization of Tau forming intracellular Tau aggregates. Remarkably, the MT network was not grossly altered by Tau displacement as demonstrated by IF (Figure 3.6A). AD brain lysates contain many different components that might potentially act as seeds for Tau aggregation, including other misfolded proteins such as the Aβ peptide. In order to verify whether the seeding is specific for Tau, or whether other factors are also responsible for Tau aggregation, we treated CST reporter cells with preparations containing Aβ oligomers (AβOs). AβOs produced by the 7PA2 fAD cell line (CHO cells overexpressing fAD human V717F APP mutant) and collected from the cellular supernatant have been used. The treatment of reporter cells with AβOs induced a significant relocalization of CST and the formation of fluorescent aggregates (Figure 3.6A). In order to confirm by a molecular approach that the observed CST-positive inclusions contain aggregated Tau proteins, the sarkosyl fractionation of the CST reporter cells treated with Tau seeds or with AβOs has been performed. Western blot analysis of the sarkosyl extracts with the anti-Tau DC25 antibody, showed a significant presence of full length CST into the sarkosyl-insoluble fraction in both treated samples, with a concomitant decrease of CST in the soluble fraction (Figure 3.6B). Taken together, these results indicate that full length Tau undergoes aggregation in response to homotypic seeding, by Tau seeds, and also in response to heterotypic seeding, by cell supernatants containing AβOs. To further verify that the AβOs mediated aggregation is not due to the peculiar structure of CST, we repeated the experiments in cells expressing unlabeled Tau.

The immunofluorescence for Tau in AβOs- or Tau- treated cells confirmed that AβOs induces Tau relocalization and aggregation as effectively as Tau seeds (Figure 3.6C). The analysis of sarkosyl-insoluble and soluble fractions showed that full length Tau accumulates into insoluble fractions in both conditions, confirming the ability of AβOs to induce Tau aggregation (Figure 3.6D). This result further confirms that the fluorophores into the CST construct do not alter the conformational changes that Tau undergoes during neurodegeneration. In order to characterize the CST response when aggregation is induced, we performed FRET experiments in reporter cells treated with AD human brain extracts, Tau seeds or AβOs. We observed that all the treatments caused the formation of intracellular CST aggregates displaying positive FRET signals (Figure 3.6E). Moreover, since the CST interaction with tubulin was impaired, the FRET signal was lost on MTs. This evidences indicate that the CST is sensitive to pathological aggregation and provides an imaging output represented by the FRET-positive signal caused by the strong proximity between CST molecules. Taken together, these results indicate that Tau undergoes aggregation in cells, in response to synthetic Tau seeds as well as to complex lysates derived from brains of Alzheimer's disease patients. Heterotypic seeding by AβOs is also observed. Moreover, the CST is able to provide information about the molecular state of Tau discriminating between physiological, destabilizing and aggregation conditions.

3.5 Development of a CST-based screening platform *in vitro*

The CST has been demonstrated to be a multifunctional tool able to investigate Tau behaviour by several approaches. Due to its ability in discriminating different conditions of Tau molecular degeneration, we applied the sensor to develop a cell-based platform to test compounds able to alter Tau aggregation. With this purpose, we expressed the CST in two cell lines. First, we used HeLa cells, for the characterization and optimization of the system, then, we used differentiated SHSY5Y cells to test the compounds in a cellular background closer to the neuronal one. We performed two different protocols for Tau aggregation, to identify the one inducing the higher formation of CST inclusions and guaranteeing the higher reproducibility. For the first protocol the CST^{WT} was expressed in HeLa cells and aggregation was induced by the synthetic seeds (297-391) from Tau^{WT}

as previously described. For the second protocol we expressed CST^{P301S} and delivered recombinant heparin-assembled Tau^{P301S} fibrils to induce aggregation (see **Materials and methods**). We observed that aggregation occurred with both protocols but its extent and reproducibility was much higher by employing the CST^{P301S}. Indeed, it has been reported also in recent papers that exploiting Tau seeds with the P301S mutation bursts the aggregation in cell cultures (Strang et al., 2018). For this reason, the development of the screening system has been performed in the second condition.

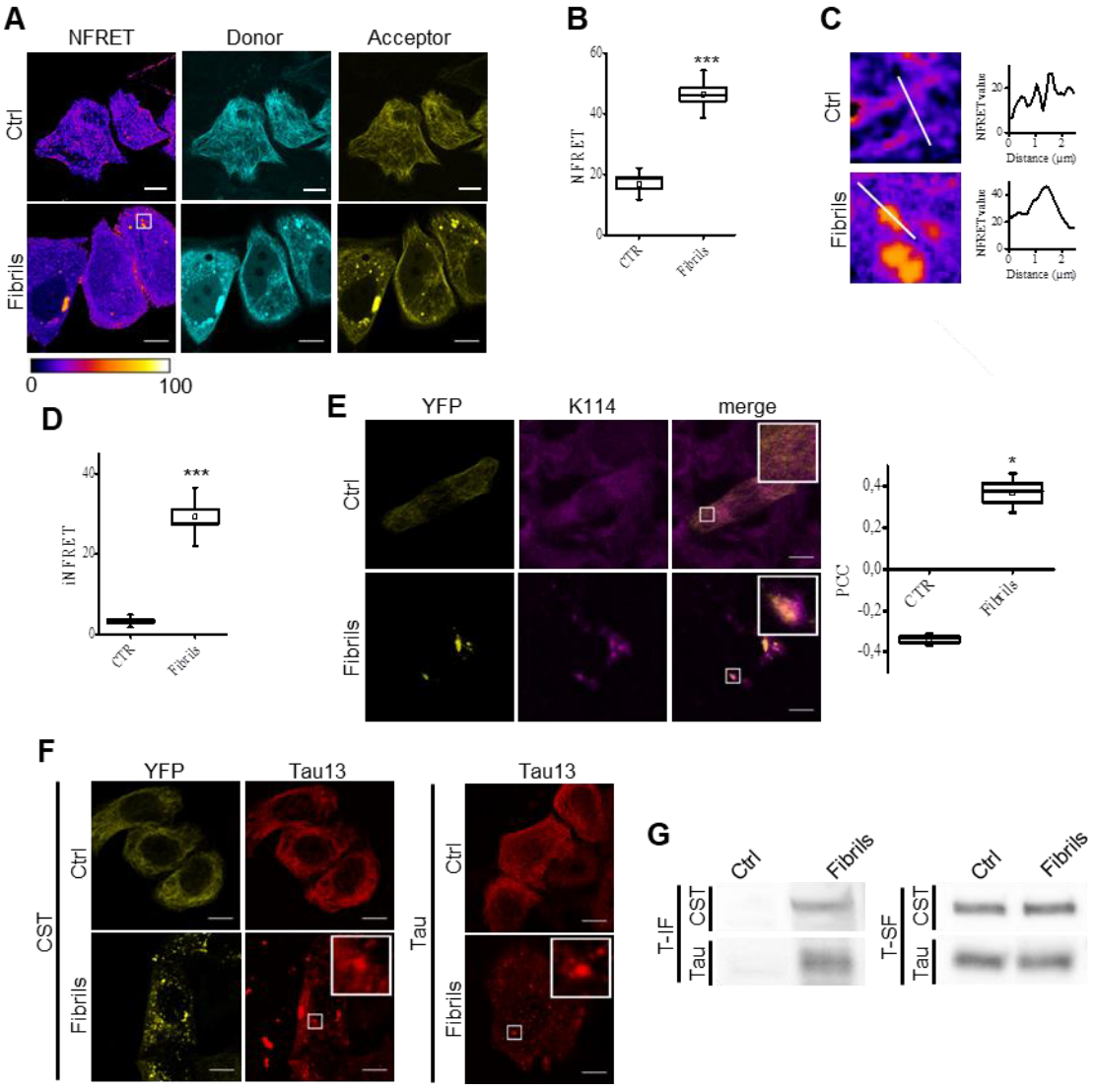

Figure 3.7. CST forms FRET-positive amyloidogenic aggregates. A. FRET images of CST^{P301S} cells untreated or treated with heparin-Tau^{P301S} aggregates (t-student test, *** p<0.001). B. NFRET quantification of A. C. Integrated NFRET (iNFRET) analysis of controls and CST aggregates. D. iNFRET quantification of controls and CST aggregates (t-student test, *** p<0.001). E. K114 staining of control or CST-aggregated reporter cells and colocalization quantification. Box spans the standard error of the mean (black square) while whiskers indicates

the standard deviation (*p < 0.05 t-student test). F. Immunofluorescence of untreated and treated cells expressing CST^{P301S} or Tau^{P301S}. Tau is detected by the Tau13 antibody (red). G. Fractionation of treated or untreated cells expressing CST^{P301S} or Tau^{P301S}. Left panel represents the Triton-X insoluble fraction (T-IF) while the right panel represents the Triton-X soluble fraction (T-SF).

Quantitative sensitized emission FRET microscopy was employed for the detection of intracellular aggregates. After CST^{P301S} aggregation, we observed the detachment of the sensor from MTs and the formation of inclusions displaying a FRET-positive signal (Figure 3.7A). NFRET values on aggregates were significantly higher than those on MTs and this might be due to because the high amount of molecules contributing to the FRET signal (Figure 3.7B), consistent with the features of an aggregate. In order to take into account at the same time the close interaction between Tau molecules and the differences in the dimension of the aggregate, the integrated NFRET signal (iNFRET) has been considered. Lines crossing MTs or aggregates were selected and NFRET profile was obtained. The integral under the curve was designed to be iNFRET (Figure 3.7C). iNFRET values on aggregates were significantly higher than those on MTs as expected (Ctrl: 3.08±0.55SE; Fibrils: 26.65±2.23SE. Figure 3.7D). To characterize the amyloidogenic nature of CST-positive intracellular aggregates, we performed a K114 staining for β-sheet fibrils (Crystal et al., 2003). Remarkably, CST signal significantly colocalized with K114 signal in the aggregates (Costes et al., 2004), confirming that CST aggregates share structural characteristics with pathological Tau aggregates (Figure 3.7E). Additionally, to demonstrate that the presence of the fluorophores on the CST do not impact on aggregation, an immunofluorescence experiment employing anti-Tau antibody was performed in cells expressing CST^{P301S} or Tau^{P301S}. Cells were treated with Tau^{P301S} fibrils and CST or Tau aggregates were detected by using a pan-Tau antibody. In both cases, aggregation was observed in treated cells while it was not detectable in untreated cells (Figure 3.7F). The result suggests that in the two conditions the aggregates have similar morphology indicating that the fluorophores do not interfere with the process of aggregation. Finally, detergent fractionation was performed to find out whether there were biochemical differences between CST^{P301S} and Tau^{P301S} aggregates. CST and Tau were increased in the Triton X-100 insoluble fraction upon treatment with preformed fibrils revealing a similar behaviour (Figure 3.7G). Altogether these results

suggest that the CST forms amyloidogenic aggregates similar to those formed by Tau and that it provides an output, the FRET signal, applicable in a cell-based platform.

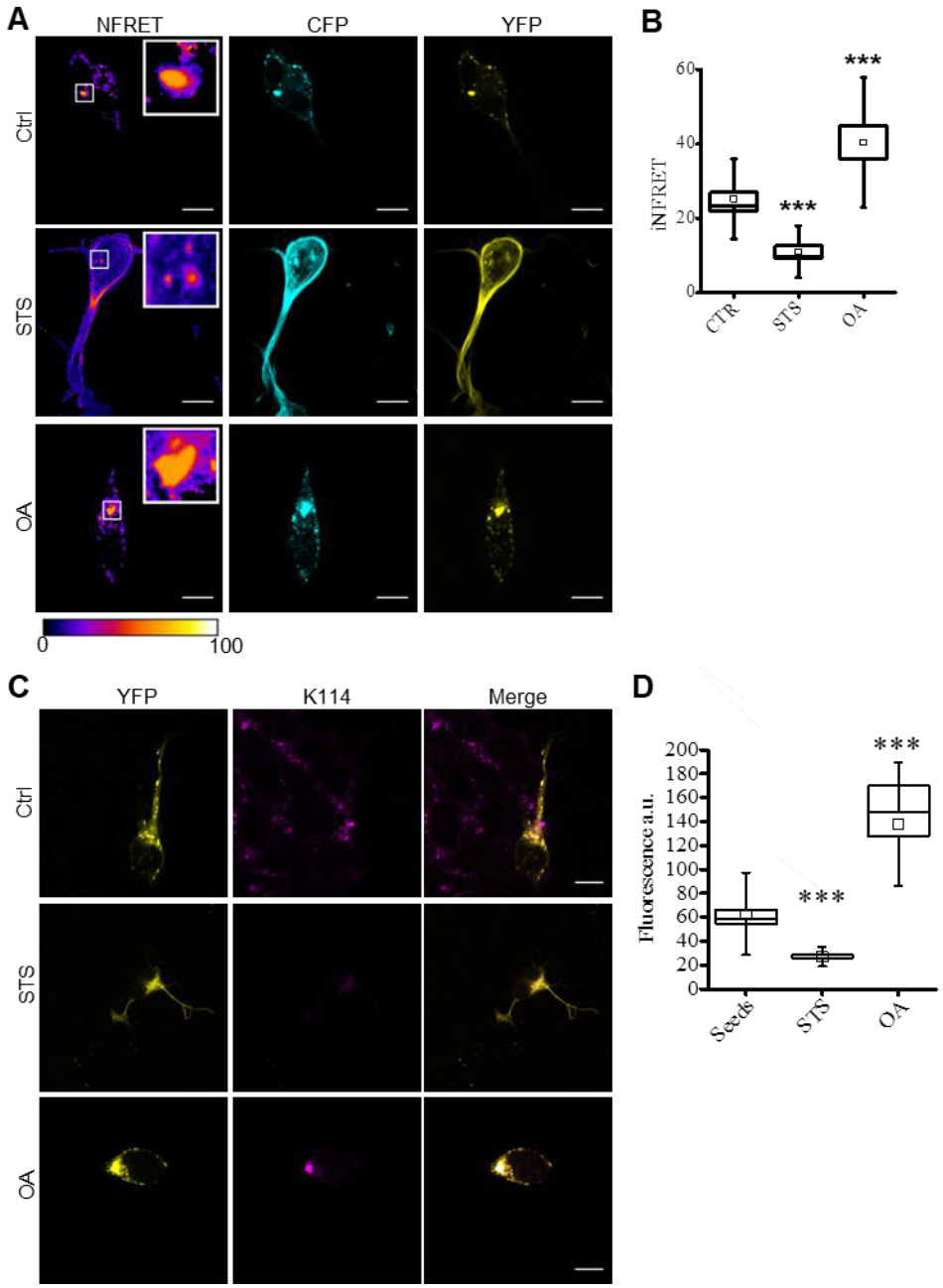

Figure 3.8. CST-based cellular platform is sensitive to compounds altering Tau phosphorylation. A. NFRET images of aggregated CST cells untreated or treated with staurosporine (STS) or okadaic acid (OA). B. iNFRET quantification of cells reported in A (ANOVA test, *** $p<0.001$). C. K114 staining of untreated or STS/OA treated cells and colocalization with the CST aggregates. D. Fluorescence quantification of K114 positive aggregates reported in C (ANOVA test, *** $p<0.001$).

The peculiar characteristics of the CST provide a reliable tool to quantify Tau aggregation in terms of structure and stability of the aggregate. After characterization of CST aggregation in HeLa cells, we chose differentiated SHSY5Y as the cellular system to develop the CST screening platform. This choice was established since Tau aggregation occurs prevalently in neurons and a cellular background close to the neuronal one is more reliable to test compounds against pathological Tau behaviour. Treatment of differentiated SHSY5Y expressing CST^{P301S} with Tau^{P301S} fibrils caused the delocalization of the sensor and its aggregation as already observed in HeLa cells. In order to optimize the cell-based platform, the effect of kinases on Tau aggregation has been evaluated since hyperphosphorylation is one of the main post-translational modifications involved in inducing and stabilizing Tau aggregate, as previously described.

After the formation of CST inclusions, cells are treated with staurosporine (STS) or okadaic acid (OA). STS is a non-specific protein kinases inhibitor which prevents Tau phosphorylation and is used here as a negative control for aggregation. OA, the positive control for aggregation, is an inhibitor of protein phosphatase PP2A and it induces Tau hyperphosphorylation. As expected, the iNFRET was significantly reduced in STS-treated cells suggesting a weaker interaction between Tau molecules and a smaller dimension of the aggregates (Figure 3.8A-B). On the contrary, the iNFRET was significantly increased in OA-treated cells compared to controls, indicating an increase in the aggregation and a stronger interaction between Tau proteins (Figure 3.8A-B). In order to verify that this finding was due to structural changes in the aggregates, K114 staining for β-sheet fibrils has been performed (Figure 3.8C). The intensity distribution of the pixels in the cells indicates that the K114 signal was significantly lower in STS-treated and it was significantly higher in OA-treated cells compared to controls (Figure 3.8D). These results support the fact that the CST cell-based platform is able to discriminate between different drugs affecting aggregation providing information about the stability and the dimension of aggregates. This optimization was followed by the application of the system to test the effect of two candidate compounds.

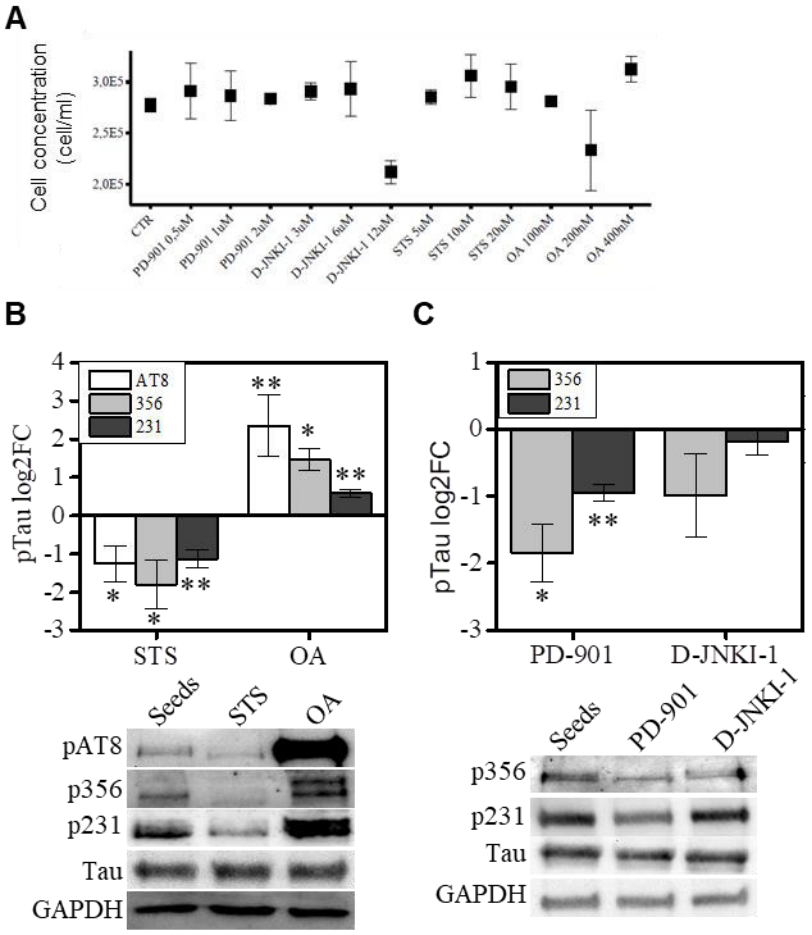

Figure 3.9. Kinase inhibitors are not toxic for cells and reduce Tau phosphorylation. A. Survival curve of reporter cells treated with PD-901, D-JNKI-1, staurosporine (STS) and okadaic acid (OA). B. Western blot and relative quantification of phosphorylated Tau residues in reporter cells expressing aggregated CST and treated with staurosporine (STS) or okadaic acid (OA). C. Western blot and relative quantification of phosphorylated Tau residues in reporter cells expressing aggregated CST and treated with PD-901 or D-JNKI-1.

In order to identify potential therapeutic molecules which could reduce Tau aggregation, we tested two kinase inhibitors in the CST cell-based system: PD-901, an ERK pathway inhibitor, and D-JNKI-1, a JNK1 inhibitor (Henderson et al., 2011; Hirt et al., 2004; Milano et al., 2007; Yap et al., 2011). The survival curve of cells treated with increasing concentration of compounds suggests that at the working range of concentrations, the drugs are not toxic for cells (Figure 3.9A). To verify the effect of the compounds on phosphorylation, reporter cells treated with Tau^{P301S} fibrils were exposed to PD-901 or D-JNKI-1 and to STS or OA as a control. Western blot experiments showed that PD-901 decreased phosphorylation at Thr231 and Ser356 residues, whose phosphorylation is usually associated to pathological aggregation (Figure 3.9C).

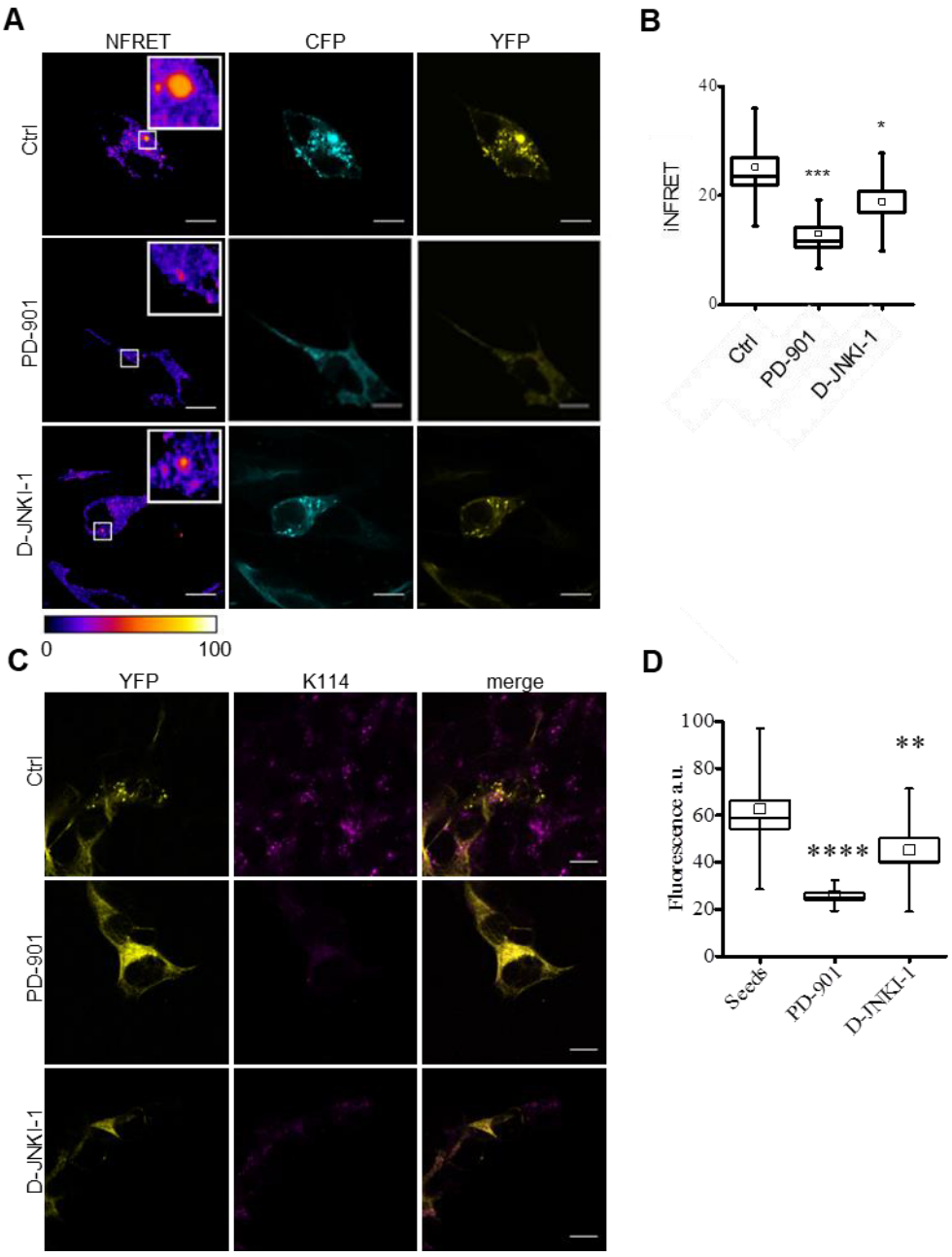

Figure 3.10. PD-901 is able to reduce CST aggregation. A. NFRET images of aggregated CST cells untreated or treated with PD-901 or D-JNKI-1. B. iNFRET quantification of cells reported in A (ANOVA test, *** p<0.001, *p<0.05). C. K114 staining of untreated or PD-901/D-JNKI-1 treated cells and colocalization with the CST aggregates. D. Fluorescence quantification of K114 positive aggregates reported in C (ANOVA test, **** p<0.0001; ** p<0.01).

To investigate the potential therapeutic effect of the drugs, upon aggregation induction, reporter cells were treated with PD-901 and D-JNKI-1 and quantitative sensitized emission FRET microscopy was employed to quantify aggregation. The iNFRET of the aggregates was significantly reduced in cells treated with PD-901 or D-JNKI-1 than in controls (Figure 3.10A-B), suggesting that the inhibition of ERK or JNK pathways is able to impair Tau aggregation. Remarkably, the

effect of PD-901 in destabilizing Tau aggregates was stronger than D-JNKI-1, resulting in a more efficient candidate compound (PD-901: 13.26±1.31SE; D-JNKI-1: 19.16±1.57SE). In order to verify this finding, K114 staining for β-sheet fibrils was performed. The intensity distribution of K114 signal was significantly lower in PD-901-treated cells than controls, while no significant difference could be detected between D-JNKI-1 and controls (Figure 3.10C-D). This effect might be caused by a weaker effect of D-JNKI-1 in altering aggregates. Altogether, these results point out that CST is a powerful tool to detect and quantify Tau aggregation. Moreover, the PD-901 could be a potential therapeutic agent to block or even to revert Tau aggregation, while D-JNKI-1 shows a little therapeutic effect.

3.6 Development of an *in vivo* screening platform based on the CST

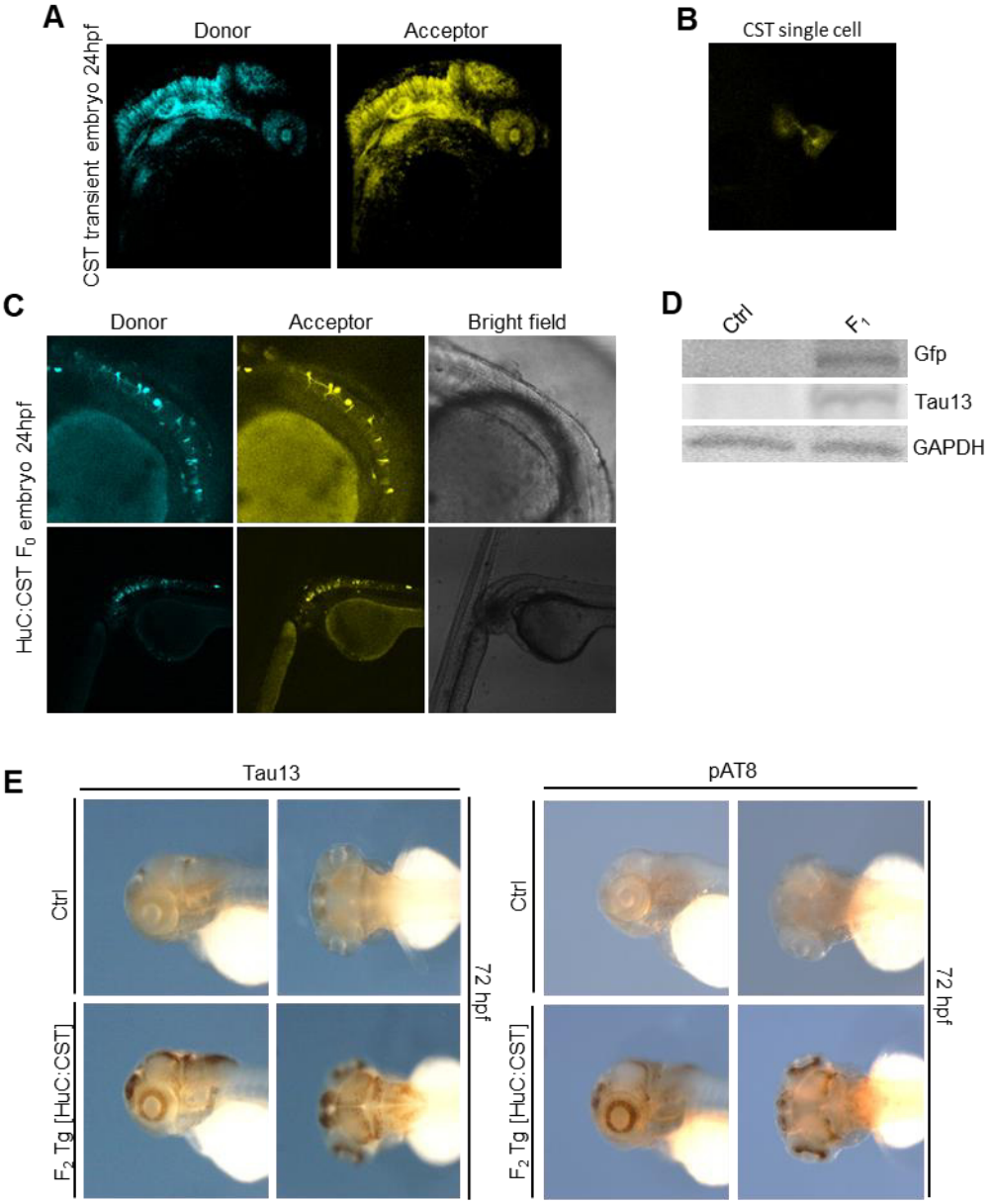

Figure 3.11. Development of a transgenic zebrafish expressing the CST. A. Confocal imaging at 24hpf of donor and acceptor channels of a zebrafish embryo microinjected with the CST mRNA. B. Single-cell imaging of the zebrafish embryo represented in A. C. CST imaging of the F_0 transgenic line expressing the CST under the HuC promoter at 24hpf. D. Western blot of control and F_1 transgenic line at 72hpf. E. IHC of F2 embryos at 72hpf and staining with Tau13 and phosphor-AT8 antibody. Experiments performed in collaboration with Miriam De Sarlo and Professor Michela Ori.

The results obtained supported also a possible application *in vivo*. CST is genetically encoded and it can be stably expressed in animal models. In order to develop the CST-*in vivo* model, we employed *D. rerio* (zebrafish). We chose zebrafish since it is an ideal choice for the CST employment due to the

transparency of embryos allowing an easy imaging approach. Moreover, transgenesis in this animal is well-validated and efficient. Finally, previous experiments with zebrafish overexpressing human Tau revealed that, in this model, Tau hyperphosphorylation and aggregation is spontaneous and occurs in a short time span (Bai and Burton, 2011; Bai et al., 2007; Kim et al., 1996; Paquet et al., 2009, 2010; Saleem and Kannan, 2018)

First, to demonstrate that CST is correctly expressed in zebrafish, the zygotes have been microinjected with CST mRNA and embryos have been analysed at 24hpf (hours post fertilization) by confocal imaging. The injection of CST mRNA led to a transient whole embryo expression of the sensor. We observed that CST is correctly expressed in zebrafish embryos, in fact both CFP and YFP fluorophores can be detected (Figure 3.11A) and, at single cell level, CST displays a network typical of Tau protein bound to MTs, as expected (Figure 3.11B). These results support the fact that CST can be used in this system and that it resembles Tau properties also *in vivo*. In order to develop a model based on CST, we cloned the CST^{WT} in a Tol2 plasmid, for the stable integration in zebrafish genome. We chose the HuC promoter which guarantees a durable expression of the sensor specifically in zebrafish neurons. Zebrafish zygotes were co-injected with Tol2-CST plasmid and the mRNA of the transposase, the enzyme which recognizes the Tol2 sequences and integrates the CST in the genome. The F_0 line was selected for the positive fluorescent signal by confocal imaging 24hpf. As shown in figure 3.11C, the F_0 is a chimera which expresses CST only in neuronal cells. Six founders were selected and inbreeded. A preliminary characterization on the F_1 generation was performed. Fluorescence could be detected 24hpf in transgenic zebrafishes and western blot experiments of protein extracts from 72hpf embryos showed that the sensor was correctly expressed and did not undergo proteolytic cleavage (Figure 3.11D). Moreover, immunohistochemistry experiments performed at the same time point confirmed the expression of CST and demonstrated that it was phosphorylated at AT8 epitope (Figure 3.11E). These preliminary analyses showed that CST is correctly expressed in zebrafish model and further characterizations, in particular the optimization of the FRET analyses *in vivo*, will be the basis for the development

of the *in vivo* platform which combines the properties of CST to those of zebrafish model.

3.7 CST is detectable in cellular nuclei and does not display FRET signal

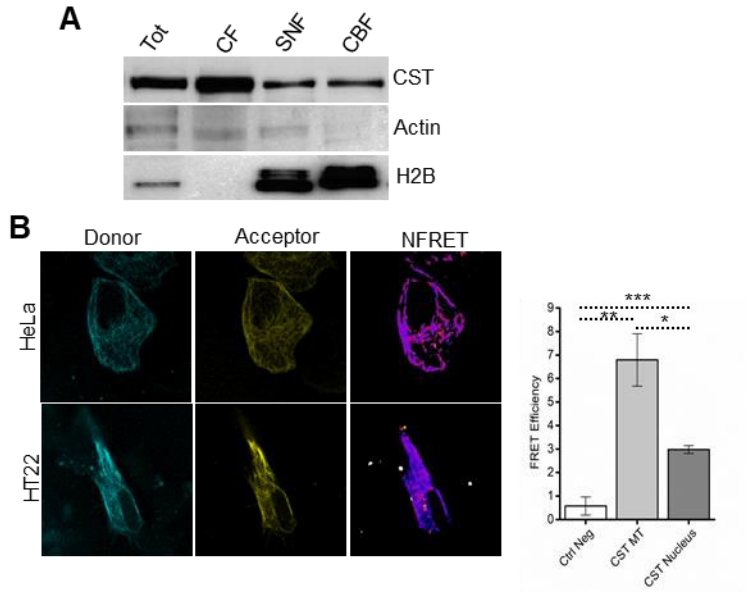

Figure 3.12. the CST is detectable in the nuclear compartment. A. Fractionation and WB of HT22 cells expressing CST. B. FRET images of HeLa and HT22 cells expressing the CST and relative FRET efficiency quantification in the cytosol and in the nucleus

The experimental procedures employed to characterize the CST showed additional evidences about the subcellular localization of Tau. The fractionation protocol, used to obtain the cytoplasmic fraction of cells expressing the Tau sensor also allowed the isolation of a soluble nuclear fraction (SNF) and a chromatin bound fraction (CBF). The analysis of these two fractions indicated the presence of the CST in the nuclear compartment (Figure 3.12A). Even if CST molecules were detectable in the HeLa and HT22 nuclei, the NFRET signal, that is independent from the total number of fluorescent molecules, was absent or extremely low (Figure 3.12B), suggesting that Tau conformation is different in this compartment compared to Tau in the cytosol or bound to MTs. This strong difference between nuclear and cytoplasmic Tau might be caused by the fact that nuclear Tau is soluble or interacts with proteins which modify its conformation.

3.8 Nuclear Tau modulates the VGluT1 expression

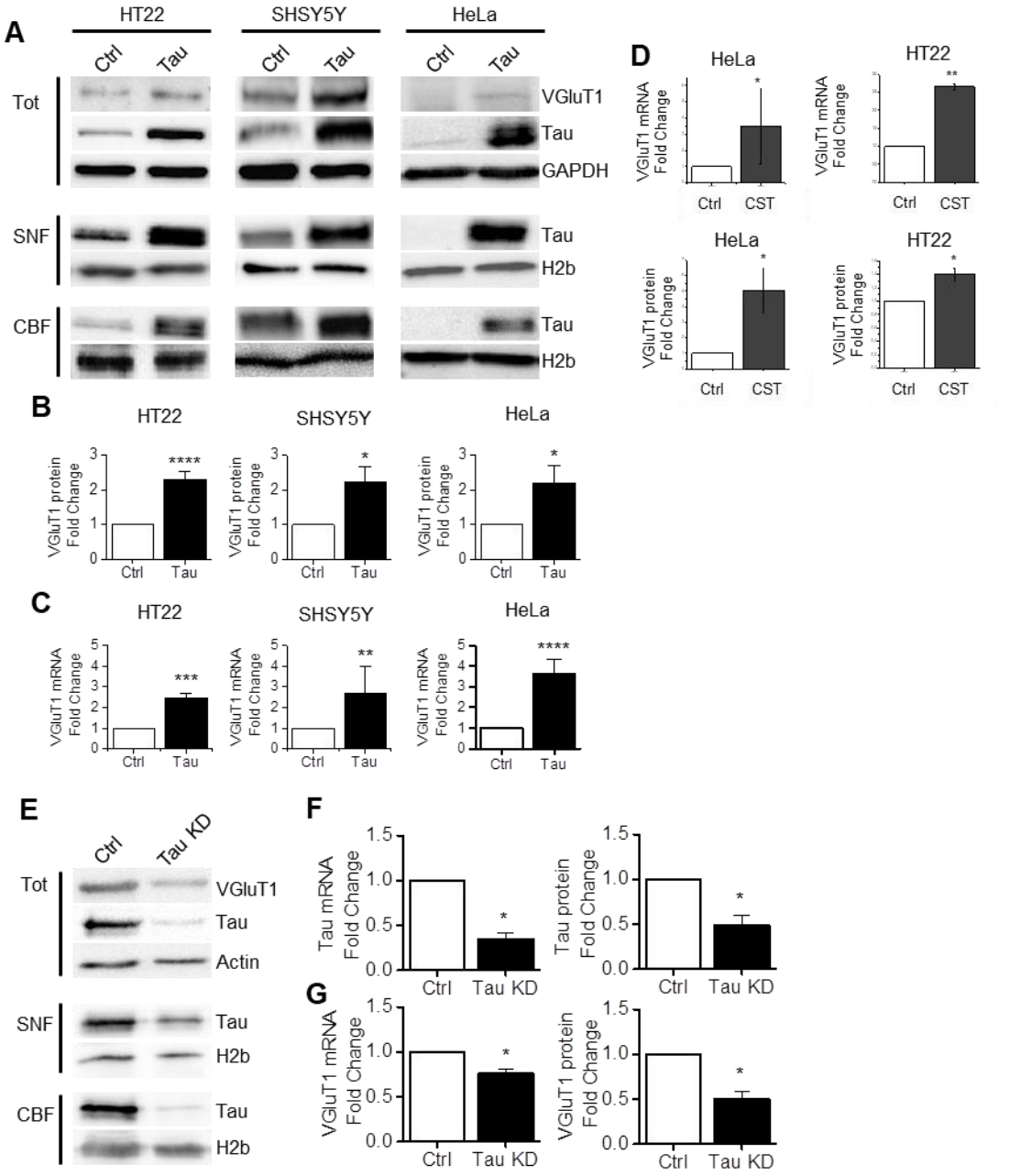

Figure 3.13. Tau alters VGluT1 expression. A. Western blot of total extracts and subcellular fraction obtained from neuronal (HT22 and differentiated SHSY5Y) and non-neuronal (HeLa) cell lines. The 0N4R overexpressed Tau is compared with the corresponding endogenous isoform. B. Quantification of VGluT1 protein level in control and Tau-expressing cells. C. VGluT1 mRNA quantification by qPCR. (Mann–Whitney test; **** p<0.0001; *** p<0.001; ** p<0.01; * p<0.05). D. Quantification of VGluT1 protein and mRNA levels in control and CST-expressing cells. E. Western blot of subcellular fractions obtained from differentiated SHSY5Y cells treated with non-targeting shRNA (Ctrl) or Tau targeting shRNAs (Tau KD). F. Quantification of Tau mRNA and protein levels in control and Tau KD cells. G. Quantification of VGluT1 mRNA and protein levels in

control and Tau KD cells. (Mann–Whitney test; * $p<0.05$). SNF: soluble nuclear fraction; CBF: chromatin-bound fraction.

Since the CST was detected in the nucleus, we verified the presence of unlabelled Tau in this compartment. Tau was detected both in the SNF and CBF and this result led to the question about the function of Tau in that subcellular area. The possible roles of nuclear Tau have been described above but this field is still largely unexplored and it is not clear if nuclear Tau could have a role in modulating gene expression, a function that might be relevant for the pathophysiology of tauopathies. In order to identify its function we investigated the impact of nuclear Tau on the glutamate release pathway which is known to be altered in the early phases of tauopathies (Dickerson et al., 2005; Jadhav et al., 2015; Khadrawyb YA, 2014; Maurin et al., 2014; Revett et al., 2013).

To investigate the role of Tau in the modulation of gene expression, we expressed the CST or the Tau isoform 0N4R in cells expressing (HT22 and differentiated SHSY5Y) and not expressing (HeLa) endogenous Tau. By a subcellular fractionation protocol, we isolated the soluble nuclear (SNF) and chromatin bound (CBF) fractions. The CST and Tau were clearly detectable in the nuclear fraction, both in the soluble and in the chromatin bound one in all the cell lines (Figure 3.12A, 3.13A). Moreover, endogenous nuclear Tau was expressed and detected only in HT22 and SHSY5Y cells as expected (Figure3.13A). To investigate whether Tau can modulate gene expression, we checked the expression of disease-related genes. A growing body of evidence suggests that the glutamate release is altered during the progression of tauopathies, causing an early synaptic hyperexcitability in pre-symptomatic phases (Dickerson et al., 2005; Jadhav et al., 2015; Khadrawyb YA, 2014; Maurin et al., 2014; Revett et al., 2013). We focused on the presynaptic vesicular glutamate transporters (VGluT1) that package glutamate into vesicles for neurotransmitter exocytosis (Martineau et al., 2017; Siksou et al., 2013; Takamori et al., 2000). A significant increase of VGluT1 protein level was observed by western blot (HT22: 2.2±0.26SE Fold Change=FC; SHSY5Y: 2.24±0.44SE FC; HeLa: 2.19±0.49SE FC; Figure 3.13B) in neuronal and non-neuronal cell lines overexpressing Tau. Remarkably, VGluT1 mRNA levels also increased after Tau expression (HT22: 2.46 ± 0.21SE FC; SHSY5Y: 2.69±1.27SE FC; HeLa:

3.6±0.75SE FC; Figure 3.13C). A similar result has been observed in cells expressing the CST, suggesting that the presence of the fluorophores does not affect significantly the gene modulation mediated by Tau (Figure 3.13D). These results indicate that Tau modulates VGluT1 gene expression, in a cell type-independent manner. To support this evidence, we performed a Tau knock-down (Tau KD) experiment by lentiviral delivery of shRNAs in differentiated SHSY5Y. A non-targeting shRNA was used as control. Cells were collected 72h after transduction and analysed to check the mRNA and protein expression of Tau and VGluT1. Tau knockdown in differentiated SHSY5Y cells was very efficient, causing a significant loss of Tau at both the protein and mRNA levels (mRNA: 0.35±0.06SE FC; protein: 0.49±0.11SE FC; Figure 3.13E-F) with respect to control cells. In Tau KD cells a decrease of Tau protein could also be observed in the nuclear fractions (Figure 3.13E). Concomitantly, the expression of VGluT1 was strongly reduced (mRNA: 0.76±0.06SE FC; protein: 0.5±0.08SE FC; Figure 3.13E-G) demonstrating that, at least partly, it depends on Tau expression.

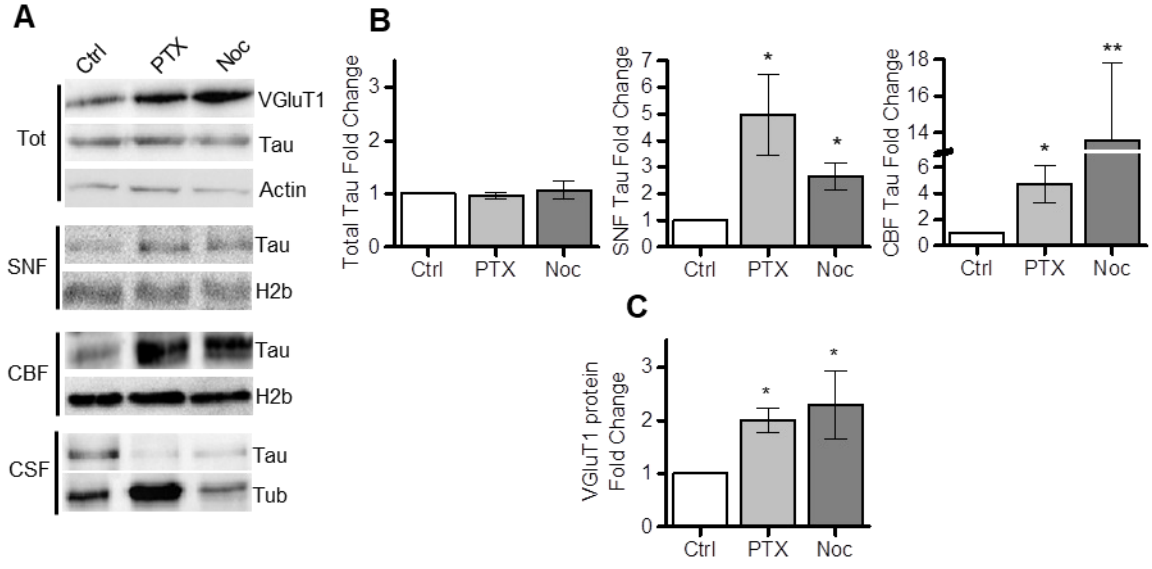

Figure 3.14. Tau displacement from MTs increases Tau nuclear accumulation and VGluT1 expression. A. Western blot of total extracts and subcellular fractions from HT22 untreated and treated cells. PTX (paclitaxel), Noc (nocodazole). B. Quantification of Tau protein levels in total extracts and nuclear fractions. C. Quantification of VGluT1 protein levels (Kruskal–Wallis ANOVA and Mann–Whitney test; ** $p<0.01$; * $p<0.05$).

At the onset of pathology, Tau stability on microtubules is reduced. The increased availability of soluble Tau protein is currently believed to slowly favour the toxic

oligomerization (Braak et al., 1994). We reasoned that this event could shift the equilibrium between Tau pools in the cytoplasmic and nuclear compartments, thus increasing Tau nuclear localization after the displacement from MTs. The overexpression of Tau leads to an increase of the protein amount in all the cellular compartments, including the cytoskeletal fraction, thus providing a condition different from what happens during the pathology progression and which could alter VGluT1 expression for mechanisms partially independent from the nuclear accumulation of Tau. In order to avoid Tau overexpression and to study the effect of the destabilization on nuclear Tau functions, we worked on HT22 cells expressing endogenous Tau which has been destabilized and detached from MTs by treatment with paclitaxel (PTX) or nocodazole (Noc). These drugs increase soluble Tau with two opposite mechanisms: PTX stabilizes MTs and competes with Tau for the same binding pocket on the tubulin dimer, causing its displacement from MTs; nocodazole disassembles the MT network, leading to an increase in soluble Tau (Kar et al., 2003; Di Primio et al., 2017). WB experiments indicated that in HT22 treated cells, a significant increase of Tau levels in both the nuclear fractions could be observed (Figure 3.14A-B). On the contrary, there was a decrease of Tau in the cytoskeletal fraction, as expected (Figure 3.14A). By WB we observed that the increase in the soluble endogenous Tau, both in the cytoplasm and nucleus, determined a concomitant significant increase in VGluT1 expression in PTX- and Noc-treated cells (PTX: 2.0±0.23SE FC; Noc: 2.29±0.64SE FC; Figure 3.14C). These results demonstrate that the destabilization of the endogenous Tau from MTs has a double effect: it favours an increase in the cytoplasmic soluble pool and at the same time Tau is translocated to the nuclear compartment. The downstream effect of this relocalization is an increase in the VGluT1 expression.

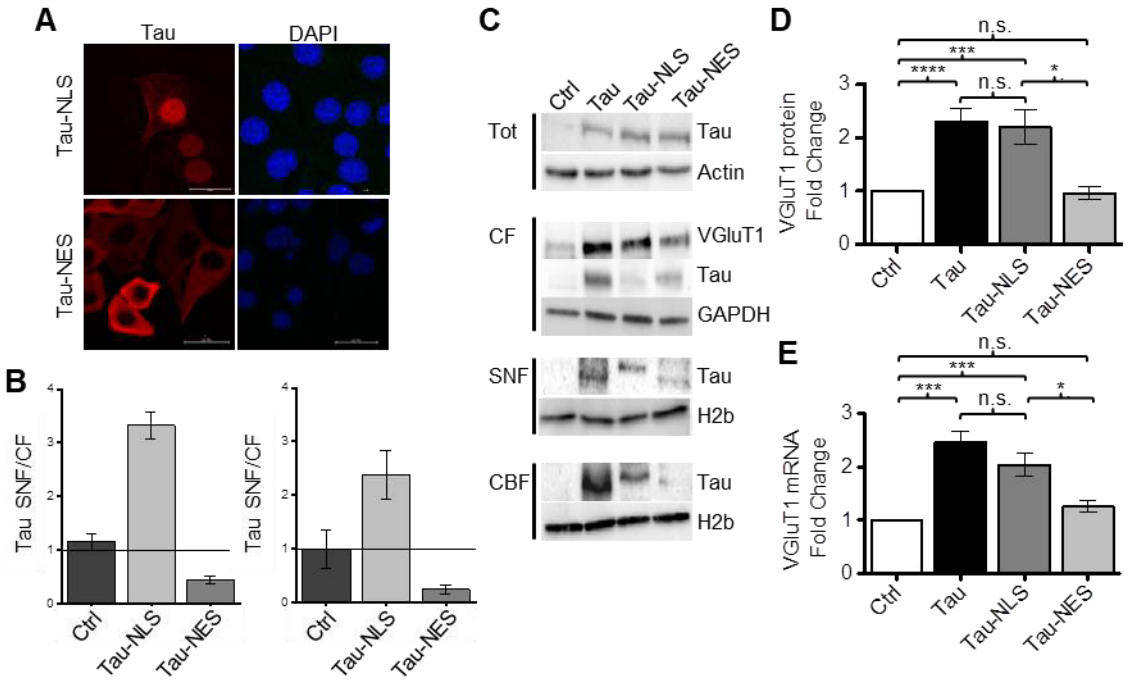

Figure 3.15. VGluT1 increased expression is dependent on nuclear Tau. A. Immunofluorescence of HT22 cells expressing Tau-NLS or Tau-NES. Tau (red), DAPI (blue). B. Quantification of SNF and DBF compared to CF in HT22 cells expressing Tau, Tau-NLS or Tau-NES. C. Western blot of HT22 cells expressing Tau-NLS or Tau-NES. D. Quantification of WB experiments (Kruskal–Wallis ANOVA and Mann–Whitney test; *** $p<0.001$, **** $p<0.0001$, n.s. $p>0.05$). E. VGluT1 mRNA quantification by qPCR in HT22 cells (Kruskal–Wallis ANOVA and Mann-Whitney test; *** $p<0.001$, n.s. $p>0.05$).

To understand if the alteration in VGluT1 levels is mediated by Tau increase in the cytoplasmic or nuclear compartments, we forced the localization of Tau in the nucleus or its retention in the cytoplasm by including a nuclear localization sequence (Tau-NLS) or a nuclear export signal (Tau-NES), respectively. As expected, Tau-NLS prevalently accumulated in the nuclear fraction, while Tau-NES was mainly detected in the cytoplasm (Figure 3.15A-B-C). Tau-NLS induced a significant increase in VGluT1 protein expression (2.0±0.36SE FC) comparable to that induced by untagged Tau. On the contrary, when the nuclear localization of Tau was prevented (Tau-NES), no increase in VGluT1 protein could be observed (Figure 3.15C-D). Likewise, cells expressing Tau-NES showed no increase in the level of VGluT1 mRNA, while cells expressing Tau-NLS showed an increase similar to that observed with untagged Tau (Tau-NLS: 2.04 ± 0.21SE FC; Tau-NES: 1.26 ± 0.12SE FC; Figure 3.15E). These results indicate that Tau proteins translocated into the nucleus regulate the expression of VGluT1.

Accordingly, shifting the equilibrium towards cytoplasmic Tau, by forcing its nuclear export, brings VGluT1 expression back to baseline. Altogether, these evidences demonstrate that nuclear Tau is able to alter the expression of VGluT1 and reasonably of other proteins.

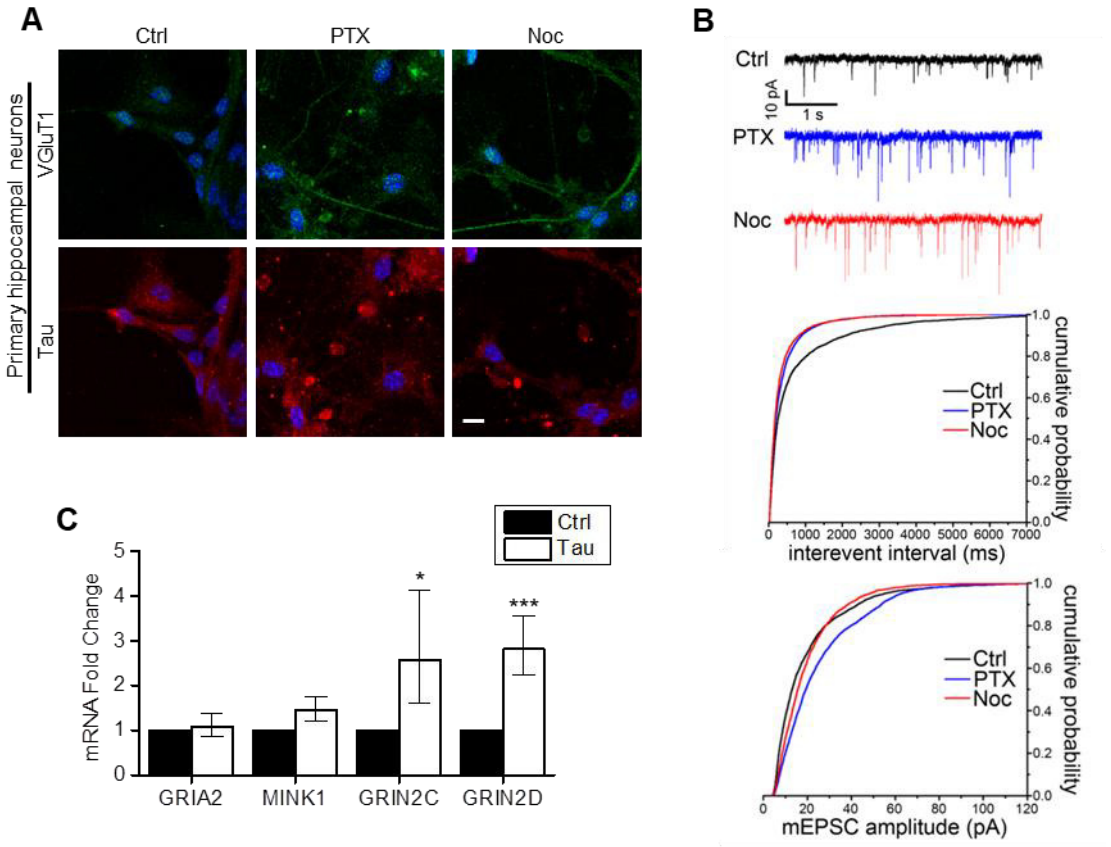

Figure 3.16. Tau displacement from MTs increases VGluT1 expression altering the synaptic transmission. A. Representative confocal imaging of IF in primary neurons. Tau (red), VGluT1 (green), DAPI (blue). B. Cumulative distributions of mEPSC frequency (i.e., interevent interval) and mEPSC amplitude following either PTX or Noc treatment, compared to untreated controls (Ctrl, n = 3002 events from 12 cells; PTX, n = 4911 events from 10 cells; Noc, n = 3576 events from 6 cells; Kolmogorov–Smirnov test, Ctrl versus PTX, $p<0.001$; Ctrl versus Noc, $p<0.001$; PTX versus Noc, $p<0.001$). C. Quantification of differentially expressed genes related to AMPA (GRIA2, MINK1) and NMDA (GRIN2C, GRIN2D) receptors.

The effect of nuclear Tau on VGluT1 expression leads to the question if this alteration might have a real functional impact on neuronal excitability. In order to address this point, we analysed the effect of Tau in primary hippocampal neurons. To induce the destabilization of endogenous Tau, we treated cells with PTX or nocodazole. An increase in VGluT1 expression, detected by IF, was observed in treated primary neuronal cultures (Figure 3.16A). A patch-clamp recordings of spontaneous synaptic transmission (miniature Excitatory

Postsynaptic Currents, mEPSCs) on primary hippocampal neuronal cultures have been performed. Consistent with the increase in VGluT1 expression, a significant increase in mEPSC frequency after either PTX or Noc treatment was observed (Figure 3.16B). This indicates a prevalent presynaptic effect on glutamatergic transmission. In addition, both PTX and Noc also increased the mEPSC amplitude (Figure 3.16B), suggesting an additional post synaptic effect induced by modulating the nuclear Tau pool. In order to assess this possibility, the mRNA levels of AMPA and NMDA receptor subunits were measured in SHSY5Y cells overexpressing Tau by RNAseq experiments (described in details below). GO analysis individuated, among the altered categories, that, after Tau overexpression, the glutamate release pathway was significantly modulated. In particular, among post-synaptic genes, the mRNAs coding for NMDA receptor subunits GRIN2C and GRIN2D were upregulated, while the mRNAs of the AMPA receptor subunit GRIA2 and the AMPA trafficking protein MINK1 were unchanged (Figure 3.16C). Altogether, these results demonstrate that the modulation of the endogenous soluble Tau levels alters VGluT1 expression, as well as that of subunits of the NMDA receptors, thus altering the glutamatergic synaptic transmission.

3.9 Pathological conditions impair Tau nuclear function in modulating VGluT1 expression

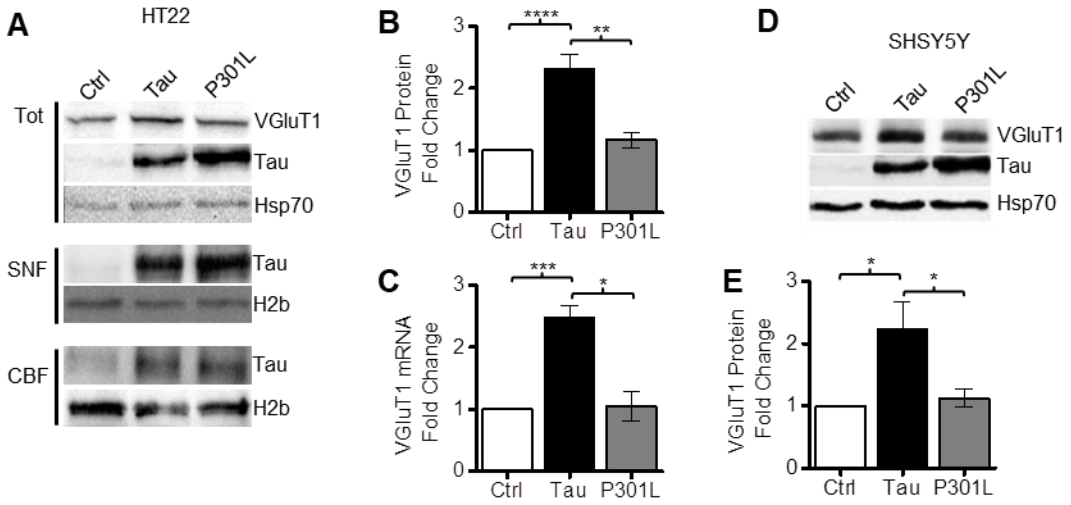

Figure 3.17. Tau pathological mutant P301L impairs Tau function of altering VGluT1 expression. A. Western blot of subcellular fractions in HT22 cells expressing Tau^{WT} or Tau^{P301L}.

B. Quantification of VGluT1 protein expression in HT22. C. VGluT1 mRNA quantification by qPCR in HT22 cells expressing Tau^{WT} or Tau^{P301L}. D. Western blot of total extracts of differentiated SHSY5Y cells expressing Tau^{WT} or Tau^{P301L}. E. Quantification of VGluT1 protein levels in SHSY5Y cells expressing Tau^{WT} or Tau^{P301L}. (Kruskal–Wallis ANOVA and Mann-Whitney test; **** p<0.0001; *** p<0.001, ** p<0.01; * p<0.05; n.s. p>0.05).

The role of nuclear Tau in gene expression regulation was performed in conditions mimicking a pre-aggregation status of Tau protein, in particular those conditions in which the interaction with MTs is impaired and the amount of soluble Tau is increased. These evidences suggest that this nuclear function might be altered by pathological mechanisms, in particular mutations associated to tauopathies and aggregation. To investigate whether pathologically mutated Tau could have an impact on its role in the nuclear compartment, we expressed Tau^{P301L} in HT22 cells and we observed that this mutant is efficiently translocated into nucleus as well as wild type Tau (Figure 3.17A). Tau^{P301L} did not increase VGluT1 expression with respect to control cells. Indeed, both the protein (1.16±0.13SE FC) and mRNA levels (1.04±0.23SE FC) were not different from those in control cells (Figure 3.17B-C). Moreover, a similar result was observed in differentiated SHSY5Y, where mutated Tau did not induce a significant increase in VGluT1 expression (Figure 3.17D-E). Taken together, these results indicate that P301L mutation does not affect nuclear translocation but abolishes the ability of Tau to induce VGluT1 expression, thus causing a loss of its nuclear function. Remarkably, the employment of Tau^{P301S} in differentiated SHSY5Y, another well-characterized Tau mutant related to the insurgency of tauopathies, is able to induce an increase in VGluT1 expression comparable to the one observed with Tau^{WT} (Figure 3.19), suggesting that two different missense mutations in the same residue can affect Tau nuclear function in different ways.

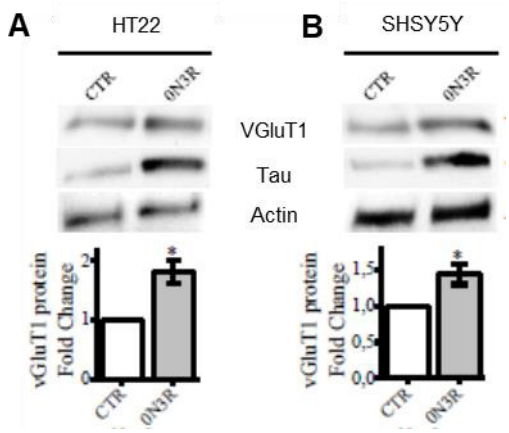

Figure 3.18. Tau isoform 0N3R alters VGluT1 expression. A. Western blot of HT22 cells expressing Tau isoform 0N3R and relative quantification of VGluT1 protein levels. B. Western blot of SHSY5Y cells expressing Tau isoform 0N3R and relative quantification of VGluT1 protein levels. (Mann-Whitney test; * p<0.05).

Since these mutations are located on the second repeat of the MTBD, we investigated if the absence of this repeat could alter the role of Tau in the modulation of VGluT1 expression. Tau 3R isoforms, due the alternative splicing of the exon 10, are physiological variants which lack of the second repeat (Andreadis et al., 1992; Goedert and Jakes, 1990; Goedert et al., 1989a). In order to clarify if this sequence can influence Tau function, we expressed the Tau isoform 0N3R in HT22 and differentiated SHSY5Y and we analysed the expression of VGluT1 (Figure 3.18A-B). The absence of the second repeat in both cell lines did not affect the nuclear Tau function. As a matter of fact, a significant increase in VGluT1 protein levels was observed (Figure 3.18A-B). Indeed, the expression of Tau 0N3R isoform induces an alteration in VGluT1 levels comparable to that observed in cells expressing the 0N4R isoform, sharing a similar function in gene modulation. These evidences suggest that Tau effect on gene expression is not dependent on the second repeat of the MTBD. Moreover, this result is associated to the effect of P301S and P301L mutations described above. In fact, even if the presence of the second repeat is not necessary for the modulation of VGluT1, P301L mutation, but not P301S, is able to impair nuclear Tau role, suggesting that this loss of function is mutation-specific.

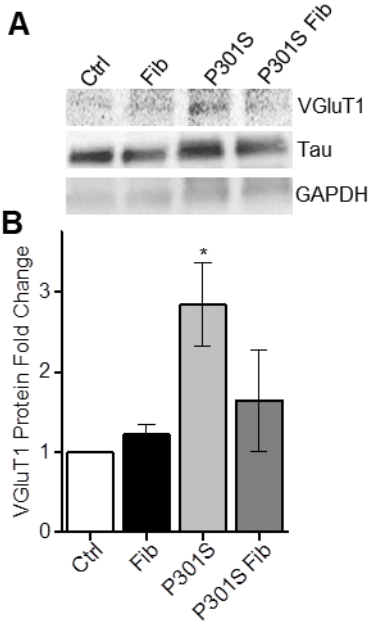

Figure 3.19. Tau pathological aggregation impairs Tau modulation of VGluT1 expression. A. Western blot of HT22 cells expressing P301S and treated with Tau^{P301S} preformed fibrils (Fib). B. Quantification of VGluT1 levels in cells represented in A. (Mann-Whitney test; * $p<0.05$).

Finally, we performed preliminary experiments to study the effect of aggregation on nuclear Tau function in gene expression. Several studies indicated that during pre-clinical stages of AD, glutamate release is increased leading to excitotoxicity but, in later stages when Tau aggregation is consolidated in the brain, a reduction in the glutamate release is observed (Dickerson et al., 2005; Jadhav et al., 2015; Khadrawyb YA, 2014; Maurin et al., 2014; Revett et al., 2013). To clarify if the aggregation can impair Tau modulation of VGluT1, we induced Tau^{P301S} aggregation by preformed fibrils administration in differentiated SHSY5Y cells (Figure 3.19A). Figure 3.19 shows that cells expressing Tau^{P301S} have a higher expression of VGluT1 compared to controls but after Tau aggregation VGluT1 amount returns to baseline levels (Figure 3.19B), suggesting that aggregation leads to a loss of Tau nuclear function in modulating gene expression.

3.10 Tau nuclear function is mediated by chromatin remodelling

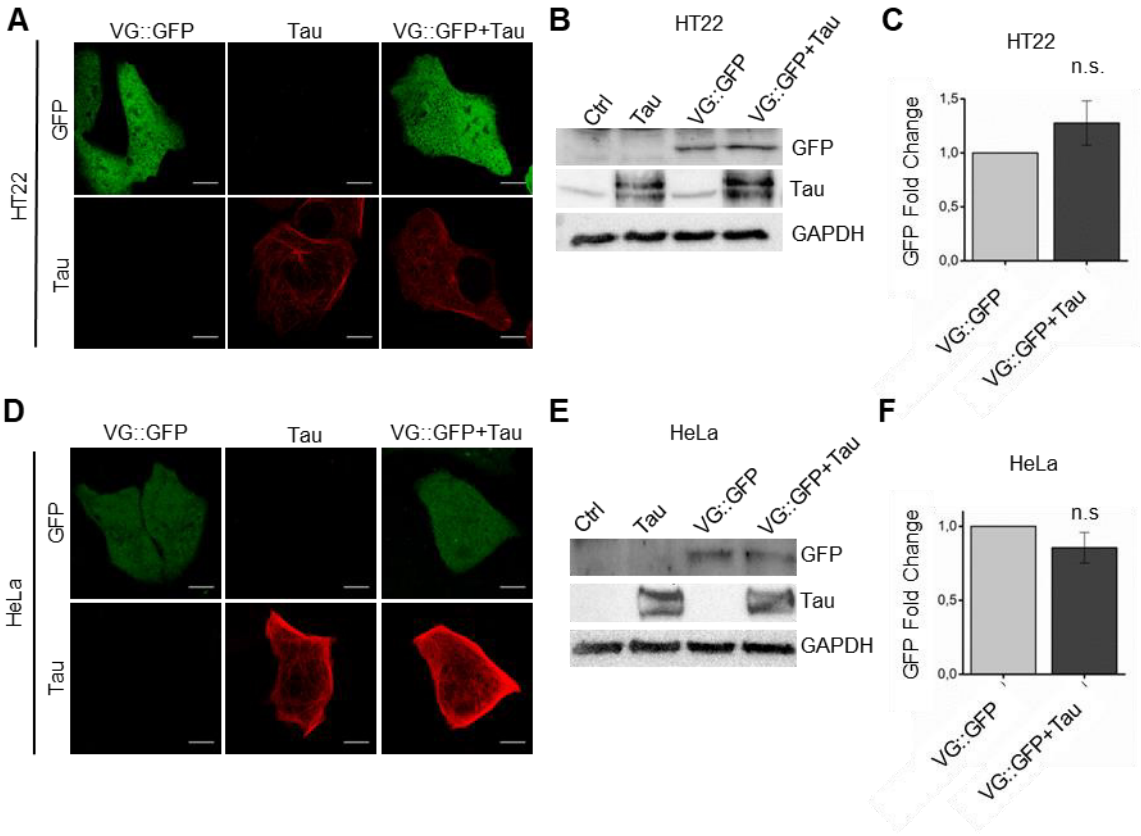

Figure 3.20. Tau modulation of VGluT1 levels is not directed to the VGluT1 promoter. A. Confocal imaging of HT22 cells expressing Tau-mCherry, GFP under the VGluT1 promoter (VG::GFP) or both. GFP is represented in green, Tau in red. B. Western blot of HT22 cells expressing Tau, VG::GFP or both to detect Tau and GFP levels. C. Quantification of GFP levels in the western blot experiment reported in B. D. Confocal imaging of HeLa cells expressing Tau-mCherry, GFP under the VGluT1 promoter (VG::GFP) or both. GFP is represented in green, Tau

in red. E. Western blot of HeLa cells expressing Tau, VG::GFP or both to detect Tau and GFP levels. F. Quantification of GFP levels in the western blot experiment reported in E (Mann-Whitney test: n.s. $p>0.05$).

We further investigated the molecular mechanism mediating the nuclear function of Tau. Since Tau interacts directly with genomic DNA (Benhelli-Mokrani et al., 2018; Qi et al., 2015), we hypothesized that Tau could alter VGluT1 expression by interacting with the VGluT1 promoter. To address this point, we expressed the reporter gene GFP under the VGluT1 promoter (VG::GFP) in control or Tau-overexpressing HeLa and HT22 cells. Imaging experiments showed that GFP signal was not altered by the increased expression of Tau in both cell types (Figure 3.20A-D). This result was confirmed by Western blot, in fact GFP expression was similar in Tau-overexpressing and control cells (Figure 3.20 B-C-E-F). These results demonstrate that the modulation of VGluT1 expression mediated by Tau is not directly dependent on the VGluT1 promoter.

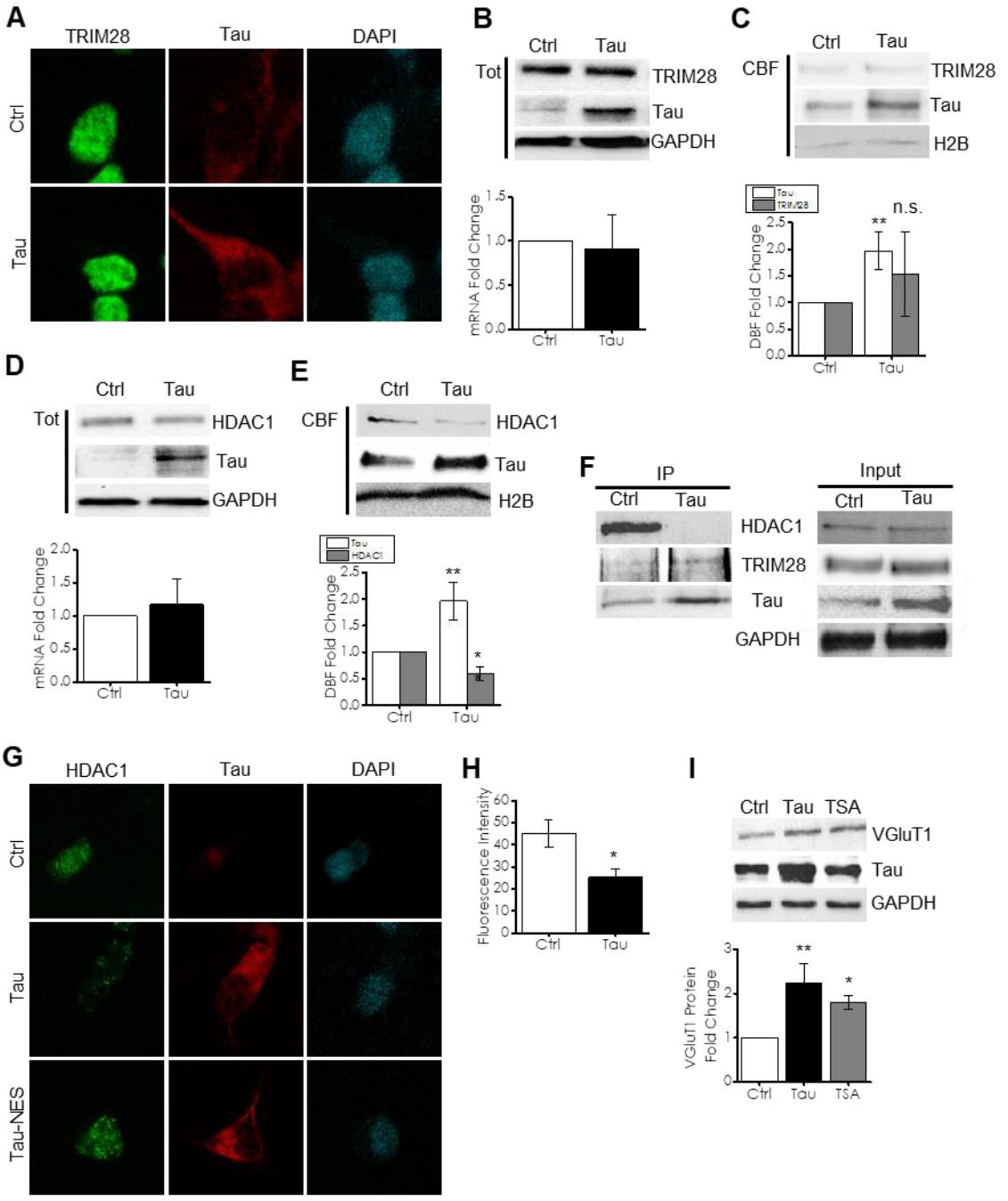

Figure 3.21. Tau competes with HDAC1 for the interaction with TRIM28 altering gene expression. A. Immunofluorescence of control or Tau-expressing SHSY5Y cells. TRIM28 staining (green) is detected mainly in the nuclear compartment as expected. Tau is represented in red, DAPI in blue. B. Western blot and qPCR quantification of total extracts in control and Tau-expressing SHSY5Ycells and detection of TRIM28 and Tau levels. C. Western blot and relative quantification of chromatin-bound fraction (CBF) in control and Tau-expressing SHSY5Y cells and detection of TRIM28 and Tau levels. D. Western blot and qPCR quantification of total extracts in control and Tau-expressing SHSY5Y cells and detection of HDAC1 and Tau levels. E. Western blot and relative quantification of CBF in control and Tau-expressing SHSY5Y cells and detection of HDAC1 and Tau levels. F. Co-IP experiment in control and Tau-expressing SHSY5Y cells. Immunoprecipitation of Tau by Tau-13 antibody and detection of TRIM28 and HDAC1. G. Immunofluorescence of SHSY5Y cells expressing Tau or Tau-NES. HDAC1 staining (green) is

detected mainly in the nuclear compartment in control cells as expected. Tau is represented in red, DAPI in blue. H. Quantification of HDAC1 nuclear signal in control and Tau-expressing SHSY5Y cells. I. Western blot and relative quantification of SHSY5Y cells expressing Tau or treated with Tricostatin-A (TSA) and detection of VGluT1 levels.

In order to elucidate the molecular mechanism exerted by nuclear Tau in the alteration of VGluT1 expression, we investigated the interaction of Tau with nuclear proteins which could influence gene expression. Recent studies identified the nuclear protein TRIM28 as a Tau interactor which mediates its translocation into the nucleus (Rousseaux et al., 2016). Remarkably, TRIM28 forms a big nuclear complex which alters the chromatin structure leading to formation of heterochromatin and, as a consequence, gene repression (Barde et al., 2013; Friedman et al., 2007).

First, we investigated the association of Tau and TRIM28 in our SHSY5Y model. Immunofluorescence experiments showed that TRIM28 is detectable in the nuclear compartment as expected, and its expression is not altered by the increase of Tau mRNA and protein levels (Figure 3.21A). This result has been confirmed by Western blot analyses on total protein extracts and by qPCR (Figure 3.21B). Moreover, the CBF obtained by subcellular fractionation showed that TRIM28 nuclear localization did not change in Tau overexpressing cells (Figure 3.21C). These evidences demonstrate that Tau has no significant effect on TRIM28 expression and localization.

Since TRIM28 has several nuclear partners which mediate the function of chromatin remodelling, we analysed the impact of Tau on TRIM28 interactors. HDAC1 is a well-known TRIM28 interactor belonging to histone deacetylases family whose function is to eliminate the acetyl group from histones favouring heterochromatin formation (Delcuve et al., 2013; Haberland et al., 2011). Due to its function and to the interaction with TRIM28 in the nucleus, HDAC1 has been investigated as a candidate for this study. Western blot in total extracts and qPCR showed that HDAC1 expression was not altered by Tau overexpression (Figure 3.21D), however, we observed a significant reduction in HDAC1 in CBF compared to control cells (Figure 3.21E). To understand if HDAC1 delocalization from the chromatin-bound fraction was due to a competitive effect with Tau, we performed a Co-IP experiment. We immune-precipitated Tau by anti-Tau antibodies and detected TRIM28 and HDAC1. Figure 3.21F shows that, while

TRIM28 is normally detected in the protein complex, HDAC1 is strongly reduced suggesting that there is a competitive effect between Tau and HDAC1 for the binding with TRIM28. This competition has been confirmed also by IF experiments. As a matter of fact, HDAC1 can be detected mainly in the nuclei of control cells as expected but, in Tau overexpressing cells, a significant reduction of HDAC1 signal in the nuclear compartment is observed with the concomintant relocalization into the cytoplasm confirming that Tau is involved in the subcellular localization of HDAC1 (Figure 3.21G-H). To discriminate if the competition between Tau and HDAC1 occurs in the cytosol or in the nucleus, we exploited the Tau-NES constructs. The retainment of Tau in the cytoplasm, by expressing Tau-NES in HT22 cells, showed that cytoplasmic Tau did not influence the nuclear localization of HDAC1 (Figure 3.21G) that is detected in the nuclear compartment as in control cells. This suggests that HDAC1 delocalization is mainly due to nuclear Tau molecules. However, the competitive mechanism between nuclear Tau and HDAC1 cannot still explain the increase in VGluT1 levels.

Our hypothesis is that the delocalization of HDAC1 from the nuclear compartment might impair its function as a chromatin remodeller. Thus, this might lead to an altered gene expression and in particular to an increase in VGluT1 expression. To address this point, we treated control cells with Tricostatin-A, a compound able to block the activity of HDAC family proteins, among these HDAC1. Western blot experiments in cells treated with TSA showed a significant increase in VGluT1 expression that was comparable to the increase observed in Tau-expressing cells (Figure 3.21I), supporting our hypotheses. In conclusion these results suggest that Tau could modulate gene expression by altering the chromatin structure, a mechanism that will be deeply investigated in future experiments.

3.11 Tau protein causes a global alteration of gene expression and modulates pathways related to L-MCI

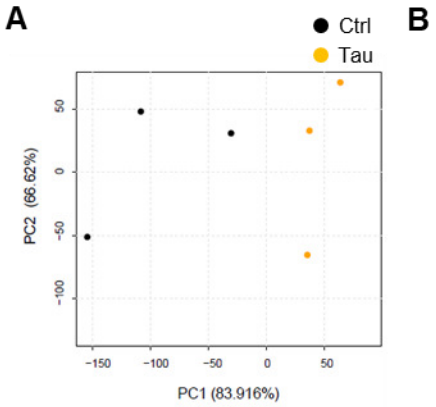

B

KEGG category	p_{adj}
ECM_receptor_interaction_:::_hsa04512	1.78E-08
PI3K_Akt_signaling_pathway_:::_hsa04151	2.19E-07
Protein_processing_in_endoplasmic_reticulum_:::_hsa04141	8.16E-07
Focal_adhesion_:::_hsa04510	8.16E-07
Glutamatergic_synapse_:::_hsa04724	1.03E-05
Thyroid_hormone_synthesis_:::_hsa04918	3.49E-05
Protein_digestion_and_absorption_:::_hsa04974	1.19E-04
Rap1_signaling_pathway_:::_hsa04015	2.04E-04
Axon_guidance_:::_hsa04360	2.37E-04
Neuroactive_ligand_receptor_interaction_:::_hsa04080	3.71E-04
Phagosome_:::_hsa04145	3.71E-04
MAPK_signaling_pathway_:::_hsa04010	4.59E-04
cAMP_signaling_pathway_:::_hsa04024	4.59E-04
GABAergic_synapse_:::_hsa04727	4.59E-04
Salivary_secretion_:::_hsa04970	4.59E-04
Pathways_in_cancer_:::_hsa05200	4.59E-04
Circadian_entrainment_:::_hsa04713	5.89E-04
Relaxin_signaling_pathway_:::_hsa04926	5.89E-04
Phosphatidylinositol_signaling_system_:::_hsa04070	7.19E-04
Amphetamine_addiction_:::_hsa05031	7.59E-04
Calcium_signaling_pathway_:::_hsa04020	7.90E-04
Retrograde_endocannabinoid_signaling_:::_hsa04723	8.12E-04
Oxytocin_signaling_pathway_:::_hsa04921	1.13E-03
Cocaine_addiction_:::_hsa05030	1.40E-03
Long_term_depression_:::_hsa04730	2.51E-03
GnRH_signaling_pathway_:::_hsa04912	2.51E-03
Inflammatory_mediator_regulation_of_TRP_channels_:::_hsa04750	3.10E-03
Transcriptional_misregulation_in_cancer_:::_hsa05202	3.25E-03
Prion_diseases_:::_hsa05020	3.40E-03
Metabolic_pathways_:::_hsa01100	4.19E-03

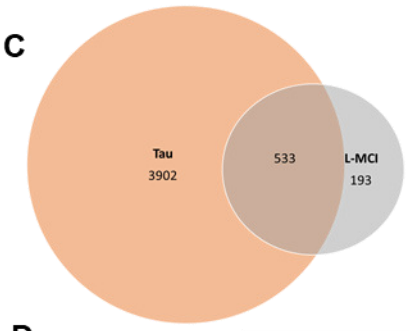

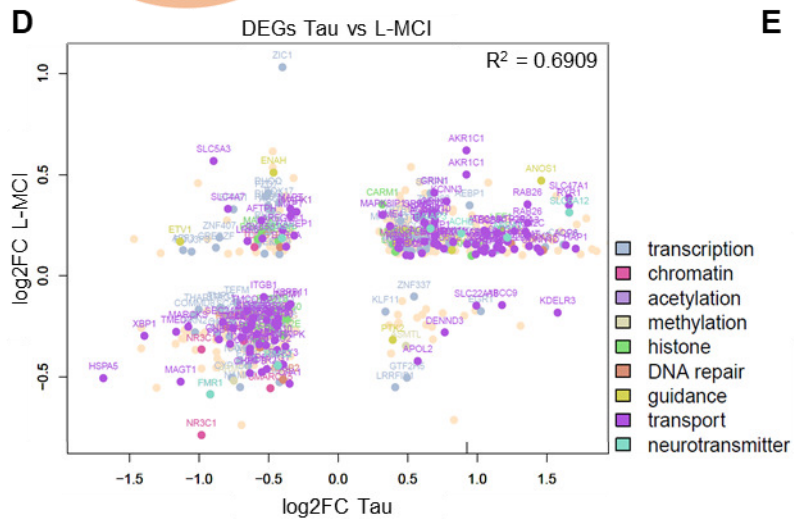

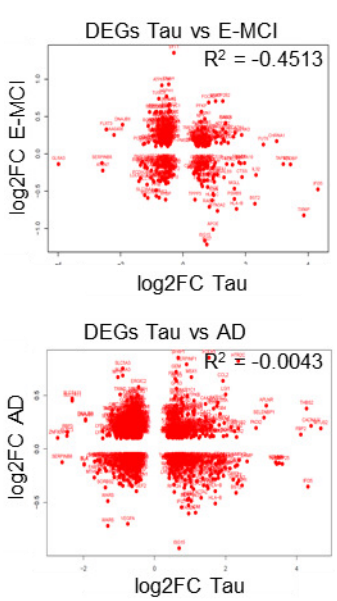

Figure 3.22. Tau overexpression alters globally gene expression and reproduces a L-MCI condition. A. PCA analysis of control and Tau-expressing differentiated SHSY5Y cells. B. DEGs clustering analysis based on KEGG database. The table reports the most significant categories identified by gene ontology of DEGs between control and Tau-expressing cells. C. Venn diagram of DEGs identified in our transcriptome, DEGs identified in hippocampi of L-MCI patients and their intersection. D. Comparison between common DEGs of Tau-expressing SHSY5Y and L-MCI hippocampi. R^2 reported in the graph is the Pearson correlation and different colours indicate different gene categories. E. Graphs reporting common DEGs between Tau-expressing SHSY5Y and E-MCI or AD hippocampi. R^2 reported in the graph is the Pearson correlation.

The discovery that nuclear Tau modulates VGluT1 gene expression suggests that this function might also have an impact on the expression of other genes. In order to identify the genes whose expression is altered by Tau protein, we performed a RNAseq experiment in differentiated SHSY5Y. We compared the transcriptome profile of three controls and three Tau-expressing samples. First, the analyses of the principal components (PCA) showed that Tau expressing and control samples group separately (Figure 3.22A). The sequencing analysis revealed that 3902 genes were differentially expressed (DEGs) after Tau expression. Moreover, gene ontology of these genes by using the KEGG database identified clusters of gene functions which were strongly regulated by the higher amount of Tau protein. Remarkably, among the most regulated pathways, several are related to the glutamate release pathway, mRNA processing, protein homeostasis and signalling pathways (Figure 3.22B). These observations indicate that the increase of Tau is able to globally alter the transcriptome, thus potentially influencing several fundamental mechanisms for cellular homeostasis.

In order to clarify if our cellular model overexpressing Tau can mimic molecular aspects characterizing AD patients, we compared the DEGs of Tau-overexpressing SHSY5Y cells with DEGs of database GSE84422. In detail, GSE84422 database contains microarray data of hippocampi from AD patients collected at different stages of disease. Three groups are available: E-MCI, L-MCI and AD. The comparison of our RNAseq data with this database indicated that there was a strong positive correlation between Tau-expressing differentiated SHSY5Y cells with hippocampi at L-MCI stage (Figure 3.22C-D). A lower correlation was observed for E-MCI and AD samples (Figure 3.22E), suggesting that the increase in soluble Tau mimics the pathological condition characterized by Tau destabilization in neuronal cells. Common DEGs between RNAseq data and L-MCI samples and gene ontology analysis showed that the cellular functions altered by Tau were also altered in L-MCI (Figure 3.22C-D), supporting this cellular system as a simple and reliable model to study the pathological effects of Tau in a pre-clinical condition. In conclusion, Tau protein alters VGluT1 expression but several genes are also modulated, mimicking conditions related to L-MCI. Further analyses and experiments will clarify which are the genes

exclusively modulated by nuclear Tau and the role that this new function might have in the development of Tau pathologies.

Chapter 4

Discussion

4.1 Development of a Tau conformational sensor and application *in vitro* and *in vivo*

Tau is an unfolded neuronal protein deeply studied because of its central role in neurodegenerative diseases. In tauopathies, Tau assumes a β-sheet structure and forms amyloidogenic aggregates that can be currently studied by high resolution techniques (Alonso et al., 2001; von Bergen et al., 2000; Fitzpatrick et al., 2017; Wang and Mandelkow, 2016). However, a few conclusions have been achieved for the structure of monomers since Tau is an intrinsically disordered protein (Cleveland et al., 1977; Hirokawa et al., 1988; Mukrasch et al., 2009). Current techniques do not allow to determine Tau atomic structure in physiological conditions or at the early onset of pathology, before aggregation. However, at a minor resolution, it is possible to investigate in a cellular system the physiological conformation of Tau and the conformational changes it undergoes in pathological conditions.

We developed and characterized the Conformational Sensitive Tau Sensor (CST) which allows to investigate Tau conformation in living cells and in different cellular contexts (Di Primio et al., 2017). The main difference of this tool with already available Tau biosensors (Kfoury et al., 2012; Tak et al., 2013) is the tagging of Tau with a FRET couple enabling to monitor, in real time, Tau conformational dynamics from the binding to MTs to displacement and aggregation. By expressing the CST in different cellular systems we confirmed that the presence of the two fluorophores does not affect the interaction of Tau with MTs (Figure 3.1-3.2) supporting the fact that Tau main physiological function is preserved in the CST as expected (Avila et al., 2004; Breuzard et al., 2013; Samsonov et al., 2004). The CST has been applied in order to study Tau behaviour in physiological conditions. The CST on MTs displays a positive FRET signal and a comparison with cells co-expressing monolabelled CFP-Tau and Tau-YFP demonstrates that the FRET signal is mainly due to an intramolecular interaction between the N- and C-terminal ends. This result shows, for the first time, that Tau

bound to MTs assumes a loop conformation in which the ends of the protein are close each other. On the contrary, a more relaxed conformation is detectable for Tau soluble molecules in the cytoplasm. As a matter of fact, by destabilizing the cytoskeleton or the interaction between Tau and tubulin, a strong reduction of FRET signal is observed and it is associated to a significant increase in the cytoplasmic fraction of Tau (figure 3.3). The employment of the CST in living cells confirmed previous *in vitro* studies indicating that in absence of MTs the soluble Tau assumes a paperclip conformation (Bibow et al., 2011; Jeganathan et al., 2006; Mukrasch et al., 2009). Our approach clarified that this paperclip conformation is distinctive of Tau bound to MTs while the soluble cytoplasmic Tau assumes a completely different conformation that was undetectable *in vitro*. Certainly, *in vitro* experiments performed in test tubes do not resemble the cellular complexity and in this case the loss of the loop conformation for soluble monomers might be due to cellular interactors or post-translational modifications.

The possibility to discriminate between physiological and destabilized state led to the application of the CST to determine the conformational changes of Tau mutants associated to tauopathies (Bugiani et al., 1999; Hutton et al., 1998; Rizzu et al., 1999; Spillantini et al., 1998a). The P301L and ΔK280 mutations have been considered. These two mutations are strongly linked to FTDP and Pick's disease and molecular studies demonstrated that they have reduced affinity to tubulin, resulting in a destabilization of MTs, and are more prone to post-translational modifications and aggregation (Goedert et al., 1999). The employment of CST^{P301L} and $CST^{\Delta K280}$ shows similar results for P301L and ΔK280 mutations. FRET analysis reveals that both mutants display a positive FRET signal on MTs but significantly lower than CST^{WT}, suggesting that the presence of mutations causes a conformational change leading to a more relaxed conformation of Tau bound to tubulin. The fraction of mutated Tau soluble in the cytosol is higher than wild-type Tau indicating a lower affinity to tubulin. Moreover, the analysis of the mutated CST network on MTs indicates a reduced number of branching points and of the total filament length. The alteration of Tau network further supports a destabilization and a lower complexity of the cytoskeleton that, associated to the increase in the soluble fraction of the protein, indicates a general impairment of Tau function. This result confirmed previous

studies indicating that these mutants reduce the MTs stability and are more subjected to post-translational modifications and aggregation (Hasegawa et al., 1998b; Spillantini et al., 1998b, 1998a). The CST adds a new evidence on these pathological mutations. As a matter of fact, the destabilization caused by P301L and ΔK280 corresponds to a conformational change of Tau protein on MTs. Mutated CST is significantly more relaxed that the wild-type, thus suggesting that the destabilization of Tau protein and its structure are closely related. This association is confirmed by employing a CST mutant more stable on MTs. By impeding the phosphorylation of the AT8 epitope by site-directed mutagenesis (CST^{AT8mut}), a significant increase in the fraction of Tau bound to cytoskeleton is observed (Figure 3.4). Moreover, the MT network analysis shows an increase in branching points and total filament length compared to the CST^{WT}, suggesting a higher network complexity. The FRET analysis of the AT8 phospho-mutant indicates that the FRET of the sensor bound to MTs is higher than the wild-type, indicating a conformation significantly closer than the CST^{WT}. Altogether these results show that there is an association between the conformation of Tau and its binding to tubulin, resulting in an alteration of the cytoskeleton network.

These evidences stimulated further investigation of mutations still not completely characterized but related to a particular tauopathy. Intriguingly, in recent years a novel Tau mutation associated to Pick's disease, Q336H, was discovered. *In vitro* experiments revealed that Tau^{Q336H} is able to increase the tubulin polymerization, a peculiar effect generally opposite to other Tau mutations (Tacik et al., 2015). We generated the CST^{Q336H} and we studied its effect on MT network and Tau conformation. The CST^{Q336H} network analysis shows a significant increase in branching points and filament length compared to CST^{WT}, in a way similar to the AT8 phospho-mutant. The FRET signal of the CST^{Q336H} is higher than wild-type, revealing a closer conformation of molecules bound to MTs than the CST^{WT}. These first results suggest a stabilizing function of Q336H mutation increasing the complexity of MTs. Remarkably, this mutation is associated to aggregation and development of Pick's disease even if its impact on Tau structure seems in contrast to other tauopathy-related mutations. A possible explanation might be that Tau conformational alteration has a double effect: the cytoskeleton stabilization and, at the same time, a higher sensitivity to post-translational

modifications and/or oligomerization leading to aggregation. Another explanation might be that the mutation alters the 3R/4R isoforms ratio which seems related to specific tauopathies (Arai et al., 2001; Buée-Scherrer et al., 1996; Delacourte et al., 1996; Sergeant et al., 1997; Togo et al., 2002). Further studies will provide new insights on the effect of Q336H on Tau functions and will clarify how it is linked to pathology.

Tau pathology development goes through different steps, from a physiological condition to Tau destabilization and oligomerization, concluding with intracellular amyloidogenic inclusions (Avila et al., 2004; Wang and Mandelkow, 2016). The employment of the CST to investigate the molecular dynamics of Tau pathology showed that it provides an imaging readout discriminating Tau conformations in different cellular conditions. To characterize how the sensor responds to pathological aggregation, CST reporter cells have been treated with different amyloidogenic aggregates. The administration of brain lysates from AD patients causes a delocalization of the CST from MTs to the cytoplasm and subsequent formation of FRET-positive aggregates, demonstrating that CST is also sensitive to pathological aggregation. The AD brain lysate represents a mixture of proteins in the final pathological stage of the disease. This means that it contains the two major inclusions detectable in AD, Tau tangles and Aβ aggregates (Lane et al., 2018). The homotypic treatment of reporter cells by Tau fibrils induces the delocalization and aggregation of the CST, resulting in a FRET positive signal and its isolation in the sarkosyl-insoluble fraction. Remarkably, a similar effect is observed with the heterotypic treatment with AβOs; the CST forms insoluble intracellular inclusions which display a FRET signal. Same results have been obtained also in cells expressing the unlabelled Tau, demonstrating that the presence of the fluorophores is negligible in this mechanism. The treatment with Tau fibrils leads to the sensor aggregation as expected and allows to add a new feature of the CST, in fact it provides a FRET positive output in aggregation conditions. The employment of AD brain lysates and, more clearly, of AβOs further supports the sensitivity of CST in response to a pathological state, indicating that heterotypic aggregates are able to alter Tau pathological dynamics. Tau aggregates forming in response to administration of AβOs suggest that these pathological proteins in AD can interact enhancing the Tau

aggregation process. The cross-reaction between Tau and Aβ has been already observed both *in vitro* and *in vivo* experiments indicating that it favours post-translational modifications of Tau (Guo et al., 2006). However, the mechanisms behind this response are still unclear and further studies are necessary to clarify how Tau and Aβ impact each other during the progression of AD.

The sensitivity of the CST to pathological conditions, led to the development of *in vitro and in vivo* systems to identify molecules or conditions able to reduce or prevent Tau pathological behaviour. Many attempts to block or revert tauopathies progression failed in providing an efficient treatment for these pathologies, even if Tau-based clinical trials are currently ongoing and are evaluating the safety and the efficacy of the Tau-directed therapy on AD patients (Novak et al., 2010, 2018c, 2018b, 2018a; West et al., 2017). However, the lack of a cure for Tau pathology is due to several factors, in particular the insufficient knowledge of its functions and mechanisms related to the pathology and the poor development of screening techniques to easily and efficiently identify therapeutic compounds. About the last point, a number of Tau biosensors are currently available and sensitive to aggregation (Kfoury et al., 2012; Tak et al., 2013). However, they are still not employed for high throughput screening assays. We developed a cellular platform based on CST to identify potential therapeutic compounds against Tau pathology.

First of all, for the assay optimization, the CST^{P301S} has been expressed in HeLa cells and aggregation has been induced by administration of heparin-Tau^{P301S} fibrils to favour a higher amount of aggregation. The characterization of aggregates shows that CST^{P301S} inclusions are insoluble and positive to K114 staining as well as amyloidogenic aggregates (Crystal et al., 2003). Moreover, the imaging analysis clearly indicates that the FRET signal of CST included in aggregates is much higher than the signal displayed by the sensor bound to MTs. These results demonstrates that, by means of different FRET values, the CST provides three different outcomes relative to three states of Tau: bound on MTs, soluble in the cytosol and aggregated. However, while the FRET signal in physiological and destabilizing conditions provides information also about the conformation of Tau, upon aggregation the FRET signal does not mean a structure or the directionality of interacting Tau molecules. In order to improve the

signal of the aggregated CST, taking into account the different dimensions of aggregates and to increase the sensitivity to different treatments, the integrated NFRET signal has been considered (iNFRET). The iNFRET value describes two aspects of the aggregate: the proximity of CST molecules and the dimension of the aggregate. By comparing iNFRET values of CST bound to MTs and aggregated we found that the iNFRET of aggregates is significantly higher. The analysis suggests that this system can be suitable for a screening application. After this preliminary characterization, the CST^{P301S} has been expressed in a disease relevant cell line: differentiated SHSY5Y cells. Upon aggregation, the FRET and iNFRET signals were comparable to those in HeLa cells indicating that this CST-based cellular system could be exploited as a platform to test potential therapeutic compounds impairing Tau aggregation.

Several candidates are available which might block specific mechanisms of Tau aggregation and we focused on kinase inhibitors since phosphorylation is the most characterized post-translational modification related to Tau pathology (Pevalova et al., 2006; Wang and Mandelkow, 2016). Initially, reporter cells have been treated with known kinase or phosphatase inhibitors, staurosporine (STS) and okadaic acid (OA) respectively, to evaluate the response of the system to these treatments and to set up optimal experimental conditions. STS is a pan-kinase inhibitor and induces a strong reduction of CST aggregation, thus it has been considered the positive control for the screening. On the contrary OA is a phosphatases inhibitor and induces hyperphosphorylation facilitating Tau aggregation (Arendt et al., 2016; Guo et al., 2017; Karaman et al., 2008). For its effect, OA is the negative control of the system. The FRET analysis of aggregates shows that STS induces a significant decrease of iNFRET values compared to untreated cells, leading to smaller aggregates where CST molecules are less packed. OA treatment, instead, causes a huge increase of iNFRET, with bigger and more stable aggregates. Moreover, the detection of phosphorylation levels at Tau specific residues related to pathology confirms that STS induces Tau phosphorylation inhibition, in particular on AT8, T231 and S356 epitopes, while OA significantly increases the Tau phosphorylation. These results indicate that the CST-based cellular platform is sensitive to the phosphorylation changes upon aggregation and it can be used to identify novel anti-aggregation

compounds. To identify potential therapeutic molecules, the platform has been challenged with two kinase inhibitors, PD-901 and D-JNKI-1, which are employed in clinical trials against thyroid carcinoma, acute hearing loss and ischemia (Henderson et al., 2011; Hirt et al., 2004; Milano et al., 2007; Yap et al., 2011). PD-901 blocks the ERK pathway, involved in the first stages of pathological Tau phosphorylation (Hanger et al., 2009). D-JNKI-1 is an inhibitor of JNK which phosphorylates Tau in later stages of aggregation (Hanger et al., 2009). The treatment of reporter cells with PD-901 or D-JNKI-1 shows that both molecules induce a significant decrease in iNFRET values of CST^{P301S} aggregates, resulting in a lower dimension of aggregates and a weaker interaction between CST proteins. Remarkably, the effect of PD-901 is much stronger than D-JNKI-1. This evidence suggests that the inhibition of the ERK pathway impairs Tau aggregation more efficiently than the inhibition of JNK and this is confirmed also by the K114 staining which is significantly lower in PD-901 treated cells. Altogether these results indicate PD-901 as a potential therapeutic compound to reduce Tau aggregation. The different effect between PD-901 and D-JNKI-1 has been investigated by analysing the phosphorylation of Tau specific epitopes. Both ERK and JNK phosphorylate several Tau residues, however, ERK is considered more involved in phosphorylation events occurring at early stages of the pathology to prime aggregation. On the contrary, JNK seems to be involved in later phases, when Tau aggregation is already consolidated. Western blot experiments show that upon aggregation the phospho-AT8 epitope is not altered by treatments with PD-901 or D-JNKI-1. Remarkably, phosphorylation at T231 and S356 residues is significantly reduced in cells treated with PD-901 while no effect is observed with D-JNKI-1 treatment. The phosphorylation of these epitopes is considered an early event in destabilization and hyperphosphorylation of Tau (Johnson, 2004), thus our results suggest that Tau aggregation is impaired when early phospho-epitopes are blocked. It is conceivable that the loss of early pathological phosphorylation signature destabilizes the protein of the forming aggregate; on the other end, this might prevent further accumulation of Tau to the inclusions. Given the promising results obtained by the CST-based platform, PD-901 will be tested in animal models for Tau pathology in order to confirm its efficacy in a more complex system.

The development of the CST-based platform and the identification of molecules preventing Tau aggregation support that the CST is a reliable tool for this kind of applications. The employment of the sensor in a cellular context leads to the possibility of an *in vivo* use in order to test drugs in a more complex system. The aim of the subsequent project was to obtain a CST-transgenic model for high-throughput screenings of compounds against Tau pathology. Several animal models are available to study Tau pathological behaviour and to generate our transgenic line, the D. rerio (zebrafish) has been chosen. The zebrafish model is a perfect candidate for screenings since embryos are transparent for days, the treatments are easy to be administrated and transgenesis is simple and efficient. Moreover, previous experiments with zebrafish overexpressing human Tau revealed that in this model Tau pathological behaviour is spontaneous and occurs after a few days post fertilization (Bai and Burton, 2011; Bai et al., 2007; Paquet et al., 2009, 2010). Preliminary experiments with transient expression of CST by mRNA injection show that the sensor can be expressed in this model and, at cellular level, it displays a fluorescent network on microtubules as expected, confirming that the CST maintains its basic characteristics in zebrafish. To develop the transgenic animal, the CST^{WT} has been integrated in the zebrafish genome under the HuC promoter which guarantees the expression only in neuronal cells (Kim et al., 1996). The analysis of the F_0 line at 24hpf clearly shows the transgene expressed in neurons as expected. The inbreeding of the F_0 provided the F_1 generation which stably expresses CST in all neurons. Currently the F_1 zebrafishes are under characterization. A preliminary imaging analysis showed the CST signal in the nervous system and the western blot analyses indicated that the sensor is correctly expressed and does not undergo any cleavage *in vivo*. Moreover, an immunohistochemistry experiment performed at 72hpf showed that the CST is highly phosphorylated at AT8 epitope in that stage while the signal is undetectable in control animals. This result confirms previous observations reporting that human Tau overexpressed in zebrafish is progressively hyperphosphorylated with aging and induces neurodegeneration (Paquet et al., 2009). Further experiments are necessary to characterize this model, in particular the FRET measurements *in vivo*. The final goal of this transgenic model is to combine the peculiar characteristics of CST and zebrafish to obtain a reliable model to screen therapeutic molecules impairing Tau

aggregation and neurodegeneration. Due to the preliminary results obtained *in vitro*, PD-901 will be the first test compound analysed in this model.

This research has the aim to study different aspects of Tau protein by molecular and cellular approaches to solve some biological problems about Tau which were still unclear. The development of a biosensor able to monitor in real time Tau conformation provides a new tool whose employment could help the investigation of the factors which modify the conformation of Tau in the first stages of the pathology, finding potential targets to prevent this important but neglected aspect of tauopathies. Moreover, the sensitivity of the CST to pathological aggregation can also be applied to clarify late pathological mechanisms and to screen candidate compounds to impair or revert the formation of Tau toxic inclusions. Even if the CST has been used mainly in a cellular context, a transgenic zebrafish is currently under development, with the aim to combine a complex biological system with a simple molecular output able to determine Tau conformational dynamics in pathological conditions. This will be the base for an *in vivo* screening model of potential therapeutic compounds preventing Tau pathologic behaviour. In addition, the CST could also be employed in tauopathy mouse models for example to study the alteration of Tau conformation in different brain areas and at different stages of tauopathy progression, an aspect still unclear and which could add new information about Tau pathological dynamics *in vivo*. Finally, the first *in vitro* application of the CST to discover molecules potentially able to alter Tau pathological progression resulted in the identification of PD-901 and D-JNKI-1 as compounds which can reduce Tau aggregation, in particular PD-901 demonstrated to have a stronger effect than D-JNKI-1, suggesting that the inhibition of the EKR pathway is more efficient in preventing Tau aggregation that the JNK pathway. The effect of PD-901 on Tau pathology needs to be evaluated in mouse models, not only to confirm its efficacy *in vivo* but also to clarify its way of action in a complex system and the administration. Remarkably, if these data would be confirmed *in vivo*, the exploitation of PD-901 in humans might be very fast and easy, since it is already used in clinical trials alone or in combination with other therapeutic molecules (ClinicalTrials.gov Identifier: NCT02022982; NCT02039336; NCT03905148) and working concentrations and side effects are already known.

4.2 The role of Tau in gene expression

Tau recent-discovered functions in the dendritic and nuclear compartments are still an open field and further investigations are necessary to understand their impact on pathology. During the characterization of the CST, the subcellular fractionation of HeLa and SHSY5Y cells allowed the isolation of the cytoplasmic fraction (CF) and of soluble nuclear (SNF) and chromatin-bound fractions (CBF). The western blot analyses of these fractions reveal that CST localizes not only in the cytosol as expected, but also in the nuclear compartment. The nuclear localization of Tau was described for the first time in neuroblastoma cells and then confirmed in neurons, suggesting that Tau may have other roles not strictly related to MTs (Loomis et al., 1990; Rady et al., 1995). In order to study the function of nuclear Tau and to avoid any interference due to the presence of the two fluorophores in the CST construct, the unlabelled Tau 0N4R has been employed for the subsequent experiments.

Tau has been transfected in HeLa, HT22 and differentiated SHSY5Y cells. The presence of Tau in the nuclear fraction is supported by previous *in vitro* experiments which demonstrated the interaction of Tau with DNA and by a genome-wide study which investigated the DNA regions bound by Tau (Benhelli-Mokrani et al., 2018; Hua and He, 2003; Padmaraju et al., 2010; Qi et al., 2015; Sjöberg et al., 2006). In our experiments we found that Tau is detectable in nuclei, confirming that the ability of Tau to translocate into the nucleus is retained also in non-neuronal cell lines. Several evidences suggest a role for nuclear Tau in nucleolar organization and DNA protection in stress conditions (Maina et al., 2018; Sjöberg et al., 2006; Sultan et al., 2011; Violet et al., 2014). Moreover, Tau has been seen to accumulate in heterochromatin during aging and to alter transposons activation suggesting a role in gene expression modulation, still debated (Gil et al., 2017; Guo et al., 2018; Sun et al., 2018). In order to clarify the nuclear role of Tau in relation to a possible alteration of gene expression, we first analysed the accumulation of Tau in the chromatin bound fraction and we found that in neuronal cell lines employed there is a detectable amount of endogenous Tau that can be significantly increased by Tau overexpression.

Then, we focused on the effect of Tau on genes involved in glutamatergic synaptic transmission. A common event occurring during the progression of Tau pathology is a strong change in synaptic transmission. In particular, in early pathologic stages, glutamate release is increased and correlates with toxic hyperexcitability; in late stages a glutamate release impairment can be observed (Avila et al., 2017; Crescenzi et al., 2017; Dickerson et al., 2005; Hall et al., 2015; Hunsberger et al., 2015; Jadhav et al., 2015; Khadrawyb YA, 2014; Maurin et al., 2014; Revett et al., 2013). Synaptic glutamate release is dependent by several proteins, and the VGluT family has a relevant role by mediating glutamate loading into synaptic vesicles (Martineau et al., 2017; Siksou et al., 2013). In tauopathy mouse models, glutamate release and VGluT1 levels are increased in the pre-symptomatic phase of the disease, when Tau is destabilized or oligomeric, while a glutamate reduction is observed in late stages, when Tau aggregation is established, a behaviour similar to that observed in human brains (Crescenzi et al., 2017; Dickerson et al., 2005; Hunsberger et al., 2015; Khadrawyb YA, 2014). This suggests that alterations of VGluT1 expression are associated to both the stage of the disease and the state of Tau protein, soluble in the cytoplasm or aggregated. It is conceivable that the nuclear role of Tau in these two stages might be distinct. The increased expression of Tau in HeLa, HT22 and SHSY5Y cells induces a significant increase of VGluT1 mRNA and protein that is not detectable for VGluT2 and VGluT3, meaning that this modulation is selective and specific.

The over-expression of Tau should mimic the pre-clinical stages of Tau pathology when it is unstable on MTs and its levels as soluble monomers are higher in the cytoplasm. Moreover, we found that the total increase of Tau favours also a significant increase in the nuclear compartment. To provide further supporting evidence, cells have been treated with PTX and Noc, chemicals that increase the Tau soluble pool by different mechanisms: Tau displacement from MTs or cytoskeletal disruption respectively (Kar et al., 2003; Di Primio et al., 2017). Both treatments increase Tau in the nucleus, highlighting an equilibrium between cytoplasmic and nuclear Tau. Concomitantly, the expression of VGluT1 protein is increased. This demonstrates that Tau detachment from MTs not only affects MTs stability but also favours its nuclear translocation, thus ultimately affecting

VGluT1 expression. A relevant point is that these experiments are performed on not-transfected cells, demonstrating that the VGluT1 modulation does not depend on Tau overexpression but on endogenous Tau delocalization. Remarkably, nuclear Tau and VGluT1 expression have a functional effect on neurons since an increased spontaneous synaptic transmission can be observed by patch-clamp experiments. In particular, the higher mEPSC frequency indicates a presynaptic effect that can be directly linked to higher VGluT1 levels. This electrophysiological observation correlates with the neuronal hyperexcitability detected in the early-stage tauopathy. The relationship between Tau and VGluT1 expression has been confirmed also by depletion experiments. As a matter of fact, Tau knock-down reduces VGluT1 levels, accounting for a bidirectional correlation between the levels of Tau and the expression of VGluT1.

In the experiments described above, the effect of Tau on VGluT1 has been analysed when Tau amount was increased both in the cytosol and in the nucleus. In order to discriminate if the effect on gene expression is due to cytoplasmic or nuclear Tau, we exploited Tau tagged with NLS or NES. The expression of these two constructs shows a disequilibrium of Tau subcellular localization, with Tau-NLS accumulated in the nucleus while Tau-NES mostly present in the cytosol as expected. Remarkably, forcing the nuclear localization of Tau increases VGluT1 expression at the same level attained by overexpression of untagged Tau. On the contrary, by forcing the export of Tau from the nucleus the expression of VGluT1 returns to control level. This is the first evidence clearly demonstrating that the modulation of VGluT1 expression is mainly depend on Tau in the nuclear compartment. The fact that the VGluT1 alteration is comparable between untagged Tau and Tau-NLS expressing cells might indicate that the amount of untagged Tau reaching the nucleus is already saturating. A suggestion about this point can be observed in PTX and Noc treated cells, where the increase in VGluT1 expression is similar to the one observed in transfected cells but Tau in the nucleus is about two fold higher than in untreated cells, indicating that a small increase of nuclear Tau is sufficient to significantly alter VGluT1 levels. Altogether these results demonstrate that the modulation of VGluT1 expression can be triggered by Tau molecules and this effect is exerted in the nuclear compartment.

The discovery of this nuclear role of Tau leads to the question if pathological mutations or aggregation could affect its function. The expression of the tauopathy related P301S or P301L mutations shows two different and unexpected effects. Subcellular fractionation indicates that both mutations lead to an increase of Tau in the nucleus that is comparable to Tau^{WT}. However, when we look at the nuclear function, Tau^{P301S} is able to induce a significant increase in VGluT1 that is not detectable in cells expressing Tau^{P301L}. This result indicates that P301L mutation causes a loss of function of Tau in the nuclear compartment while P301S does not affect nuclear Tau. Intriguingly, previous characterizations of these two mutations indicated that they similarly destabilize Tau on MTs and induce aggregation leading to pathology. On the contrary, the study of their nuclear behaviour demonstrates a significant difference in modulating VGluT1 expression even if the mechanism is still unclear and under investigation. A possibility is that they undergo different post-translational modifications which differentially influence nuclear Tau function. Another cause might be the nature of the substituted aminoacids since the leucine is apolar and might have a stronger impact on Tau properties than the polar serine. The Pro301 residue is located in the second repeat of the MTBD that is absent in 3R Tau isoforms so we expressed the Tau 0N3R in order to clarify if the absence of R2 could impair the modulation of VGluT1 levels. The expression of Tau 0N3R induces an increase of VGluT1 comparable to the one observed by Tau 0N4R suggesting that the R2 is not necessary for Tau nuclear function even if *in vitro* studies showed that it is important for the interaction with DNA (Hua and He, 2003; Qi et al., 2015). Moreover, this result suggests that the loss of function caused by the P301L mutation is specific and independent from the repeats in the MTBD. Although the molecular mechanisms involved are still unclear, a more extensive study on gene expression might be performed to elucidate the role of wild-type and mutated Tau on the modulation of genes involved in glutamatergic synaptic transmission. It would be interesting to investigate whether other pathological mutations impair Tau modulation of gene expression.

This novel function might have a relevant role in the onset of the pathology as it has been widely demonstrated that the glutamate release is increased and causes hippocampal hyperexcitability in the pre-symptomatic phase of

tauopathies. To study the nuclear effect in later stages, Tau aggregation has been induced. However, VGluT1 expression is comparable to control cells, demonstrating that pathological inclusions impair Tau nuclear function. Remarkably, Tau aggregation is an hallmark of late stages of neurodegeneration which corresponds to a reduction in the excitability and glutamate release (Braak et al., 2006; Dickerson et al., 2005). It's still unsolved how aggregation affects Tau nuclear function, it may aggregate also in the nucleus blocking its function or it may alter cytoplasmic mechanisms related to nuclear Tau. A possible mechanism has been suggested in a recent study by Benhelli-Mokrani et al. They demonstrated that Tau oligomers in neuronal nuclei induce a repression of gene expression on specific targets bound directly by Tau (Benhelli-Mokrani et al., 2018). However further experiments will be performed to better characterize the role of Tau aggregation in the nuclear compartment.

To investigate whether other genes are modulated by Tau a high-throughput approach has been employed by RNAseq technique. The overexpression of Tau 0N4R in differentiated SHSY5Y induces a global transcriptome alteration. Indeed, ~4000 genes are differentially expressed (DEGs) and GO analysis for cellular functions identifies several clusters that are significantly altered and mostly related to neurodegeneration. Remarkably the glutamate release pathway cluster is represented, suggesting that Tau influences not only VGluT1 expression but several genes involved in this function. Moreover, a further analysis reveals that Tau alters post-synaptic genes specific for the NMDA receptors, for example NMDA subunits GRIN2C and GRIN2D, but not AMPA receptors, demonstrating that its function is selective. Remarkably, the post-synaptic modulation has a functional counterpart observed by patch-clamp in primary hippocampal neurons. As a matter of fact, we observe a significant increase of mEPSC amplitude in treated cells which is usually attributed to a post-synaptic effect, supporting the transcriptome analysis. Other clusters are deregulated in Tau expressing cells, such as those regarding protein synthesis and genome stability, which are also altered in AD models and patients (Garcia-Esparcia et al., 2017; Hernández-Ortega et al., 2016; Sultan et al., 2011). Our transcriptome has been compared to a database of hippocampi from patients at different stages of AD in order to understand if the genes and clusters identified in our cellular model are also

represented in the human pathological context. Indeed, the DEGs observed in our model strongly correlate with DEGs individuated in L-MCI patients, while the correlation is lower with both E-MCI and AD patients. These evidences suggest that Tau overexpression mimics a L-MCI pathological context which generally corresponds at cellular level to Tau destabilization and the first step of aggregation (Braak et al., 2006; Lowe et al., 2018). These data support our cellular model as a reliable and easy system for preliminary studies of Tau pathological behaviour in destabilizing conditions, in particular for studies of gene modulation and functional alteration. These preliminary results open to further experiments in order to clarify how the deregulation of gene expression observed in tauopathies is directly caused by Tau protein, in particular by its nuclear pool, leading to a new relevant pathological Tau function which can be targeted to prevent neurodegeneration.

It's a key point to further investigate this function to identify possible targets for therapeutic intervention. Since Tau has been seen to bind directly the DNA in the nucleus (Benhelli-Mokrani et al., 2018), we evaluated if Tau modulates VGluT1 levels by acting on its promoter. However, we demonstrated that Tau effect on VGluT1 is not directed to the promoter. This result does not exclude that Tau can influence VGluT1 expression by interacting directly or indirectly to other regulatory genetic regions, such as enhancers or silencers, and this hypothesis will be investigated in future experiments. A possible mechanism which could explain nuclear Tau alteration of gene expression is that by interacting with other proteins, it may influence the expression of genes as a transcription factor or it may induce a chromatin modification. Indeed, recent studies suggest that nuclear Tau is associated to heterochromatin regions. Analysis of human brains showed that Tau phosphorylated at AT100 epitope increases during aging and colocalizes with heterochromatin. Moreover, the loss of Tau causes the activation of transposons which are usually silenced in heterochromatic regions (Gil et al., 2017; Guo et al., 2018; Sun et al., 2018). The mechanisms by which Tau localizes to the nucleus are still unknown, although it has been shown that the interaction of Tau with TRIM28 stabilizes and promotes Tau nuclear accumulation. In addition, both nuclear Tau and nuclear TRIM28 are increased in AD brains (Rousseaux et al., 2016). Remarkably, TRIM28 is a key nuclear

protein whose function is to form a big complex with several interactors, leading to chromatin condensation (Barde et al., 2013; Friedman et al., 2007). The interaction between Tau and TRIM28 and the association of Tau and heterochromatin lead to the hypothesis that nuclear Tau may alter gene expression by chromatin remodelling. Our experiments indicate that TRIM28 expression and subcellular localization is not altered by the increase in Tau nuclear levels. Remarkably, by checking the expression of HDAC1, a TRIM28 well-characterized interactor, a significant reduction can be seen in the chromatin-bound fraction confirmed also by immunofluorescence experiments. These results suggest that the increase in Tau levels is able to induce a delocalization of HDAC1 with no effect on HDAC1 and TRIM28 expression. A preliminary co-IP experiment shows that Tau might have a competitive effect on HDAC1 for the interaction with TRIM28 which could explain the HDAC1 delocalization from the chromatin fraction. However, the properties of this putative complex have to be further confirmed and investigated and other TRIM28 interactors will be considered. The open question is if HDAC1 delocalization is due to cytoplasmic or nuclear Tau. A preliminary result with Tau-NES suggests that cytoplasmic Tau does not influence HDAC1 nuclear localization, indicating that the competition for the interaction with TRIM28 is probably due to the nuclear fraction of Tau. In addition, we evaluated if the delocalization of HDAC1 from the chromatin is sufficient to explain the alteration of VGluT1 expression observed when Tau levels are increased. To clarify this point cells were treated with TSA, an inhibitor of HDACs family members, among these HDAC1 (Delcuve et al., 2013). Western blot analysis shows that VGluT1 levels in TSA-treated cells are higher than control cells and comparable to the increase observed in Tau expressing cells, suggesting that the delocalization and the impairment of HDAC1 function might induce an increase in VGluT1 expression. Further investigation is needed as knock-down experiments of TRIM28 and HDAC1, Tau effect on other TRIM28 interactors and studies in animal models for tauopathies. However, these preliminary results indicate a mechanism associated to a Tau-dependent chromatin remodelling which has also been observed in a Drosophila model for tauopathies (Frost et al., 2014). Remarkably a global chromatin relaxation was also seen in AD human brains, with altered levels of HDAC class I and histone acetylation influencing gene

expression (Frost et al., 2014; Sun et al., 2018). Another possible mechanism explaining the gene expression modulation mediated by nuclear Tau and the interaction with TRIM28 can be related to an alteration in the acetylation profile of Tau. Indeed, TRIM28 cofactors, in particular proteins of the HDAC family, may modify the acetylation of Tau, currently associated to destabilization and pathological aggregation, thus altering its nuclear amount or function (Carlomagno et al., 2017; Ulrich et al., 2018). Moreover, Tau has been seen to interact with HDAC6 in the cytosol reducing its deacetylation activity and increasing the acetylation of HDAC6 targets as a consequence (Ding et al., 2008; Perez et al., 2009; Selenica et al., 2014). This evidence suggests that other mechanisms involving Tau and HDACs have been identified and similar processes could also take place in the nuclear compartment with members of the same family. However, further studies are necessary such as the identification of acetylated residues of Tau in the nucleus and the acetylation level of TRIM28 and HDACs targets in presence or absence of Tau.

Altogether these results indicate that Tau has a role in gene expression modulation which can be altered if the protein is destabilized and its soluble amount is increased as a consequence. Remarkably, the evidence that nuclear Tau affects exclusively VGluT1 expression influencing neuronal excitability, suggests that the progressive pathological functional alterations that neurons undergo in tauopathies might be dependent more on the unbalancing of soluble Tau which becomes more available to be translocated into the nucleus than on modifications of cytoplasmic Tau functions. This is also supported by the fact that the increase in Tau amount induces not only an increase in VGluT1 levels but also a global gene alteration, mimicking specifically a L-MCI condition in patients. However, in order to determine which neuronal functions are dependent exclusively on nuclear Tau alteration, further studies are needed in particular transcriptomic analyses on cells expressing Tau-NLS or Tau-NES will discriminate the gene sets modulated by Tau in the nucleus or in the cytosol and this experiment will be coupled to functional validations in neuronal cells to evaluate that the gene altered by nuclear Tau have a real impact in the cellular context. Moreover, to clarify if nuclear Tau could be a new therapeutic target to treat tauopathies progression, its role needs to be confirmed in mouse models for

tauopathies, focusing on different phases of Tau pathology progression or developing a new model in which Tau subcellular localization is unbalanced towards the nuclear compartment. Another important point is to understand the effect of Tau aggregation on nuclear Tau both *in vitro* and *in vivo*, above all in relation to the late stages of tauopathies. The discovery of Tau as a gene modulator in the nucleus, if its centrality will be confirmed with further investigations, could lead to a different way to approach Tau pathologies, not only focusing on the aggregate and its spreading but considering a new subcellular compartment where Tau is localized. Therapeutic strategies could target different aspects of nuclear Tau to prevent its pathological effect for example the regulation of its transport into the nucleus or its mechanism in gene modulation or cofactors which mediate its nuclear function.

In conclusion, with this research we investigated Tau alternative functions, a field that was underestimated in past decades but that is currently growing due to strong evidences which support the importance of these functions both in physiology and pathology. In particular, we focused on the nuclear localization of Tau which is important in physiology to maintain genome stability but this protective action is impaired during tauopathies leading to neuronal damage. We discovered an additional Tau function in the nucleus as a matter of fact Tau is able to modulate gene expression altering the neuronal excitability in conditions mimicking early pathological stages of tauopathies. In addition, this function seems related to an effect of Tau on chromatin remodelling suggesting that nuclear Tau can be more important than previously hypothesized since a chromatin structural reorganization is associated to a global gene alteration, an hallmark typical of tauopathies. However further studies are needed to clarify the behaviour of nuclear Tau in late pathological stages when Tau is aggregated but also a complete picture of the nuclear mechanisms in order to identify a potential target to impede the damages caused by Tau functional alteration in the nuclear compartment, opening to new therapeutic approaches to challenge the neurodegeneration mediated by Tau.

Bibliography

Abraha, A., Ghoshal, N., Gamblin, T.C., Cryns, V., Berry, R.W., Kuret, J., and Binder, L.I. (2000). C-terminal inhibition of tau assembly in vitro and in Alzheimer's disease. J. Cell Sci. *113 Pt 21*, 3737–3745.

Ahmed, T., Van der Jeugd, A., Blum, D., Galas, M.-C., D'Hooge, R., Buee, L., and Balschun, D. (2014). Cognition and hippocampal synaptic plasticity in mice with a homozygous tau deletion. Neurobiol. Aging *35*, 2474–2478.

Ali, Y.O., Ruan, K., and Zhai, R.G. (2012). NMNAT suppresses tau-induced neurodegeneration by promoting clearance of hyperphosphorylated tau oligomers in a Drosophila model of tauopathy. Hum. Mol. Genet. *21*, 237–250.

Allen, B., Ingram, E., Takao, M., Smith, M.J., Jakes, R., Virdee, K., Yoshida, H., Holzer, M., Craxton, M., Emson, P.C., et al. (2002). Abundant tau filaments and nonapoptotic neurodegeneration in transgenic mice expressing human P301S tau protein. J. Neurosci. *22*, 9340–9351.

Alonso, A., Zaidi, T., Novak, M., Grundke-Iqbal, I., and Iqbal, K. (2001). Hyperphosphorylation induces self-assembly of tau into tangles of paired helical filaments/straight filaments. Proc. Natl. Acad. Sci. U. S. A. *98*, 6923–6928.

Alonso, A. del C., Mederlyova, A., Novak, M., Grundke-Iqbal, I., and Iqbal, K. (2004). Promotion of hyperphosphorylation by frontotemporal dementia tau mutations. J. Biol. Chem. *279*, 34873–34881.

Alonso, A.D., Grundke-Iqbal, I., Barra, H.S., and Iqbal, K. (1997). Abnormal phosphorylation of tau and the mechanism of Alzheimer neurofibrillary degeneration: sequestration of microtubule-associated proteins 1 and 2 and the disassembly of microtubules by the abnormal tau. Proc. Natl. Acad. Sci. U. S. A. *94*, 298–303.

Alonso, A.D., Di Clerico, J., Li, B., Corbo, C.P., Alaniz, M.E., Grundke-Iqbal, I., and Iqbal, K. (2010). Phosphorylation of tau at Thr212, Thr231, and Ser262 combined causes neurodegeneration. J. Biol. Chem. *285*, 30851–30860.

Amos, L.A. (2004). Microtubule structure and its stabilisation. Org. Biomol. Chem.

2, 2153–2160.

Anders, S., and Huber, W. (2010). Differential expression analysis for sequence count data. Genome Biol. *11*, R106.

Andorfer, C.A., and Davies, P. (2000). PKA Phosphorylations on Tau: Developmental Studies in the Mouse. Dev. Neurosci. *22*, 303–309.

Andreadis, A., Brown, W.M., and Kosik, K.S. (1992). Structure and novel exons of the human tau gene. Biochemistry *31*, 10626–10633.

Arai, T., Ikeda, K., Akiyama, H., Shikamoto, Y., Tsuchiya, K., Yagishita, S., Beach, T., Rogers, J., Schwab, C., and McGeer, P.L. (2001). Distinct isoforms of tau aggregated in neurons and glial cells in brains of patients with Pick's disease, corticobasal degeneration and progressive supranuclear palsy. Acta Neuropathol. *101*, 167–173.

Arai, T., Miklossy, J., Klegeris, A., Guo, J.-P., and McGeer, P.L. (2006). Thrombin and prothrombin are expressed by neurons and glial cells and accumulate in neurofibrillary tangles in Alzheimer disease brain. J. Neuropathol. Exp. Neurol. *65*, 19–25.

Arendt, T., Stieler, J.T., and Holzer, M. (2016). Tau and tauopathies. Brain Res. Bull. *126*, 238–292.

Arriagada, P. V, Growdon, J.H., Hedley-Whyte, E.T., and Hyman, B.T. (1992). Neurofibrillary tangles but not senile plaques parallel duration and severity of Alzheimer's disease. Neurology *42*, 631–639.

Avila, J., Lucas, J.J., Perez, M., and Hernandez, F. (2004). Role of tau protein in both physiological and pathological conditions. Physiol. Rev. *84*, 361–384.

Avila, J., Llorens-Martín, M., Pallas-Bazarra, N., Bolós, M., Perea, J.R., Rodríguez-Matellán, A., and Hernández, F. (2017). Cognitive decline in neuronal aging and Alzheimer's disease: Role of NMDA receptors and associated proteins. Front. Neurosci. *11*, 1–9.

Azoury, J., Lee, K.W., Georget, V., Rassinier, P., Leader, B., Curie, M., Bat, C., Bernard, Q. Saint, Bat, B., and Bernard, Q. Saint (2008). Report Spindle

Positioning in Mouse Oocytes Relies on a Dynamic Meshwork of Actin Filaments. 1514–1519.

Bai, Q., and Burton, E.A. (2011). Zebrafish models of Tauopathy. Biochim. Biophys. Acta - Mol. Basis Dis. *1812*, 353–363.

Bai, Q., Garver, J.A., Hukriede, N.A., and Burton, E.A. (2007). Generation of a transgenic zebrafish model of Tauopathy using a novel promoter element derived from the zebrafish eno2 gene. Nucleic Acids Res. *35*, 6501–6516.

Baker, M., Litvan, I., Houlden, H., Adamson, J., Dickson, D., Perez-Tur, J., Hardy, J., Lynch, T., Bigio, E., and Hutton, M. (1999). Association of an extended haplotype in the tau gene with progressive supranuclear palsy. Hum. Mol. Genet. *8*, 711–715.

Barde, I., Rauwel, B., Marin-Florez, R.M., Corsinotti, A., Laurenti, E., Verp, S., Offner, S., Marquis, J., Kapopoulou, A., Vanicek, J., et al. (2013). A KRAB/KAP1-miRNA Cascade Regulates Erythropoiesis Through Stage-Specific Control of Mitophagy. Science (80-.). *340*, 350–353.

Barghorn, S., and Mandelkow, E. (2002). Toward a unified scheme for the aggregation of tau into Alzheimer paired helical filaments. Biochemistry *41*, 14885–14896.

Beevers, J.E., Lai, M.C., Collins, E., Booth, H.D.E., Zambon, F., Parkkinen, L., Vowles, J., Cowley, S.A., Wade-Martins, R., and Caffrey, T.M. (2017). MAPT Genetic Variation and Neuronal Maturity Alter Isoform Expression Affecting Axonal Transport in iPSC-Derived Dopamine Neurons. Stem Cell Reports *9*, 587–599.

Benhelli-Mokrani, H., Mansuroglu, Z., Chauderlier, A., Albaud, B., Gentien, D., Sommer, S., Schirmer, C., Laqueuvre, L., Josse, T., Buée, L., et al. (2018). Genome-wide identification of genic and intergenic neuronal DNA regions bound by Tau protein under physiological and stress conditions. Nucleic Acids Res. *1*, 1–18.

Bentley, D.R., Balasubramanian, S., Swerdlow, H.P., Smith, G.P., Milton, J., Brown, C.G., Hall, K.P., Evers, D.J., Barnes, C.L., Bignell, H.R., et al. (2008).

Accurate whole human genome sequencing using reversible terminator chemistry. Nature *456*, 53–59.

von Bergen, M., Friedhoff, P., Biernat, J., Heberle, J., Mandelkow, E.M., and Mandelkow, E. (2000). Assembly of tau protein into Alzheimer paired helical filaments depends on a local sequence motif ((306)VQIVYK(311)) forming beta structure. Proc. Natl. Acad. Sci. U. S. A. *97*, 5129–5134.

Bertrand, J., Plouffe, V., Sénéchal, P., and Leclerc, N. (2010). The pattern of human tau phosphorylation is the result of priming and feedback events in primary hippocampal neurons. Neuroscience *168*, 323–334.

Bibow, S., Ozenne, V., Biernat, J., Blackledge, M., Mandelkow, E., and Zweckstetter, M. (2011). Structural Impact of Proline-Directed Pseudophosphorylation at AT8, AT100, and PHF1 Epitopes on 441-Residue Tau. J. Am. Chem. Soc. *133*, 15842–15845.

Bier, E. (2005). Drosophila, the golden bug, emerges as a tool for human genetics. Nat. Rev. Genet. *6*, 9–23.

Bilen, J., and Bonini, N.M. (2005). Drosophila as a Model for Human Neurodegenerative Disease. Annu. Rev. Genet. *39*, 153–171.

Bindea, G., Mlecnik, B., Hackl, H., Charoentong, P., Tosolini, M., Kirilovsky, A., Fridman, W.-H., Pagès, F., Trajanoski, Z., and Galon, J. (2009). ClueGO: a Cytoscape plug-in to decipher functionally grouped gene ontology and pathway annotation networks. Bioinformatics *25*, 1091–1093.

Binder, L.I., Frankfurter, A., and Rebhun, L.I. (1985). The distribution of tau in the mammalian central nervous system. J. Cell Biol. *101*, 1371–1378.

Birks, J. (2006). Cholinesterase inhibitors for Alzheimer's disease. Cochrane Database Syst. Rev. CD005593.

Boekhoorn, K., Terwel, D., Biemans, B., Borghgraef, P., Wiegert, O., Ramakers, G.J.A., de Vos, K., Krugers, H., Tomiyama, T., Mori, H., et al. (2006). Improved long-term potentiation and memory in young tau-P301L transgenic mice before onset of hyperphosphorylation and tauopathy. J. Neurosci. *26*, 3514–3523.

Bondulich, M.K., Guo, T., Meehan, C., Manion, J., Rodriguez Martin, T., Mitchell, J.C., Hortobagyi, T., Yankova, N., Stygelbout, V., Brion, J.-P., et al. (2016). Tauopathy induced by low level expression of a human brain-derived tau fragment in mice is rescued by phenylbutyrate. Brain *139*, 2290–2306.

Bonneau, C., Gurard-Levin, Z.A., Andre, F., Pusztai, L., and Rouzier, R. (2015). Predictive and prognostic value of the Tau protein in breast cancer. Anticancer Res. *35*, 5179–5184.

Braak, H., Braak, E., and Strothjohann, M. (1994). Abnormally phosphorylated tau protein related to the formation of neurofibrillary tangles and neuropil threads in the cerebral cortex of sheep and goat. Neurosci. Lett. *171*, 1–4.

Braak, H., Alafuzoff, I., Arzberger, T., Kretzschmar, H., and Del Tredici, K. (2006). Staging of Alzheimer disease-associated neurofibrillary pathology using paraffin sections and immunocytochemistry. Acta Neuropathol. *112*, 389–404.

Bretteville, A., Marcouiller, F., Julien, C., El Khoury, N.B., Petry, F.R., Poitras, I., Mouginot, D., Lévesque, G., Hébert, S.S., and Planel, E. (2012). Hypothermia-induced hyperphosphorylation: a new model to study tau kinase inhibitors. Sci. Rep. *2*, 480.

Breuzard, G., Hubert, P., Nouar, R., De Bessa, T., Devred, F., Barbier, P., Sturgis, J.N., and Peyrot, V. (2013). Molecular mechanisms of Tau binding to microtubules and its role in microtubule dynamics in live cells. J. Cell Sci. *126*, 2810–2819.

Buée-Scherrer, V., Hof, P.R., Buée, L., Leveugle, B., Vermersch, P., Perl, D.P., Olanow, C.W., and Delacourte, A. (1996). Hyperphosphorylated tau proteins differentiate corticobasal degeneration and Pick's disease. Acta Neuropathol. *91*, 351–359.

Bugiani, O., Murrell, J.R., Giaccone, G., Hasegawa, M., Ghigo, G., Tabaton, M., Morbin, M., Primavera, A., Carella, F., Solaro, C., et al. (1999). Frontotemporal dementia and corticobasal degeneration in a family with a P301S mutation in tau. J. Neuropathol. Exp. Neurol. *58*, 667–677.

Caffrey, T.M., Joachim, C., Paracchini, S., Esiri, M.M., and Wade-Martins, R.

(2006). Haplotype-specific expression of exon 10 at the human MAPT locus. Hum. Mol. Genet. *15*, 3529–3537.

Carlomagno, Y., Chung, D.C., Yue, M., Castanedes-Casey, M., Madden, B.J., Dunmore, J., Tong, J., DeTure, M., Dickson, D.W., Petrucelli, L., et al. (2017). An acetylation–phosphorylation switch that regulates tau aggregation propensity and function. J. Biol. Chem. *292*, 15277–15286.

Carlyle, B.C., Nairn, A.C., Wang, M., Yang, Y., Jin, L.E., Simen, A.A., Ramos, B.P., Bordner, K.A., Craft, G.E., Davies, P., et al. (2014). cAMP-PKA phosphorylation of tau confers risk for degeneration in aging association cortex. Proc. Natl. Acad. Sci. *111*, 5036–5041.

Cataldo, A.M., Barnett, J.L., Pieroni, C., and Nixon, R.A. (1997). Increased neuronal endocytosis and protease delivery to early endosomes in sporadic Alzheimer's disease: neuropathologic evidence for a mechanism of increased beta-amyloidogenesis. J. Neurosci. *17*, 6142–6151.

Chauderlier, A., Gilles, M., Spolcova, A., Caillierez, R., Chwastyniak, M., Kress, M., Drobecq, H., Bonnefoy, E., Pinet, F., Weil, D., et al. (2018). Tau/DDX6 interaction increases microRNA activity. Biochim. Biophys. Acta. Gene Regul. Mech. *1861*, 762–772.

Chen, J., Kanai, Y., Cowan, N.J., and Hirokawa, N. (1992). Projection domains of MAP2 and tau determine spacings between microtubules in dendrites and axons. Nature *360*, 674–677.

Cho, J.-H., and Johnson, G.V.W. (2003). Glycogen synthase kinase 3beta phosphorylates tau at both primed and unprimed sites. Differential impact on microtubule binding. J. Biol. Chem. *278*, 187–193.

Cho, J.-H., and Johnson, G.V.W. (2004). Glycogen synthase kinase 3 beta induces caspase-cleaved tau aggregation in situ. J. Biol. Chem. *279*, 54716–54723.

Clavaguera, F., Bolmont, T., Crowther, R.A., Abramowski, D., Frank, S., Probst, A., Fraser, G., Stalder, A.K., Beibel, M., Staufenbiel, M., et al. (2009). Transmission and spreading of tauopathy in transgenic mouse brain. Nat. Cell

Biol. *11*, 909–913.

Cleveland, D.W., Hwo, S.Y., and Kirschner, M.W. (1977). Purification of tau, a microtubule-associated protein that induces assembly of microtubules from purified tubulin. J. Mol. Biol. *116*, 207–225.

Cohen, T.J., Guo, J.L., Hurtado, D.E., Kwong, L.K., Mills, I.P., Trojanowski, J.Q., and Lee, V.M.Y. (2011). The acetylation of tau inhibits its function and promotes pathological tau aggregation. Nat. Commun. *2*, 252.

Colodner, K.J., and Feany, M.B. (2010). Glial fibrillary tangles and JAK/STAT-mediated glial and neuronal cell death in a Drosophila model of glial tauopathy. J. Neurosci. *30*, 16102–16113.

Le Corre, S., Klafki, H.W., Plesnila, N., Hübinger, G., Obermeier, A., Sahagún, H., Monse, B., Seneci, P., Lewis, J., Eriksen, J., et al. (2006). An inhibitor of tau hyperphosphorylation prevents severe motor impairments in tau transgenic mice. Proc. Natl. Acad. Sci. U. S. A. *103*, 9673–9678.

Costes, S. V., Daelemans, D., Cho, E.H., Dobbin, Z., Pavlakis, G., and Lockett, S. (2004). Automatic and quantitative measurement of protein-protein colocalization in live cells. Biophys. J. *86*, 3993–4003.

Crescenzi, R., DeBrosse, C., Nanga, R.P.R., Byrne, M.D., Krishnamoorthy, G., D'Aquilla, K., Nath, H., Morales, K.H., Iba, M., Hariharan, H., et al. (2017). Longitudinal imaging reveals sub-hippocampal dynamics in glutamate levels associated with histopathologic events in a mouse model of tauopathy and healthy mice. Hippocampus *27*, 285–302.

Cruz, J.C., Tseng, H.-C., Goldman, J.A., Shih, H., and Tsai, L.-H. (2003). Aberrant Cdk5 activation by p25 triggers pathological events leading to neurodegeneration and neurofibrillary tangles. Neuron *40*, 471–483.

Crystal, A.S., Giasson, B.I., Crowe, A., Kung, M.P., Zhuang, Z.P., Trojanowski, J.Q., and Lee, V.M.Y. (2003). A comparison of amyloid fibrillogenesis using the novel fluorescent compound K114. J. Neurochem. *86*, 1359–1368.

Daebel, V., Chinnathambi, S., Biernat, J., Schwalbe, M., Habenstein, B., Loquet,

A., Akoury, E., Tepper, K., Müller, H., Baldus, M., et al. (2012). β-Sheet core of tau paired helical filaments revealed by solid-state NMR. J. Am. Chem. Soc. *134*, 13982–13989.

Daly, N.L., Hoffmann, R., Otvos, L., and Craik, D.J. (2000). Role of phosphorylation in the conformation of tau peptides implicated in Alzheimer's disease. Biochemistry *39*, 9039–9046.

Dayanandan, R., Van Slegtenhorst, M., Mack, T.G.A., Ko, L., Yen, S.-H., Leroy, K., Brion, J.-P., Anderton, B.H., Hutton, M., and Lovestone, S. (1999). Mutations in tau reduce its microtubule binding properties in intact cells and affect its phosphorylation. FEBS Lett. *446*, 228–232.

Delacourte, A., Robitaille, Y., Sergeant, N., Buée, L., Hof, P.R., Wattez, A., Laroche-Cholette, A., Mathieu, J., Chagnon, P., and Gauvreau, D. (1996). Specific pathological Tau protein variants characterize Pick's disease. J. Neuropathol. Exp. Neurol. *55*, 159–168.

Delcuve, G., Khan, D., and Davie, J. (2013). Roles of Histone Deacetylases in Epigenetic Regulation. Epigenetics Pathol. 143–172.

Devos, S.L., Miller, R.L., Schoch, K.M., Holmes, B.B., Kebodeaux, C.S., Wegener, A.J., Chen, G., Shen, T., Tran, H., Nichols, B., et al. (2017). Tau reduction prevents neuronal loss and reverses pathological tau deposition and seeding in mice with tauopathy. *0481*.

DeVos, S.L., Goncharoff, D.K., Chen, G., Kebodeaux, C.S., Yamada, K., Stewart, F.R., Schuler, D.R., Maloney, S.E., Wozniak, D.F., Rigo, F., et al. (2013). Antisense Reduction of Tau in Adult Mice Protects against Seizures. J. Neurosci. *33*, 12887–12897.

DeVos, S.L., Corjuc, B.T., Commins, C., Dujardin, S., Bannon, R.N., Corjuc, D., Moore, B.D., Bennett, R.E., Jorfi, M., Gonzales, J.A., et al. (2018). Tau reduction in the presence of amyloid-β prevents tau pathology and neuronal death in vivo. Brain *141*, 2194–2212.

Dickerson, B.C., Salat, D.H., Greve, D.N., Chua, E.F., Rand-Giovannetti, E., Rentz, D.M., Bertram, L., Mullin, K., Tanzi, R.E., Blacker, D., et al. (2005).

Increased hippocampal activation in mild cognitive impairment compared to normal aging and AD. Neurology *65*, 404–411.

Ding, H., Dolan, P.J., and Johnson, G.V.W. (2008). Histone deacetylase 6 interacts with the microtubule-associated protein tau. J. Neurochem. *106*, 2119–2130.

Dixit, R., Ross, J.L., Goldman, Y.E., and Holzbaur, E.L.F. (2008). Differential regulation of dynein and kinesin motor proteins by tau. Science *319*, 1086–1089.

Dotti, C.G., Banker, G.A., and Binder, L.I. (1987). The expression and distribution of the microtubule-associated proteins tau and microtubule-associated protein 2 in hippocampal neurons in the rat in situ and in cell culture. Neuroscience *23*, 121–130.

Ebneth, A., Godemann, R., Stamer, K., Illenberger, S., Trinczek, B., and Mandelkow, E. (1998). Overexpression of tau protein inhibits kinesin-dependent trafficking of vesicles, mitochondria, and endoplasmic reticulum: implications for Alzheimer's disease. J. Cell Biol. *143*, 777–794.

Eckermann, K., Mocanu, M.-M., Khlistunova, I., Biernat, J., Nissen, A., Hofmann, A., Schönig, K., Bujard, H., Haemisch, A., Mandelkow, E., et al. (2007). The beta-propensity of Tau determines aggregation and synaptic loss in inducible mouse models of tauopathy. J. Biol. Chem. *282*, 31755–31765.

Feige, J.N., Sage, D., Wahli, W., Desvergne, B., and Gelman, L. (2005). PixFRET, an ImageJ plug-in for FRET calculation that can accommodate variations in spectral bleed-throughs. Microsc. Res. Tech. *68*, 51–58.

Filipcik, P., Zilka, N., Bugos, O., Kucerak, J., Koson, P., Novak, P., and Novak, M. (2012). First transgenic rat model developing progressive cortical neurofibrillary tangles. Neurobiol. Aging *33*, 1448–1456.

Fitzpatrick, A.W.P., Falcon, B., He, S., Murzin, A.G., Murshudov, G., Garringer, H.J., Crowther, R.A., Ghetti, B., Goedert, M., and Scheres, S.H.W. (2017). Cryo-EM structures of tau filaments from Alzheimer's disease. Nature *547*, 185–190.

Förster, T. (1948). Zwischenmolekulare Energiewanderung und Fluoreszenz.

Ann. Phys. *437*, 55–75.

Frandemiche, M.L., De Seranno, S., Rush, T., Borel, E., Elie, A., Arnal, I., Lante, F., and Buisson, A. (2014). Activity-Dependent Tau Protein Translocation to Excitatory Synapse Is Disrupted by Exposure to Amyloid-Beta Oligomers. J. Neurosci. *34*, 6084–6097.

Friedman, J.R., Neilson, E.G., Speicher, D.W., Rauscher, F.J., Fredericks, W.J., Jensen, D.E., and Huang, X.P. (2007). KAP-1, a novel corepressor for the highly conserved KRAB repression domain. Genes Dev. *10*, 2067–2078.

Frost, B., Jacks, R.L., and Diamond, M.I. (2009). Propagation of tau misfolding from the outside to the inside of a cell. J. Biol. Chem. *284*, 12845–12852.

Frost, B., Hemberg, M., Lewis, J., and Feany, M.B. (2014). Tau promotes neurodegeneration through global chromatin relaxation. Nat. Neurosci. *17*, 357–366.

Futerman, A.H., and Banker, G.A. (1996). The economics of neurite outgrowth--the addition of new membrane to growing axons. Trends Neurosci. *19*, 144–149.

Gamblin, T.C., Chen, F., Zambrano, A., Abraha, A., Lagalwar, S., Guillozet, A.L., Lu, M., Fu, Y., Garcia-Sierra, F., LaPointe, N., et al. (2003). Caspase cleavage of tau: linking amyloid and neurofibrillary tangles in Alzheimer's disease. Proc. Natl. Acad. Sci. U. S. A. *100*, 10032–10037.

Garcia-Esparcia, P., Sideris-Lampretsas, G., Hernandez-Ortega, K., Grau-Rivera, O., Sklaviadis, T., Gelpi, E., and Ferrer, I. (2017). Altered mechanisms of protein synthesis in frontal cortex in Alzheimer disease and a mouse model. Am. J. Neurodegener. Dis. *6*, 15–25.

Gil, L., Federico, C., Pinedo, F., Bruno, F., Rebolledo, A.B., Montoya, J.J., Olazabal, I.M., Ferrer, I., and Saccone, S. (2017). Aging dependent effect of nuclear tau. Brain Res. *1677*, 129–137.

Gistelinck, M., Lambert, J.-C., Callaerts, P., Dermaut, B., and Dourlen, P. (2012). Drosophila Models of Tauopathies: What Have We Learned? Int. J. Alzheimers. Dis. *2012*, 1–14.

Goedert, M., and Jakes, R. (1990). Expression of sepearate isoforms of human tau protein. Embo *9*, 4225–4230.

Goedert, M., Spillantini, M.G., Jakes, R., Rutherford, D., and Crowther, R.A. (1989a). Multiple isoforms of human microtubule-associated protein tau: sequences and localization in neurofibrillary tangles of Alzheimer's disease. Neuron *3*, 519–526.

Goedert, M., Spillantini, M.G., Potier, M.C., Ulrich, J., and Crowther, R.A. (1989b). Cloning and sequencing of the cDNA encoding an isoform of microtubule-associated protein tau containing four tandem repeats: differential expression of tau protein mRNAs in human brain. EMBO J. *8*, 393–399.

Goedert, M., Spillantini, M.G., and Crowther, R.A. (1992). Cloning of a big tau microtubule-associated protein characteristic of the peripheral nervous system. Proc. Natl. Acad. Sci. *89*, 1983–1987.

Goedert, M., Jakes, R., and Crowther, R.A. (1999). Effects of frontotemporal dementia FTDP-17 mutations on heparin-induced assembly of tau filaments. FEBS Lett. *450*, 306–311.

Gómez-Isla, T., Hollister, R., West, H., Mui, S., Growdon, J.H., Petersen, R.C., Parisi, J.E., and Hyman, B.T. (1997). Neuronal loss correlates with but exceeds neurofibrillary tangles in Alzheimer's disease. Ann. Neurol. *41*, 17–24.

Gómez de Barreda, E., Dawson, H.N., Vitek, M.P., and Avila, J. (2010). Tau deficiency leads to the upregulation of BAF-57, a protein involved in neuron-specific gene repression. FEBS Lett. *584*, 2265–2270.

Gong, C.-X., Liu, F., Grundke-Iqbal, I., and Iqbal, K. (2005). Post-translational modifications of tau protein in Alzheimer's disease. J. Neural Transm. *112*, 813–838.

Gong, C.X., Singh, T.J., Grundke-Iqbal, I., and Iqbal, K. (1993). Phosphoprotein phosphatase activities in Alzheimer disease brain. J. Neurochem. *61*, 921–927.

Gu, Y., Oyama, F., and Ihara, Y. (1996). Tau is widely expressed in rat tissues. J. Neurochem. *67*, 1235–1244.

Guillozet-Bongaarts, A.L., Garcia-Sierra, F., Reynolds, M.R., Horowitz, P.M., Fu, Y., Wang, T., Cahill, M.E., Bigio, E.H., Berry, R.W., and Binder, L.I. (2005). Tau truncation during neurofibrillary tangle evolution in Alzheimer's disease. Neurobiol. Aging *26*, 1015–1022.

Guillozet-Bongaarts, A.L., Cahill, M.E., Cryns, V.L., Reynolds, M.R., Berry, R.W., and Binder, L.I. (2006). Pseudophosphorylation of tau at serine 422 inhibits caspase cleavage: in vitro evidence and implications for tangle formation in vivo. J. Neurochem. *97*, 1005–1014.

Guo, C., Jeong, H.H., Hsieh, Y.C., Klein, H.U., Bennett, D.A., De Jager, P.L., Liu, Z., and Shulman, J.M. (2018). Tau Activates Transposable Elements in Alzheimer's Disease. Cell Rep. *23*, 2874–2880.

Guo, J.-P., Arai, T., Miklossy, J., and McGeer, P.L. (2006). Abeta and tau form soluble complexes that may promote self aggregation of both into the insoluble forms observed in Alzheimer's disease. Proc. Natl. Acad. Sci. U. S. A. *103*, 1953–1958.

Guo, T., Noble, W., and Hanger, D.P. (2017). Roles of tau protein in health and disease. Acta Neuropathol. *133*, 665–704.

Haase, C., Stieler, J.T., Arendt, T., and Holzer, M. (2004). Pseudophosphorylation of tau protein alters its ability for self-aggregation. J. Neurochem. *88*, 1509–1520.

Haberland, M., Montgomery, R.L., and Olson, E.N. (2011). Physiology : Implications for Disease and Therapy. Nat. Rev. Genet. *10*, 32–42.

Hall, A.M., Throesch, B.T., Buckingham, S.C., Markwardt, S.J., Peng, Y., Wang, Q., Hoffman, D.A., and Roberson, E.D. (2015). Tau-Dependent Kv4.2 Depletion and Dendritic Hyperexcitability in a Mouse Model of Alzheimer's Disease. J. Neurosci. *35*, 6221–6230.

Hanger, D.P., Anderton, B.H., and Noble, W. (2009). Tau phosphorylation: the therapeutic challenge for neurodegenerative disease. Trends Mol. Med. *15*, 112–119.

Hardcastle, T.J., and Kelly, K.A. (2010). baySeq: Empirical Bayesian methods for identifying differential expression in sequence count data. BMC Bioinformatics *11*, 422.

Hasegawa, M., Smith, M.J., and Goedert, M. (1998a). Tau proteins with FTDP-17 mutations have a reduced ability to promote microtubule assembly. FEBS Lett. *437*, 207–210.

Hasegawa, M., Smith, M.J., and Goedert, M. (1998b). Tau proteins with FTDP-17 mutations have a reduced ability to promote microtubule assembly. FEBS Lett. *437*, 207–210.

Henderson, Y.C., Chen, Y., Frederick, M.J., Lai, S.Y., and Gary, L. (2011). MEK Inhibitor PD0325901 Significantly Reduces the Growth of Papillary Thyroid Carcinoma Cells In vitro and In vivo. Mol. Cancer Ther. *9*, 1968–1976.

Hernández-Ortega, K., Garcia-Esparcia, P., Gil, L., Lucas, J.J., and Ferrer, I. (2016). Altered Machinery of Protein Synthesis in Alzheimer's: From the Nucleolus to the Ribosome. Brain Pathol. *26*, 593–605.

Hernández, F., García-García, E., and Avila, J. (2013). Microtubule Depolymerization and Tau Phosphorylation. J. Alzheimer's Dis. *37*, 507–513.

Himmel, M., Ritter, A., Rothemund, S., Pauling, V., Rottner, K., Gingras, A.R., and Ziegler, W.H. (2009). Control of High Affinity Interactions in the Talin C Terminus. *284*, 13832–13842.

Hirokawa, N., Shiomura, Y., and Okabe, S. (1988). Tau proteins: the molecular structure and mode of binding on microtubules. J. Cell Biol. *107*, 1449–1459.

Hirt, L., Badaut, J., Thevenet, J., Granziera, C., Regli, L., Maurer, F., Bonny, C., and Bogousslavsky, J. (2004). D-JNKI1, a cell-penetrating c-Jun-N-terminal kinase inhibitor, protects against cell death in severe cerebral ischemia. Stroke *35*, 1738–1743.

Holmes, B.B., Furman, J.L., Mahan, T.E., Yamasaki, T.R., Mirbaha, H., Eades, W.C., Belaygorod, L., Cairns, N.J., Holtzman, D.M., and Diamond, M.I. (2014). Proteopathic tau seeding predicts tauopathy in vivo. Proc. Natl. Acad. Sci. *111*,

E4376–E4385.

Holth, J.K., Bomben, V.C., Reed, J.G., Inoue, T., Younkin, L., Younkin, S.G., Pautler, R.G., Botas, J., and Noebels, J.L. (2013). Tau loss attenuates neuronal network hyperexcitability in mouse and Drosophila genetic models of epilepsy. J. Neurosci. *33*, 1651–1659.

Hua, Q., and He, R.Q. (2003). Tau could protect DNA double helix structure. Biochim. Biophys. Acta - Proteins Proteomics *1645*, 205–211.

Hunsberger, H.C., Rudy, C.C., Batten, S.R., Gerhardt, G.A., and Reed, N. (2015). P301L Tau Expression Affects Glutamate Release and Clearance in the Hippocampal Trisynaptic Pathway. J Neurochem. *132*, 169–182.

Hutton, M. (2006). Molecular Genetics of Chromosome 17 Tauopathies. Ann. N. Y. Acad. Sci. *920*, 63–73.

Hutton, M., Lendon, C.L., Rizzu, P., Baker, M., Froelich, S., Houlden, H.H., Pickering-Brown, S., Chakraverty, S., Isaacs, A., Grover, A., et al. (1998). Association of missense and 5'-splice-site mutations in tau with the inherited dementia FTDP-17. Nature *393*, 702–704.

Hwang, S.C., Jhon, D.-Y., Bae, Y.S., Kim, J.H., and Rhee, S.G. (1996). Activation of Phospholipase C-γ by the Concerted Action of Tau Proteins and Arachidonic Acid. J. Biol. Chem. *271*, 18342–18349.

Ingelson, M., Vanmechelen, E., and Lannfelt, L. (1996). Microtubule-associated protein tau in human fibroblasts with the Swedish Alzheimer mutation. Neurosci. Lett. *220*, 9–12.

Irwin, D.J., Cohen, T.J., Grossman, M., Arnold, S.E., Xie, S.X., Lee, V.M.-Y., and Trojanowski, J.Q. (2012). Acetylated tau, a novel pathological signature in Alzheimer's disease and other tauopathies. Brain *135*, 807–818.

Ittner, L.M., Ke, Y.D., Delerue, F., Bi, M., Gladbach, A., van Eersel, J., Wölfing, H., Chieng, B.C., Christie, M.J., Napier, I.A., et al. (2010). Dendritic function of tau mediates amyloid-beta toxicity in Alzheimer's disease mouse models. Cell *142*, 387–397.

Iyengar, S., and Farnham, P.J. (2011). KAP1 protein: an enigmatic master regulator of the genome. J. Biol. Chem. *286*, 26267–26276.

Jadhav, S., Cubinkova, V., Zimova, I., Brezovakova, V., Madari, A., Cigankova, V., and Zilka, N. (2015). Tau-mediated synaptic damage in Alzheimer's disease. Transl. Neurosci. *6*, 214–226.

Jeganathan, S., Bergen, M. Von, and Brutlach, H. (2006). Global Hairpin Folding of Tau in Solution †. 2283–2293.

Van der Jeugd, A., Ahmed, T., Burnouf, S., Belarbi, K., Hamdame, M., Grosjean, M.-E., Humez, S., Balschun, D., Blum, D., Buée, L., et al. (2011). Hippocampal tauopathy in tau transgenic mice coincides with impaired hippocampus-dependent learning and memory, and attenuated late-phase long-term depression of synaptic transmission. Neurobiol. Learn. Mem. *95*, 296–304.

Johnson, G.V.W. (2004). Tau phosphorylation in neuronal cell function and dysfunction. J. Cell Sci. *117*, 5721–5729.

Kaláb, P., and Soderholm, J. (2010). The design of Förster (fluorescence) resonance energy transfer (FRET)-based molecular sensors for Ran GTPase. Methods *51*, 220–232.

Kar, S., Fan, J., Smith, M.J., Goedert, M., and Amos, L.A. (2003). Repeat motifs of tau bind to the insides of microtubules in the absence of taxol. EMBO J. *22*, 70–77.

Karaman, M.W., Herrgard, S., Treiber, D.K., Gallant, P., Atteridge, C.E., Campbell, B.T., Chan, K.W., Ciceri, P., Davis, M.I., Edeen, P.T., et al. (2008). A quantitative analysis of kinase inhibitor selectivity. Nat. Biotechnol. *26*, 127–132.

Kfoury, N., Holmes, B.B., Jiang, H., Holtzman, D.M., and Diamond, M.I. (2012). Trans-cellular Propagation of Tau Aggregation by Fibrillar Species. J. Biol. Chem. *287*, 19440–19451.

Khadrawyb YA, E.H. (2014). Glutamate Excitotoxicity and Neurodegeneration. J. Mol. Genet. Med. *08*, 8–11.

KIDD, M. (1963). Paired helical filaments in electron microscopy of Alzheimer's

disease. Nature *197*, 192–193.

Kim, C.H., Ueshima, E., Muraoka, O., Tanaka, H., Yeo, S.Y., Huh, T.L., and Miki, N. (1996). Zebrafish elav/HuC homologue as a very early neuronal marker. Neurosci. Lett. *216*, 109–112.

Kim, W., Lee, S., Jung, C., Ahmed, A., Lee, G., and Hall, G.F. (2010). Interneuronal transfer of human tau between Lamprey central neurons in situ. J. Alzheimers. Dis. *19*, 647–664.

Kinoshita, A., Fukumoto, H., Shah, T., Whelan, C.M., Irizarry, M.C., and Hyman, B.T. (2003). Demonstration by FRET of BACE interaction with the amyloid precursor protein at the cell surface and in early endosomes. J. Cell Sci. *116*, 3339–3346.

Kolarova, M., García-Sierra, F., Bartos, A., Ricny, J., and Ripova, D. (2012). Structure and pathology of tau protein in Alzheimer disease. Int. J. Alzheimers. Dis. *2012*, 731526.

Kontsekova, E., Zilka, N., Kovacech, B., Novak, P., and Novak, M. (2014). First-in-man tau vaccine targeting structural determinants essential for pathological tau-tau interaction reduces tau oligomerisation and neurofibrillary degeneration in an Alzheimer's disease model. Alzheimer's Res. Ther. *6*, 1–12.

Kosmidis, S., Grammenoudi, S., Papanikolopoulou, K., and Skoulakis, E.M.C. (2010). Differential effects of Tau on the integrity and function of neurons essential for learning in Drosophila. J. Neurosci. *30*, 464–477.

Kremer, A., Maurin, H., Demedts, D., Devijver, H., Borghgraef, P., and Van Leuven, F. (2011). Early improved and late defective cognition is reflected by dendritic spines in Tau.P301L mice. J. Neurosci. *31*, 18036–18047.

KrishnaKumar, V.G., and Gupta, S. (2017). Simplified method to obtain enhanced expression of tau protein from E. coli and one-step purification by direct boiling. Prep. Biochem. Biotechnol. *47*, 530–538.

Kwok, J.B.J., Teber, E.T., Loy, C., Hallupp, M., Nicholson, G., Mellick, G.D., Buchanan, D.D., Silburn, P.A., and Schofield, P.R. (2004). Tau haplotypes

regulate transcription and are associated with Parkinson's disease. Ann. Neurol. *55*, 329–334.

Lane, C.A., Hardy, J., and Schott, J.M. (2018). Alzheimer's disease. Eur. J. Neurol. *25*, 59–70.

Langmead, B., Trapnell, C., Pop, M., and Salzberg, S.L. (2009). Ultrafast and memory-efficient alignment of short DNA sequences to the human genome. Genome Biol. *10*, R25.

Lau, D.H.W., Hogseth, M., Phillips, E.C., O'Neill, M.J., Pooler, A.M., Noble, W., and Hanger, D.P. (2016). Critical residues involved in tau binding to fyn: implications for tau phosphorylation in Alzheimer's disease. Acta Neuropathol. Commun. *4*, 49.

Lee, M., Kwon, Y.T., Li, M., Peng, J., Friedlander, R.M., and Tsai, L.-H. (2000). Neurotoxicity induces cleavage of p35 to p25 by calpain. Nature *405*, 360–364.

Lee, V.M.-Y., Goedert, M., and Trojanowski, J.Q. (2001). Neurodegenerative Tauopathies. Annu. Rev. Neurosci. *24*, 1121–1159.

Leugers, C.J., and Lee, G. (2010). Tau potentiates nerve growth factor-induced mitogen-activated protein kinase signaling and neurite initiation without a requirement for microtubule binding. J. Biol. Chem. *285*, 19125–19134.

Lewis, J., McGowan, E., Rockwood, J., Melrose, H., Nacharaju, P., Van Slegtenhorst, M., Gwinn-Hardy, K., Paul Murphy, M., Baker, M., Yu, X., et al. (2000). Neurofibrillary tangles, amyotrophy and progressive motor disturbance in mice expressing mutant (P301L) tau protein. Nat. Genet. *25*, 402–405.

Lewis, J., Dickson, D.W., Lin, W.L., Chisholm, L., Corral, A., Jones, G., Yen, S.H., Sahara, N., Skipper, L., Yager, D., et al. (2001). Enhanced neurofibrillary degeneration in transgenic mice expressing mutant tau and APP. Science *293*, 1487–1491.

Liu, C., and Götz, J. (2013). Profiling Murine Tau with 0N, 1N and 2N Isoform-Specific Antibodies in Brain and Peripheral Organs Reveals Distinct Subcellular Localization, with the 1N Isoform Being Enriched in the Nucleus. PLoS One *8*,

e84849.

Liu, F., and Gong, C.-X. (2008). Tau exon 10 alternative splicing and tauopathies. Mol. Neurodegener. *3*, 8.

Liu, F., Grundke-Iqbal, I., Iqbal, K., and Gong, C.-X. (2005). Contributions of protein phosphatases PP1, PP2A, PP2B and PP5 to the regulation of tau phosphorylation. Eur. J. Neurosci. *22*, 1942–1950.

Liu, F., Shi, J., Tanimukai, H., Gu, J., Gu, J., Grundke-Iqbal, I., Iqbal, K., and Gong, C.-X. (2009). Reduced O-GlcNAcylation links lower brain glucose metabolism and tau pathology in Alzheimer's disease. Brain *132*, 1820–1832.

Loomis, P. a, Howard, T.H., Castleberry, R.P., and Binder, L.I. (1990). Identification of nuclear tau isoforms in human neuroblastoma cells. Proc Natl Acad Sci U S A *87*, 8422–8426.

Lowe, V.J., Wiste, H.J., Senjem, M.L., Weigand, S.D., Therneau, T.M., Boeve, B.F., Josephs, K.A., Fang, P., Pandey, M.K., Murray, M.E., et al. (2018). Widespread brain tau and its association with ageing, Braak stage and Alzheimer's dementia. Brain *141*, 271–287.

Lu, M., and Kosik, K.S. (2001). Competition for microtubule-binding with dual expression of tau missense and splice isoforms. Mol. Biol. Cell *12*, 171–184.

Luna-Munoz, J., R., C., M., C., Flores-Rodriguez, P., Avila, J., R., S., la Cruz, F. De, Mena, R., A., M., and Floran-Garduno, B. (2013). Phosphorylation of Tau Protein Associated as a Protective Mechanism in the Presence of Toxic, C-Terminally Truncated Tau in Alzheimer's Disease. In Understanding Alzheimer's Disease, (InTech), p.

Luna-Muñoz, J., Peralta-Ramirez, J., Chávez-Macías, L., Harrington, C.R., Wischik, C.M., and Mena, R. (2008). Thiazin red as a neuropathological tool for the rapid diagnosis of Alzheimer's disease in tissue imprints. Acta Neuropathol. *116*, 507–515.

Maccioni, R.B., Otth, C., Concha, I.I., and Muñoz, J.P. (2001). The protein kinase Cdk5. Structural aspects, roles in neurogenesis and involvement in Alzheimer's

pathology. Eur. J. Biochem. *268*, 1518–1527.

Magnani, E., Fan, J., Gasparini, L., Golding, M., Williams, M., Schiavo, G., Goedert, M., Amos, L.A., and Spillantini, M.G. (2007). Interaction of tau protein with the dynactin complex. EMBO J. *26*, 4546–4554.

Maina, M.B., Bailey, L.J., Wagih, S., Biasetti, L., Pollack, S.J., Quinn, J.P., Thorpe, J.R., Doherty, A.J., and Serpell, L.C. (2018). The involvement of tau in nucleolar transcription and the stress response. Acta Neuropathol. Commun. *6*, 70.

Mainardi, M., Spinelli, M., Scala, F., Mattera, A., Fusco, S., D'Ascenzo, M., and Grassi, C. (2017). Loss of Leptin-Induced Modulation of Hippocampal Synaptic Trasmission and Signal Transduction in High-Fat Diet-Fed Mice. Front. Cell. Neurosci. *11*, 1–11.

Makin, S. (2018). The amyloid hypothesis on trial. Nature *559*, S4–S7.

Makrides, V., Massie, M.R., Feinstein, S.C., and Lew, J. (2004). Evidence for two distinct binding sites for tau on microtubules. 1–6.

Mandell, J.W., and Banker, G.A. (1996). A spatial gradient of tau protein phosphorylation in nascent axons. J. Neurosci. *16*, 5727–5740.

Di Maria, E., Tabaton, M., Vigo, T., Abbruzzese, G., Bellone, E., Donati, C., Frasson, E., Marchese, R., Montagna, P., Munoz, D.G., et al. (2000). Corticobasal degeneration shares a common genetic background with progressive supranuclear palsy. Ann. Neurol. *47*, 374–377.

Martineau, M., Guzman, R.E., Fahlke, C., and Klingauf, J. (2017). VGLUT1 functions as a glutamate/proton exchanger with chloride channel activity in hippocampal glutamatergic synapses. Nat. Commun. *8*.

Maurin, H., Chong, S.A., Kraev, I., Davies, H., Kremer, A., Seymour, C.M., Lechat, B., Jaworski, T., Borghgraef, P., Devijver, H., et al. (2014). Early structural and functional defects in synapses and myelinated axons in stratum lacunosum moleculare in two preclinical models for tauopathy. PLoS One *9*.

McEwan, W.A., Falcon, B., Vaysburd, M., Clift, D., Oblak, A.L., Ghetti, B.,

Goedert, M., and James, L.C. (2017). Cytosolic Fc receptor TRIM21 inhibits seeded tau aggregation. Proc. Natl. Acad. Sci. U. S. A. *114*, 574–579.

Medina, M., and Avila, J. (2014). The role of extracellular Tau in the spreading of neurofibrillary pathology. Front. Cell. Neurosci. *8*, 113.

Mershin, A. (2004). Learning and Memory Deficits Upon TAU Accumulation in Drosophila Mushroom Body Neurons. Learn. Mem. *11*, 277–287.

Milano, G., Morel, S., Bonny, C., Samaja, M., von Segesser, L.K., Nicod, P., and Vassalli, G. (2007). A peptide inhibitor of c-Jun NH2-terminal kinase reduces myocardial ischemia-reperfusion injury and infarct size in vivo. Am. J. Physiol. Heart Circ. Physiol. *292*, H1828-35.

Mirbaha, H., Holmes, B.B., Sanders, D.W., Bieschke, J., and Diamond, M.I. (2015). Tau Trimers Are the Minimal Propagation Unit Spontaneously Internalized to Seed Intracellular Aggregation. J. Biol. Chem. *290*, 14893–14903.

Mirbaha, H., Chen, D., Morazova, O.A., Ruff, K.M., Sharma, A.M., Liu, X., Goodarzi, M., Pappu, R. V, Colby, D.W., Mirzaei, H., et al. (2018). Inert and seed-competent tau monomers suggest structural origins of aggregation. Elife *7*.

Momeni, P., Pittman, A., Lashley, T., Vandrovcova, J., Malzer, E., Luk, C., Hulette, C., Lees, A., Revesz, T., Hardy, J., et al. (2009). Clinical and pathological features of an Alzheimer's disease patient with the MAPT ΔK280 mutation. Neurobiol. Aging *30*, 388–393.

Mondragón-Rodríguez, S., Trillaud-Doppia, E., Dudilot, A., Bourgeois, C., Lauzon, M., Leclerc, N., and Boehm, J. (2012). Interaction of endogenous tau protein with synaptic proteins is regulated by N-methyl-D-aspartate receptor-dependent tau phosphorylation. J. Biol. Chem. *287*, 32040–32053.

Mortazavi, A., Williams, B.A., McCue, K., Schaeffer, L., and Wold, B. (2008). Mapping and quantifying mammalian transcriptomes by RNA-Seq. Nat. Methods *5*, 621–628.

Mukrasch, M.D., Bibow, S., Korukottu, J., Jeganathan, S., Biernat, J., Griesinger, C., Mandelkow, E., and Zweckstetter, M. (2009). Structural polymorphism of 441-

residue tau at single residue resolution. PLoS Biol. *7*, e34.

Münch, G., Deuther-Conrad, W., and Gasic-Milenkovic, J. (2002). Glycoxidative stress creates a vicious cycle of neurodegeneration in Alzheimer's disease--a target for neuroprotective treatment strategies? J. Neural Transm. Suppl. 303–307.

Myers, A.J., Kaleem, M., Marlowe, L., Pittman, A.M., Lees, A.J., Fung, H.C., Duckworth, J., Leung, D., Gibson, A., Morris, C.M., et al. (2005). The H1c haplotype at the MAPT locus is associated with Alzheimer's disease. Hum. Mol. Genet. *14*, 2399–2404.

Nakanishi, H., Amano, T., Sastradipura, D.F., Yoshimine, Y., Tsukuba, T., Tanabe, K., Hirotsu, I., Ohono, T., and Yamamoto, K. (1997). Increased expression of cathepsins E and D in neurons of the aged rat brain and their colocalization with lipofuscin and carboxy-terminal fragments of Alzheimer amyloid precursor protein. J. Neurochem. *68*, 739–749.

Noble, W., Planel, E., Zehr, C., Olm, V., Meyerson, J., Suleman, F., Gaynor, K., Wang, L., LaFrancois, J., Feinstein, B., et al. (2005). Inhibition of glycogen synthase kinase-3 by lithium correlates with reduced tauopathy and degeneration in vivo. Proc. Natl. Acad. Sci. U. S. A. *102*, 6990–6995.

Nouar, R., Devred, F., Breuzard, G., and Peyrot, V. (2013). FRET and FRAP imaging: approaches to characterise tau and stathmin interactions with microtubules in cells. Biol. Cell *105*, 149–161.

Novak, M., Kabat, J., and Wischik, C.M. (1993). Molecular characterization of the minimal protease resistant tau unit of the Alzheimer's disease paired helical filament. EMBO J. *12*, 365–370.

Novak, P., Schmidt, R., Kontsekova, E., Zilka, N., Kovacech, B., Skrabana, R., and Vince-kazmerova, Z. (2010). Safety and immunogenicity of the tau vaccine AADvac1 in patients with Alzheimer ' s disease : a randomised , double-blind , placebo-controlled , phase 1 trial. Lancet Neurol. *16*, 123–134.

Novak, P., Kontsekova, E., Zilka, N., and Novak, M. (2018a). Ten Years of Tau-Targeted Immunotherapy : The Path Walked and the Roads Ahead. *12*, 1–14.

Novak, P., Schmidt, R., Kontsekova, E., Kovacech, B., Smolek, T., Katina, S., Fialova, L., Prcina, M., Parrak, V., Dal-bianco, P., et al. (2018b). FUNDAMANT : an interventional 72-week phase 1 follow-up study of AADvac1 , an active immunotherapy against tau protein pathology in Alzheimer ' s disease. *1*, 1–16.

Novak, P., Zilka, N., Zilkova, M., Kovacech, B., Skrabana, R., Ondrus, M., Fialova, L., Kontsekova, E., Otto, M., and Novak, M. (2018c). AADvac1, an Active Immunotherapy for Alzheimer's Disease and Non Alzheimer Tauopathies: An Overview of Preclinical and Clinical Development. 1–7.

Oddo, S., Caccamo, A., Shepherd, J.D., Murphy, M.P., Golde, T.E., Kayed, R., Metherate, R., Mattson, M.P., Akbari, Y., and LaFerla, F.M. (2003). Triple-transgenic model of Alzheimer's disease with plaques and tangles: intracellular Abeta and synaptic dysfunction. Neuron *39*, 409–421.

Okamura, N., Harada, R., Ishiki, A., Kikuchi, A., Nakamura, T., and Kudo, Y. (2018). The development and validation of tau PET tracers: current status and future directions. Clin. Transl. Imaging *6*, 305–316.

Oyama, F., Kotliarova, S., Harada, A., Ito, M., Miyazaki, H., Ueyama, Y., Hirokawa, N., Nukina, N., and Ihara, Y. (2004). Gem GTPase and tau: morphological changes induced by gem GTPase in cho cells are antagonized by tau. J. Biol. Chem. *279*, 27272–27277.

P. Vasudevaraju, E.G., Hegde, M.L., Collen, T.B., Britton, G.B., and Rao, K.S. (2012). New evidence on α-synuclein and Tau binding to conformation and sequence specific GC* rich DNA: Relevance to neurological disorders. J. Pharm. Bioallied Sci. *4*, 112–117.

Padmaraju, V., Indi, S.S., and Rao, K.S.J. (2010). New evidences on Tau-DNA interactions and relevance to neurodegeneration. Neurochem. Int. *57*, 51–57.

Paquet, D., Bhat, R., Sydow, A., Mandelkow, E.-M., Berg, S., Hellberg, S., Fälting, J., Distel, M., Köster, R.W., Schmid, B., et al. (2009). A zebrafish model of tauopathy allows in vivo imaging of neuronal cell death and drug evaluation. J. Clin. Invest. *119*, 1382–1395.

Paquet, D., Schmid, B., and Haass, C. (2010). Transgenic zebrafish as a novel

animal model to study tauopathies and other neurodegenerative disorders in vivo. Neurodegener. Dis. *7*, 99–102.

Pei, J.J., Tanaka, T., Tung, Y.C., Braak, E., Iqbal, K., and Grundke-Iqbal, I. (1997). Distribution, levels, and activity of glycogen synthase kinase-3 in the Alzheimer disease brain. J. Neuropathol. Exp. Neurol. *56*, 70–78.

Perez, M., Santa-Maria, I., Gomez de Barreda, E., Zhu, X., Cuadros, R., Cabrero, J.R., Sanchez-Madrid, F., Dawson, H.N., Vitek, M.P., Perry, G., et al. (2009). Tau--an inhibitor of deacetylase HDAC6 function. J. Neurochem. *109*, 1756–1766.

Perry, G., Roder, H., Nunomura, A., Takeda, A., Friedlich, A.L., Zhu, X., Raina, A.K., Holbrook, N., Siedlak, S.L., Harris, P.L., et al. (1999). Activation of neuronal extracellular receptor kinase (ERK) in Alzheimer disease links oxidative stress to abnormal phosphorylation. Neuroreport *10*, 2411–2415.

Pevalova, M., Filipcik, P., Novak, M., Avila, J., and Iqbal, K. (2006). Post-translational modifications of tau protein. Bratisl. Lek. Listy *107*, 346–353.

Pfaffl, M.W. (2001). A new mathematical model for relative quantification in real-time RT-PCR. Nucleic Acids Res. *29*, 45e – 45.

Piacentini, R., Li Puma, D.D., Mainardi, M., Lazzarino, G., Tavazzi, B., Arancio, O., and Grassi, C. (2017). Reduced gliotransmitter release from astrocytes mediates tau-induced synaptic dysfunction in cultured hippocampal neurons. Glia *65*, 1302–1316.

Piedrahita, D., Hernández, I., López-Tobón, A., Fedorov, D., Obara, B., Manjunath, B.S., Boudreau, R.L., Davidson, B., Laferla, F., Gallego-Gómez, J.C., et al. (2010). Silencing of CDK5 reduces neurofibrillary tangles in transgenic alzheimer's mice. J. Neurosci. *30*, 13966–13976.

Planel, E., Miyasaka, T., Launey, T., Chui, D.-H., Tanemura, K., Sato, S., Murayama, O., Ishiguro, K., Tatebayashi, Y., and Takashima, A. (2004). Alterations in glucose metabolism induce hypothermia leading to tau hyperphosphorylation through differential inhibition of kinase and phosphatase activities: implications for Alzheimer's disease. J. Neurosci. *24*, 2401–2411.

Plouffe, V., Mohamed, N.-V., Rivest-McGraw, J., Bertrand, J., Lauzon, M., and Leclerc, N. (2012). Hyperphosphorylation and cleavage at D421 enhance tau secretion. PLoS One *7*, e36873.

Di Primio, C., Quercioli, V., Siano, G., Rovere, M., Kovacech, B., Novak, M., and Cattaneo, A. (2017). The Distance between N and C Termini of Tau and of FTDP-17 Mutants Is Modulated by Microtubule Interactions in Living Cells. Front. Mol. Neurosci. *10*, 1–13.

Prince, M., Wimo, A., M, G., GC, A., YT, W., and M, P. (2015). World Alzheimer Report 2015 The Global Impact of Dementia An analysis of prevalence, incidence, cost and trends. Alzheimer's Dis. Int.

Qi, H., Cantrelle, F.-X., Benhelli-Mokrani, H., Smet-Nocca, C., Buée, L., Lippens, G., Bonnefoy, E., Galas, M.-C., and Landrieu, I. (2015). Nuclear Magnetic Resonance Spectroscopy Characterization of Interaction of Tau with DNA and Its Regulation by Phosphorylation. Biochemistry *54*, 1525–1533.

Rady, R.M., Zinkowski, R.P., and Binder, L.I. (1995). Presence of tau in isolated nuclei from human brain. Neurobiol. Aging *16*, 479–486.

Rao, M. V, Mohan, P.S., Peterhoff, C.M., Yang, D.-S., Schmidt, S.D., Stavrides, P.H., Campbell, J., Chen, Y., Jiang, Y., Paskevich, P.A., et al. (2008). Marked calpastatin (CAST) depletion in Alzheimer's disease accelerates cytoskeleton disruption and neurodegeneration: neuroprotection by CAST overexpression. J. Neurosci. *28*, 12241–12254.

Revett, T.J., Baker, G.B., Jhamandas, J., and Kar, S. (2013). Glutamate system, amyloid β peptides and tau protein: Functional interrelationships and relevance to Alzheimer disease pathology. J. Psychiatry Neurosci. *38*, 6–23.

Rissman, R.A., Poon, W.W., Blurton-Jones, M., Oddo, S., Torp, R., Vitek, M.P., LaFerla, F.M., Rohn, T.T., and Cotman, C.W. (2004). Caspase-cleavage of tau is an early event in Alzheimer disease tangle pathology. J. Clin. Invest. *114*, 121–130.

Rizzu, P., Van Swieten, J.C., Joosse, M., Hasegawa, M., Stevens, M., Tibben, A., Niermeijer, M.F., Hillebrand, M., Ravid, R., Oostra, B.A., et al. (1999). High

prevalence of mutations in the microtubule-associated protein tau in a population study of frontotemporal dementia in the Netherlands. Am. J. Hum. Genet. *64*, 414–421.

Robinson, M.D., McCarthy, D.J., and Smyth, G.K. (2010). edgeR: a Bioconductor package for differential expression analysis of digital gene expression data. Bioinformatics *26*, 139–140.

Rossi, G., Dalprà, L., Crosti, F., Lissoni, S., Sciacca, F.L., Catania, M., Di Fede, G., Mangieri, M., Giaccone, G., Croci, D., et al. (2008). A new function of microtubule-associated protein tau: Involvement in chromosome stability. Cell Cycle *7*, 1788–1794.

Rossi, G., Conconi, D., Panzeri, E., Redaelli, S., Piccoli, E., Paoletta, L., Dalprà, L., and Tagliavini, F. (2013). Mutations in MAPT gene cause chromosome instability and introduce copy number variations widely in the genome. J. Alzheimer's Dis. *33*, 969–982.

Rossi, G., Conconi, D., Panzeri, E., Paoletta, L., Piccoli, E., Ferretti, M.G., Mangieri, M., Ruggerone, M., Dalprà, L., and Tagliavini, F. (2014). Mutations in MAPT give rise to aneuploidy in animal models of tauopathy. Neurogenetics *15*, 31–40.

Rossi, G., Redaelli, V., Contiero, P., Fabiano, S., Tagliabue, G., Perego, P., Benussi, L., Bruni, A.C., Filippini, G., Farinotti, M., et al. (2018). Tau mutations serve as a novel risk factor for cancer. Cancer Res. canres.3175.2017.

Rousseaux, M.W.C., de Haro, M., Lasagna-Reeves, C.A., de Maio, A., Park, J., Jafar-Nejad, P., Al-Ramahi, I., Sharma, A., See, L., Lu, N., et al. (2016). TRIM28 regulates the nuclear accumulation and toxicity of both alpha-synuclein and tau. Elife *5*, 1–24.

Sabbagh, J.J., and Dickey, C.A. (2016). The Metamorphic Nature of the Tau Protein: Dynamic Flexibility Comes at a Cost. Front. Neurosci. *10*, 1–5.

Sadot, E., Heicklen-Klein, A., Barg, J., Lazarovici, P., and Ginzburg, I. (1996). Identification of a tau promoter region mediating tissue-specific-regulated expression in PC12 cells. J. Mol. Biol. *256*, 805–812.

Saint-Aubert, L., Lemoine, L., Chiotis, K., Leuzy, A., Rodriguez-Vieitez, E., and Nordberg, A. (2017). Tau PET imaging: present and future directions. Mol. Neurodegener. *12*, 19.

Saito, K., Elce, J.S., Hamos, J.E., and Nixon, R.A. (1993). Widespread activation of calcium-activated neutral proteinase (calpain) in the brain in Alzheimer disease: a potential molecular basis for neuronal degeneration. Proc. Natl. Acad. Sci. U. S. A. *90*, 2628–2632.

Saleem, S., and Kannan, R.R. (2018). Zebrafish: an emerging real-time model system to study Alzheimer's disease and neurospecific drug discovery. Cell Death Discov. *4*.

Samsonov, A., Yu, J.-Z., Rasenick, M., and Popov, S. V (2004). Tau interaction with microtubules in vivo. J. Cell Sci. *117*, 6129–6141.

Santa-María, I., Pérez, M., Hernández, F., Avila, J., and Moreno, F.J. (2006). Characteristics of the binding of thioflavin S to tau paired helical filaments. J. Alzheimer's Dis. *9*, 279–285.

Schindowski, K., Bretteville, A., Leroy, K., Bégard, S., Brion, J.-P., Hamdane, M., and Buée, L. (2006). Alzheimer's disease-like tau neuropathology leads to memory deficits and loss of functional synapses in a novel mutated tau transgenic mouse without any motor deficits. Am. J. Pathol. *169*, 599–616.

Selenica, M.-L., Benner, L., Housley, S.B., Manchec, B., Lee, D.C., Nash, K.R., Kalin, J., Bergman, J.A., Kozikowski, A., Gordon, M.N., et al. (2014). Histone deacetylase 6 inhibition improves memory and reduces total tau levels in a mouse model of tau deposition. Alzheimers. Res. Ther. *6*, 12.

Sengupta, A., Kabat, J., Novak, M., Wu, Q., Grundke-Iqbal, I., and Iqbal, K. (1998). Phosphorylation of tau at both Thr 231 and Ser 262 is required for maximal inhibition of its binding to microtubules. Arch. Biochem. Biophys. *357*, 299–309.

Sergeant, N., David, J.P., Lefranc, D., Vermersch, P., Wattez, A., and Delacourte, A. (1997). Different distribution of phosphorylated tau protein isoforms in Alzheimer's and Pick's diseases. FEBS Lett. *412*, 578–582.

Sergeant, N., Delacourte, A., and Buée, L. (2005). Tau protein as a differential biomarker of tauopathies. Biochim. Biophys. Acta - Mol. Basis Dis. *1739*, 179–197.

Shahpasand, K., Uemura, I., Saito, T., Asano, T., Hata, K., Shibata, K., Toyoshima, Y., Hasegawa, M., and Hisanaga, S.-I. (2012). Regulation of mitochondrial transport and inter-microtubule spacing by tau phosphorylation at the sites hyperphosphorylated in Alzheimer's disease. J. Neurosci. *32*, 2430–2441.

Sharma, A.M., Thomas, T.L., Woodard, D.R., Kashmer, O.M., and Diamond, M.I. (2018). Tau monomer encodes strains. Elife *7*.

Shi, Y., Kirwan, P., Smith, J., MacLean, G., Orkin, S.H., and Livesey, F.J. (2012). A human stem cell model of early Alzheimer's disease pathology in Down syndrome. Sci. Transl. Med. *4*, 124ra29.

Shipton, O.A., Leitz, J.R., Dworzak, J., Acton, C.E.J., Tunbridge, E.M., Denk, F., Dawson, H.N., Vitek, M.P., Wade-Martins, R., Paulsen, O., et al. (2011). Tau protein is required for amyloid {beta}-induced impairment of hippocampal long-term potentiation. J. Neurosci. *31*, 1688–1692.

Shrestha, D., Jenei, A., Nagy, P., Vereb, G., and Szöllősi, J. (2015). Understanding FRET as a research tool for cellular studies. Int. J. Mol. Sci. *16*, 6718–6756.

Siksou, L., Silm, K., Biesemann, C., Nehring, R.B., Wojcik, S.M., Triller, A., El Mestikawy, S., Marty, S., and Herzog, E. (2013). A role for vesicular glutamate transporter 1 in synaptic vesicle clustering and mobility. Eur. J. Neurosci. *37*, 1631–1642.

Singh, T.J., Wang, J.Z., Novak, M., Kontzekova, E., Grundke-Iqbal, I., and Iqbal, K. (1996). Calcium/calmodulin-dependent protein kinase II phosphorylates tau at Ser-262 but only partially inhibits its binding to microtubules. FEBS Lett. *387*, 145–148.

Sjöberg, M.K., Shestakova, E., Mansuroglu, Z., Maccioni, R.B., and Bonnefoy, E. (2006). Tau protein binds to pericentromeric DNA: a putative role for nuclear tau

in nucleolar organization. J. Cell Sci. *119*, 2025–2034.

Spillantini, M.G., Murrell, J.R., Goedert, M., Farlow, M.R., Klug, A., and Ghetti, B. (1998a). Mutation in the tau gene in familial multiple system tauopathy with presenile dementia. Proc. Natl. Acad. Sci. U. S. A. *95*, 7737–7741.

Spillantini, M.G., Bird, T.D., and Ghetti, B. (1998b). Frontotemporal dementia and Parkinsonism linked to chromosome 17: a new group of tauopathies. Brain Pathol. *8*, 387–402.

Stefansson, H., Helgason, A., Thorleifsson, G., Steinthorsdottir, V., Masson, G., Barnard, J., Baker, A., Jonasdottir, A., Ingason, A., Gudnadottir, V.G., et al. (2005). A common inversion under selection in Europeans. Nat. Genet. *37*, 129–137.

Steiner, B., Mandelkow, E.M., Biernat, J., Gustke, N., Meyer, H.E., Schmidt, B., Mieskes, G., Söling, H.D., Drechsel, D., Kirschner, M.W., et al. (1990). Phosphorylation of microtubule-associated protein tau: identification of the site for Ca2(+)-calmodulin dependent kinase and relationship with tau phosphorylation in Alzheimer tangles. EMBO J. *9*, 3539–3544.

Strang, K.H., Croft, C.L., Sorrentino, Z.A., Chakrabarty, P., Golde, T.E., and Giasson, B.I. (2018). Distinct differences in prion-like seeding and aggregation between Tau protein variants provide mechanistic insights into tauopathies. J. Biol. Chem. *293*, 2408–2421.

Sultan, A., Nesslany, F., Violet, M., Bégard, S., Loyens, A., Talahari, S., Mansuroglu, Z., Marzin, D., Sergeant, N., Humez, S., et al. (2011). Nuclear Tau, a key player in neuronal DNA protection. J. Biol. Chem. *286*, 4566–4575.

Sun, W., Samimi, H., Gamez, M., Zare, H., and Frost, B. (2018). Pathogenic tau-induced piRNA depletion promotes neuronal death through transposable element dysregulation in neurodegenerative tauopathies. Nat. Neurosci. *21*, 1038–1048.

Tacik, P., DeTure, M., Hinkle, K.M., Lin, W.-L., Sanchez-Contreras, M., Carlomagno, Y., Pedraza, O., Rademakers, R., Ross, O.A., Wszolek, Z.K., et al. (2015). A Novel Tau Mutation in Exon 12, p.Q336H, Causes Hereditary Pick Disease. J. Neuropathol. Exp. Neurol. *74*, 1042–1052.

Tak, H., Haque, M.M., Kim, M.J., Lee, J.H., Baik, J.-H., Kim, Y., Kim, D.J., Grailhe, R., and Kim, Y.K. (2013). Bimolecular fluorescence complementation; lighting-up tau-tau interaction in living cells. PLoS One *8*, e81682.

Takahashi, T., and Mihara, H. (2012). FRET detection of amyloid β-peptide oligomerization using a fluorescent protein probe presenting a pseudo-amyloid structure. Chem. Commun. (Camb). *48*, 1568–1570.

Takamori, S., Rhec, J.S., Rosenmund, C., and Jahn, R. (2000). Identification of a vesicular glutamate transporter that defines a glutamatergic phenotype in neurons. Nature *407*, 189–194.

Talmat-Amar, Y., Arribat, Y., Redt-Clouet, C., Feuillette, S., Bougé, A.-L., Lecourtois, M., and Parmentier, M.-L. (2011). Important neuronal toxicity of microtubule-bound Tau in vivo in Drosophila. Hum. Mol. Genet. *20*, 3738–3745.

Tang, Z., Ioja, E., Bereczki, E., Hultenby, K., Li, C., Guan, Z., Winblad, B., and Pei, J.-J. (2015). mTor mediates tau localization and secretion: Implication for Alzheimer's disease. Biochim. Biophys. Acta - Mol. Cell Res. *1853*, 1646–1657.

Terwel, D., Lasrado, R., Snauwaert, J., Vandeweert, E., Van Haesendonck, C., Borghgraef, P., and Van Leuven, F. (2005). Changed conformation of mutant Tau-P301L underlies the moribund tauopathy, absent in progressive, nonlethal axonopathy of Tau-4R/2N transgenic mice. J. Biol. Chem. *280*, 3963–3973.

Togo, T., Sahara, N., Yen, S.-H., Cookson, N., Ishizawa, T., Hutton, M., de Silva, R., Lees, A., and Dickson, D.W. (2002). Argyrophilic grain disease is a sporadic 4-repeat tauopathy. J. Neuropathol. Exp. Neurol. *61*, 547–556.

Tomasiewicz, H.G., Flaherty, D.B., Soria, J.P., and Wood, J.G. (2002). Transgenic zebrafish model of neurodegeneration. J. Neurosci. Res. *70*, 734–745.

Tournissac, M., Bourassa, P., Martinez-Cano, R.D., Vu, T.-M., Hébert, S.S., Planel, E., and Calon, F. (2019). Repeated cold exposures protect a mouse model of Alzheimer's disease against cold-induced tau phosphorylation. Mol. Metab. *22*, 110–120.

Trinczek, B., Ebneth, A., Mandelkow, E.M., and Mandelkow, E. (1999). Tau regulates the attachment/detachment but not the speed of motors in microtubule-dependent transport of single vesicles and organelles. J. Cell Sci. *112 (Pt 1*, 2355–2367.

Trojanowski, J.Q., and Lee, V.M. (1995). Phosphorylation of paired helical filament tau in Alzheimer's disease neurofibrillary lesions: focusing on phosphatases. FASEB J. *9*, 1570–1576.

Tsai, L.-H., Lee, M.-S., and Cruz, J. (2004). Cdk5, a therapeutic target for Alzheimer's disease? Biochim. Biophys. Acta *1697*, 137–142.

Ulrich, G., Salvadè, A., Boersema, P., Calì, T., Foglieni, C., Sola, M., Picotti, P., Papin, S., and Paganetti, P. (2018). Phosphorylation of nuclear Tau is modulated by distinct cellular pathways. Sci. Rep. *8*, 17702.

Vandal, M., White, P.J., Tournissac, M., Tremblay, C., St-Amour, I., Drouin-Ouellet, J., Bousquet, M., Traversy, M.-T., Planel, E., Marette, A., et al. (2016). Impaired thermoregulation and beneficial effects of thermoneutrality in the 3×Tg-AD model of Alzheimer's disease. Neurobiol. Aging *43*, 47–57.

Vanier, M.T., Neuville, P., Michalik, L., and Launay, J.F. (1998). Expression of specific tau exons in normal and tumoral pancreatic acinar cells. J. Cell Sci. *111 (Pt 1*, 1419–1432.

Violet, M., Delattre, L., Tardivel, M., Sultan, A., Chauderlier, A., Caillierez, R., Talahari, S., Nesslany, F., Lefebvre, B., Bonnefoy, E., et al. (2014). A major role for Tau in neuronal DNA and RNA protection in vivo under physiological and hyperthermic conditions. Front. Cell. Neurosci. *8*, 1–11.

Wang, R., and Reddy, P.H. (2017). Role of Glutamate and NMDA Receptors in Alzheimer's Disease. J. Alzheimer's Dis. *57*, 1041–1048.

Wang, Y., and Mandelkow, E. (2016). Tau in physiology and pathology. Nat. Rev. Neurosci. *17*, 5–21.

Wang, J.-Z., Grundke-Iqbal, I., and Iqbal, K. (1996). Glycosylation of microtubule–associated protein tau: An abnormal posttranslational modification in

Alzheimer's disease. Nat. Med. *2*, 871–875.

Wang, Y., Xue, D., Li, Y., Pan, X., Zhang, X., Kuang, B., Zhou, M., Li, X., Xiong, W., Li, G., et al. (2016). The Long Noncoding RNA MALAT-1 is A Novel Biomarker in Various Cancers: A Meta-analysis Based on the GEO Database and Literature. J. Cancer *7*, 991–1001.

Wei, Y., Qu, M.H., Wang, X.S., Chen, L., Wang, D.L., Liu, Y., Hua, Q., and He, R.Q. (2008). Binding to the minor groove of the double-strand, Tau protein prevents DNA damage by peroxidation. PLoS One *3*.

Weingarten, M.D., Lockwood, A.H., Hwo, S.-Y., and Kirschner, M.W. (1975). A Protein Factor Essential for Microtubule Assembly (tau factor/tubulin/electron microscopy/phosphocellulose). Proc.Nat.Acad.Sci *72*, 1858–1862.

West, T., Hu, Y., Verghese, P.B., Bateman, R.J., Braunstein, J.B., Fogelman, I., Budur, K., Florian, H., Mendonca, N., and Holtzman, D.M. (2017). Preclinical and Clinical Development of ABBV-8E12, a Humanized Anti-Tau Antibody, for Treatment of Alzheimer's Disease and Other Tauopathies. *4*, 236–241.

Whittington, R.A., Bretteville, A., Dickler, M.F., and Planel, E. (2013). Anesthesia and tau pathology. Prog. Neuro-Psychopharmacology Biol. Psychiatry *47*, 147–155.

Wischik, C.M., Harrington, C.R., and Storey, J.M.D. (2014). Tau-aggregation inhibitor therapy for Alzheimer's disease. Biochem. Pharmacol. *88*, 529–539.

Xia, Z., and Liu, Y. (2001). Reliable and global measurement of fluorescence resonance energy transfer using fluorescence microscopes. Biophys. J. *81*, 2395–2402.

Yagishita, S., Itoh, Y., Nan, W., and Amano, N. (1981). Reappraisal of the fine structure of Alzheimer's neurofibrillary tangles. Acta Neuropathol. *54*, 239–246.

Yan, S.D., Yan, S.F., Chen, X., Fu, J., Chen, M., Kuppusamy, P., Smith, M.A., Perry, G., Godman, G.C., and Nawroth, P. (1995). Non-enzymatically glycated tau in Alzheimer's disease induces neuronal oxidant stress resulting in cytokine gene expression and release of amyloid beta-peptide. Nat. Med. *1*, 693–699.

Yap, J.L., Worlikar, S., MacKerell, A.D., Shapiro, P., and Fletcher, S. (2011). Small-Molecule Inhibitors of the ERK Signaling Pathway: Towards Novel Anticancer Therapeutics. ChemMedChem *6*, 38–48.

Yeh, P.-A., Chien, J.-Y., Chou, C.-C., Huang, Y.-F., Tang, C.-Y., Wang, H.-Y., and Su, M.-T. (2010). Drosophila notal bristle as a novel assessment tool for pathogenic study of Tau toxicity and screening of therapeutic compounds. Biochem. Biophys. Res. Commun. *391*, 510–516.

Yoshiyama, Y., Higuchi, M., Zhang, B., Huang, S.-M., Iwata, N., Saido, T.C., Maeda, J., Suhara, T., Trojanowski, J.Q., and Lee, V.M.-Y. (2007). Synapse loss and microglial activation precede tangles in a P301S tauopathy mouse model. Neuron *53*, 337–351.

Yu, J.-Z., and Rasenick, M.M. (2006). Tau associates with actin in differentiating PC12 cells. FASEB J. *20*, 1452–1461.

Zheng-Fischhöfer, Q., Biernat, J., Mandelkow, E.M., Illenberger, S., Godemann, R., and Mandelkow, E. (1998). Sequential phosphorylation of Tau by glycogen synthase kinase-3beta and protein kinase A at Thr212 and Ser214 generates the Alzheimer-specific epitope of antibody AT100 and requires a paired-helical-filament-like conformation. Eur. J. Biochem. *252*, 542–552.

Zhu, X., Raina, A.K., Rottkamp, C.A., Aliev, G., Perry, G., Boux, H., and Smith, M.A. (2001). Activation and redistribution of c-jun N-terminal kinase/stress activated protein kinase in degenerating neurons in Alzheimer's disease. J. Neurochem. *76*, 435–441.